Analysis and Performance of Antenna Baluns

Lötter Kock

Thesis presented in partial fulfilment of the requirements
for the degree of Master of Science in Electronic Engineering
at the
University of Stellenbosch

Study Leader: Prof. K.D. Palmer

April 2005

Stellenbosch University http://scholar.sun.ac.za

- Declaration -

"I, the undersigned, hereby declare that the work contained in this thesis is my own original work and that I have not previously in its entirety or in part submitted it at any university for a degree."

Stellenbosch University http://scholar.sun.ac.za

Abstract

Data transmission plays a cardinal role in today's society. The key element of such a system is the antenna which is the interface between the air and the electronics. To operate optimally, many antennas require baluns as an interface between the electronics and the antenna. This thesis presents the problem definition, analysis and performance characterization of baluns. Examples of existing baluns are designed, computed and measured. A comparison is made between the analyzed baluns' results and recommendations are made.

Stellenbosch University http://scholar.sun.ac.za

Opsomming

Data transmissie is van kardinale belang in vandag se samelewing. Antennas is die voegvlak tussen die lug en die elektronika en vorm dus die basis van die sisteme. Vir baie antennas word `n balun, wat die elektronika aan die antenna koppel, benodig om optimaal te funktioneer. Die tesis omskryf die probleemstelling, analiese en `n prestasie maatstaf vir baluns. Prakties word daar gekyk na huidige baluns se ontwerp, simulasie, en metings. Die resultate word krities vergelyk en aanbevelings word gemaak.

Stellenbosch University http://scholar.sun.ac.za

Acknowledgements

First and foremost, I would like to thank God for affording me this life.

To my family: Thank you for support and love during the course of my studies. Thank you for the opportunity to be able to study. Without you I would literally not be here.

To Prof K.D Palmer: Thank you for your guidance, wisdom and good advice the past two years.

To Prof P. Meyer: Thank you for the guidance at the end of my final year.

To Prof J.H Cloete: Thank you for your enthusiasm and wisdom.

To all the guys in the *Molshoop*: Thanks for all the help during the past two years. It was an honor to work with you.

To Wessel Croukamp and Ashley Cupido: Thank for all your patience and help. I learnt a lot from you.

Lastly, I would like to thank OMNIPLESS and the NRF for their financial support during the past two years.

Stellenbosch University http://scholar.sun.ac.za

Table of Contents

ABSTRACT 2

OPSOMMING 3

ACKNOWLEDGEMENTS 4

TABLE OF CONTENTS 5

Chapter 1. Introduction to Baluns 11
1.1 Aim of Thesis 11
1.2 Balun Definitions 11
Chapter 2. Balun Theory 14
2.1 Antenna and Transmission line model 14
2.2 Balun Families 17
2.3 Performance characteristics 18
Chapter 3. Computation of Balun Performance 19
3.1 FEKO 19
3.2 Data Processing 19
3.3 Wu-King Feed line 22
3.4 Test Antennas 23
Chapter 4. Balun Measurements 30
4.1 Back to back 30
4.2 Combined Even and Odd mode S – parameters 30
4.3 Measurement system proposed by Palmer and Van Rooyen, [6] 31
4.4 Other Techniques 32
4.5 Comparison 33
Chapter 5. Analysis of Popular Baluns 34
5.1 The Sleeve or "Bazooka" Balun 34
5.2 Quarter wave Balun 36
5.3 Planar Marchand Balun [8, 9] 39
5.4 Double Y Balun [13, 14 & 15] 46
5.5 Tapered-line/Split Coaxial Balun [16 & 17] 48
5.6 Log-Periodic Balun [19] 50
5.7 Coplanar-Slot balun [21] 51
Chapter 6. Computational Results 53
6.1 The Sleeve or "Bazooka" Balun 53
6.2 Quarter wave Balun 57
6.3 Marchand Balun 62
6.4 Double Y Balun [13, 14 & 15] 67
6.5 Tapered-line/Split Coaxial Balun [16 & 17] 71
6.6 Log-Periodic Balun [19] 76
6.7 Coplanar-Slot balun [21] 80
6.8 Using Infinite Dipole Results to Predict Finite Antenna Performance 83
Chapter 7. Conclusion 90
7.1 Comparison of Different Balun Performances 90
7.2 Conclusion 91

REFERENCES 92

Stellenbosch University http://scholar.sun.ac.za

BIBLIOGRAPHY.....94

APPENDIX A. Examples of Marchand Baluns.....96

APPENDIX B. Balun Performance.....98

APPENDIX C. Impedance Profile for Wu-King Antenna.....110

Stellenbosch University http://scholar.sun.ac.za

List of Figures

Figure 1-1 Transmission line, Balun and Antenna Configuration 12
Figure 2-1 Dipole fed with an ideal source. 14
Figure 2-2 Current on Dipole arms. 14
Figure 2-3 Practical dipole fed with a coaxial cable. 15
Figure 2-4 Current on Dipole arms 15
Figure 2-5 Practical Dipole with feed schematic representation of impedances. 16
Figure 2-6 Two network models of generalized Baluns. (a) Delta Model (b) Y Model 16
Figure 2-7 Schematic diagram explaining differential and common mode feeds. 17
Figure 3-1 Computation Parameters and Results 22
Figure 3-2 Models of the antennas fed asymmetrical and symmetrical. 23
Figure 3-3 Schematic of Wu-King Loaded Infinite Dipole Antenna 24
Figure 3-4 Ideal and with feed line input impedance of Infinite Dipole 25
Figure 3-5 Schematic of Half Wave Dipole 25
Figure 3-6 Ideal and with feed line input impedance of Dipole 26
Figure 3-7 Schematic of Ninety Degree Half Wave Bow-Tie 27
Figure 3-8 Ideal and with feed line input impedance of Bow-Tie 28
Figure 3-9 Balun Ratio of test antennas terminated with a transmission line model 28
Figure 3-10 Percentage common to differential mode current for the 3 test antennas terminated with a transmission line 29
Figure 4-1 Measurement jig proposed by [5] 31
Figure 5-1 Photograph manufactured balun terminated with a Dipole 34
Figure 5-2 Schematic diagram of the sectioned front and top view of the Bazooka Balun 35
Figure 5-3 Network model 36
Figure 5-4 Photograph of manufactured balun with dipole. 37
Figure 5-5 Schematic diagram of Quarter wave Balun 37
Figure 5-6 Network model of quarter wave balun 38
Figure 5-7 Photograph manufactured balun. 39
Figure 5-8 Cross section of a single frequency transformer 40
Figure 5-9 Distributed element equivalent circuit of Figure 5-8 40
Figure 5-10 Second stage of development 41
Figure 5-11 Distributed element equivalent circuit of Figure 5-10 41
Figure 5-12 Coaxial Marchand Balun 41
Figure 5-13 Distributed element equivalent circuit of Figure 5-12 42
Figure 5-14 Basic Network Forms [10] 43
Figure 5-15 Coupled line model of planar Marchand Balun 43
Figure 5-16 Derivation of network model of planar Marchand Balun 44
Figure 5-17 Network model of system 45
Figure 5-18 Dimensions of designed and manufactured Marchand Balun 46
Figure 5-19 Diagram of Double Y junction with equivalent circuit 47
Figure 5-20 Photograph manufactured balun terminated with a Dipole (Top and bottom view). 49
Figure 5-21 Network Model of Tapered-line Balun 50
Figure 5-22 Dimensions of designed Tapered line balun 50
Figure 5-23 Schematic diagram of the Log-Periodic Balun 51
Figure 5-24 Schematic diagram of the Coplanar-Slot Balun 52
Figure 6-1 Computational model 53
Figure 6-2 Detailed view of the feed section for Figure 6-1 54
Figure 6-3 Currents on Infinite Dipole Arms (Magnitude & Phase) and Balun Ratio for Infinite Dipole 54

Stellenbosch University http://scholar.sun.ac.za

Figure 6-4 Feed Impedance and Differential and Common Mode Impedance Calculated from Currents on Infinite Dipole Arms (At Feed Point) 55
Figure 6-5 Balun Ratios for the Three test antennas 56
Figure 6-6 Measured and Computed $|S_{11}|$ 57
Figure 6-7 Computational model 58
Figure 6-8 Detailed view of the feed section for Figure 6-7 58
Figure 6-9 Currents on Infinite Dipole Arms (Magnitude & Phase) and Balun Ratio for Infinite Dipole. 59
Figure 6-10 Feed Impedance and Differential and Common Mode Impedance Calculated from Currents on Infinite Dipole Arms (At Feed Point) 60
Figure 6-11 Balun Ratios for the Three test antennas 61
Figure 6-12 Measured and Computed $|S_{11}|$ 62
Figure 6-13 Computational model 63
Figure 6-14 Detailed view of the feed section for Figure 6-13 63
Figure 6-15 Currents on Infinite Dipole Arms (Magnitude & Phase) and Balun Ratio for Infinite Dipole 64
Figure 6-16 Feed Impedance and Differential and Common Mode Impedance Calculated from Currents on Infinite Dipole Arms (At Feed Point) 65
Figure 6-17 Balun Ratios for the Three test antennas 66
Figure 6-18 Measured and Computed System Input Impedance 67
Figure 6-19 Computational model (Detailed view of antenna termination section is the same as for the Marchand Balun) 68
Figure 6-20 Detailed view of the feed section of Figure 6-19 68
Figure 6-21 Currents on Infinite Dipole Arms (Magnitude & Phase) and Balun Ratio for Infinite Dipole 69
Figure 6-22 Feed Impedance and Differential and Common Mode Impedance Calculated from Currents on Infinite Dipole Arms (At Feed Point) 70
Figure 6-23 Balun Ratios for the Three test antennas 71
Figure 6-24 Computational model 72
Figure 6-25 Detailed view of the antenna termination and feed section for Figure 6-24 72
Figure 6-26 Currents on Infinite Dipole Arms (Magnitude & Phase) and Balun Ratio for Infinite Dipole 73
Figure 6-27 Feed Impedance and Differential and Common Mode Impedance Calculated from Currents on Infinite Dipole Arms (At Feed Point) 74
Figure 6-28 Balun Ratios for the Three test antennas 75
Figure 6-29 Measured and Computed System Input Impedance 76
Figure 6-30 Computational model 77
Figure 6-31 Currents on Infinite Dipole Arms (Magnitude & Phase) and Balun Ratio for Infinite Dipole 78
Figure 6-32 Feed Impedance and Differential and Common Mode Impedance Calculated from Currents on Infinite Dipole Arms (At Feed Point) 79
Figure 6-33 Balun Ratios for the Three test antennas 80
Figure 6-34 Computational model (Detailed view of the feed section is shown in Figure 6-20) 80
Figure 6-35 Currents on Infinite Dipole Arms (Magnitude & Phase) and Balun Ratio for Infinite Dipole 81
Figure 6-36 Feed Impedance and Differential and Common Mode Impedance Calculated from Currents on Infinite Dipole Arms (At Feed Point) 82
Figure 6-37 Balun Ratios for the Three test antennas 83

Stellenbosch University http://scholar.sun.ac.za

Figure 6-38 Predicted and Computed Input Impedance for Dipole Terminated to a Bazooka Balun 84
Figure 6-39 Predicted and Computed Input Impedance for Bow-Tie Terminated to a Bazooka Balun 84
Figure 6-40 Predicted and Computed Input Impedance for Dipole Terminated to a Quarter Wave Balun 85
Figure 6-41 Predicted and Computed Input Impedance for Bow-Tie Terminated to a Quarter Wave Balun 86
Figure 6-42 Predicted and Computed Input Impedance for Dipole Terminated to a Marchand Balun 86
Figure 6-43 Predicted and Computed Input Impedance for Bow-Tie Terminated to a Marchand Balun 87
Figure 6-44 Predicted and Computed Input Impedance for Dipole Terminated to a Double Y Balun 88
Figure 6-45 Predicted and Computed Input Impedance for Bow-Tie Terminated to a Double Y Balun 88
Figure 6-46 Predicted and Computed Input Impedance for Dipole Terminated to a Tapered Line Balun 89
Figure 6-47 Predicted and Computed Input Impedance for Bow-Tie Terminated to a Double Y Balun 89
Figure 7-1 Current on Dipole Arms 98
Figure 7-2 Common and differential mode impedances measured from Dipole arms at feed point 98
Figure 7-3 Currents on Bow-Tie arms 99
Figure 7-4 Common and differential mode impedances measured from Bow-Tie arms at feed point 99
Figure 7-5 Currents on dipole arms 100
Figure 7-6 Common and differential mode impedances measured from dipole arms at feed point. 100
Figure 7-7 Currents on Bow-tie arms 101
Figure 7-8 Common and differential mode impedances measured from Bow-tie arms at feed point. 101
Figure 7-9 Currents on Dipole arms 102
Figure 7-10 Common and differential mode impedances measured from Dipole arms at feed point. 102
Figure 7-11 Currents on Bow-Tie Arms. 103
Figure 7-12 Common and differential mode impedances measured from Bow-Tie arms at feed point. 103
Figure 7-13 Current on Dipole Arms 104
Figure 7-14 Common and differential mode impedances measured from Dipole arms at feed point 104
Figure 7-15 Currents on Bow-Tie Arms. 105
Figure 7-16 Common and differential mode impedances measured from Bow-Tie arms at feed point 105
Figure 7-17 Current on Dipole Arms 106
Figure 7-18 Common and differential mode impedances measured from Dipole arms at feed point 106
Figure B-7-19 Current on Bow-Tie Arms 107
Figure 7-20 Common and differential mode impedances measured from Bow-Tie arms at feed point 107

UNIVERSITEIT STELLENBOSCH
BIBLIOTEEK

Stellenbosch University http://scholar.sun.ac.za

Figure 7-21 Currents on Dipole Arms 108
Figure 7-22 Common and differential mode impedances measured from Dipole arms at feed points 108
Figure B-7-23 Currents on Dipole Arms 109
Figure B-7-24 Common and differential mode impedances measured from Dipole arms at feed points 109

List of Tables

Table 3-1 Inputs for Infinite Dipole Applet 24
Table 3-2 Design data for Half Wave Dipole 26
Table 3-3 Design data for Ninety Degree Half Wave Bow-Tie 27
Table 4-1 Results available for various measurement techniques. 33
Table 5-1 Investigated Baluns sorted into families. 34
Table 5-2 Transmission line dimensions for CPS - CPW_{FGP} Double Y Balun 48
Table 5-3 Dimensions of the Slot-line balun 52
Table 7-1 Comparison of different balun performances 90

Stellenbosch University http://scholar.sun.ac.za

Chapter 1. Introduction to Baluns

1.1 Aim of Thesis

Baluns form a critical part of many high frequency systems and surprisingly, very little detailed work is published on the theory, design and performance characteristics of these devices to date. This thesis presents an in depth study of the balun. The following aspects concerning baluns will be covered in detail.

- The definition of the problem
- Model development
- Characterization of baluns
- Computational simulations of these baluns
- Modeling, operation and design of baluns
- Comparison between different balun performances

1.2 Balun Definitions

The following terms will be used to explain balun principles and properties in this thesis.

1.2.1 Problem Definition

Antennas with a physical symmetric structure require balanced signals for proper operation. This, in theory, is not a problem since many topologies of balanced transmission lines exist to feed these antennas. However this is just one side of the story. It has become popular practice in the years past to use coaxial transmission lines as the standard transmission line in the industry, and coaxial transmission lines are unbalanced (This will be discussed in detail in Chapter 1.). The problem occurs when the unbalanced transmission line is connected to the balanced antenna.

The consequences of this problem is unbalanced currents on the antenna arms and radiating currents on the feed line, which causes a distorted radiation pattern and

Stellenbosch University http://scholar.sun.ac.za

differing input impedance. To solve this problem the antenna/transmission line system requires some sort of transition to convert an unbalanced environment to a balanced environment. The class of transition that only propagates a balanced signal to the antenna is called a balun. The word balun is derived from the words "**BAL**ance to **UN**balanced" converter and gives a good indication of the function of the device. An advantage of many balun structures is that they can implement an impedance transformation which is a desirable property since antennas rarely have a 50 Ω input impedance.

It should be noted that baluns used for mixers and amplifiers operate in a different environments and are not the focus of this work. In this case the load can be modelled as lumped elements, which simplifies the analysis.

1.2.2 Balanced conditions

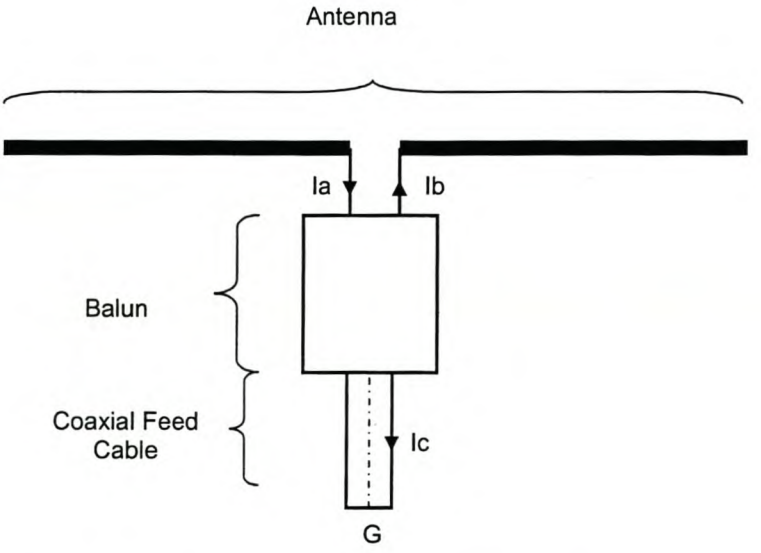

Figure 1-1 Transmission line, Balun and Antenna Configuration

The schematic diagram in Figure 1-1 shows the scenario was a practical coaxial cable is connected to an antenna through a balun transformer. Currents Ia, Ib and Ic are all possible currents in the system, where Ic is the current on the exterior of the coaxial line. For this system to be balanced the following condition has to be met.

Stellenbosch University http://scholar.sun.ac.za

- The currents, Ia and Ib, at the antenna feed point should be equal in amplitude and in of phase with respect to Figure 1-1.

Stellenbosch University http://scholar.sun.ac.za

Chapter 2. Balun Theory

2.1 Antenna and Transmission line model

This section explains the chronological development of the antenna and transmission line network model. A simple half wave dipole connected to a coaxial transmission line will be used as an example to explain the problem and illustrate its consequences. Starting of with the ideal case; the dipole is driven at the feed point as if no feed cable is connected. Figure 2-1 shows this scenario while Figure 2-2 shows the current on the dipole arms.

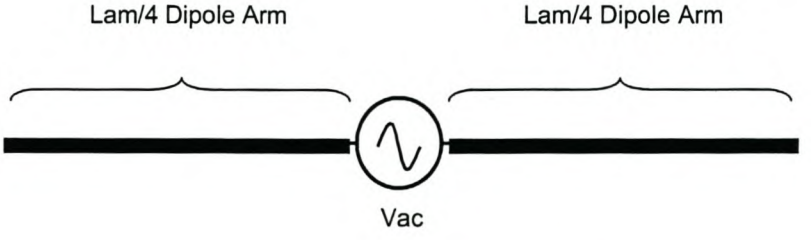

Figure 2-1 Dipole fed with an ideal source.

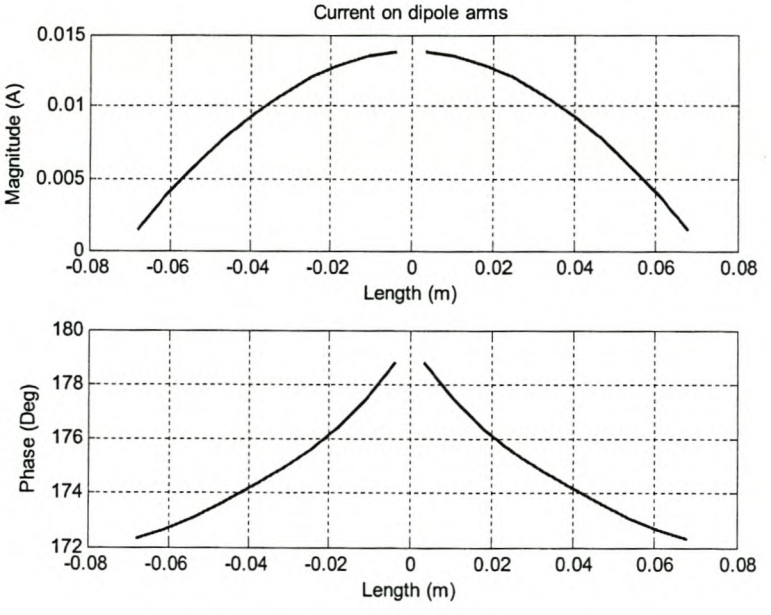

Figure 2-2 Current on Dipole arms.

Stellenbosch University http://scholar.sun.ac.za

From Figure 2-2 it can be seen that the current on the dipole is perfectly balanced and shaped for a resonant half wave dipole.

The next step is to add the unbalanced coaxial feed line. This is shown in Figure 2-3 and the effect on the arm currents can be seen in Figure 2-4.

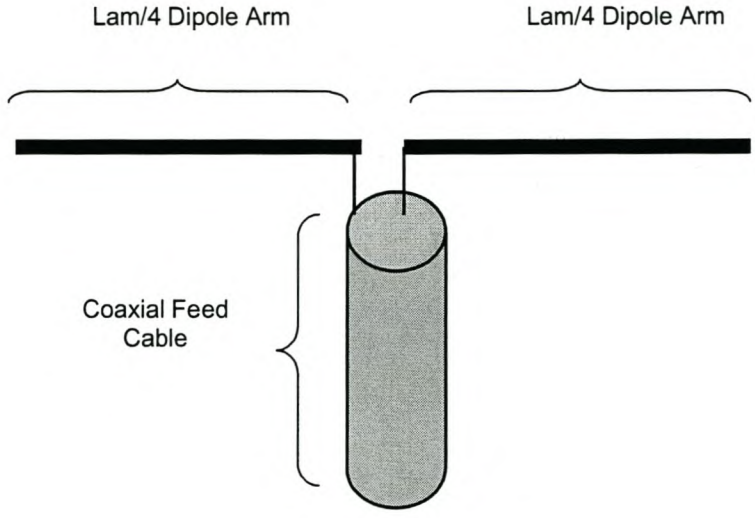

Figure 2-3 Practical dipole fed with a coaxial cable.

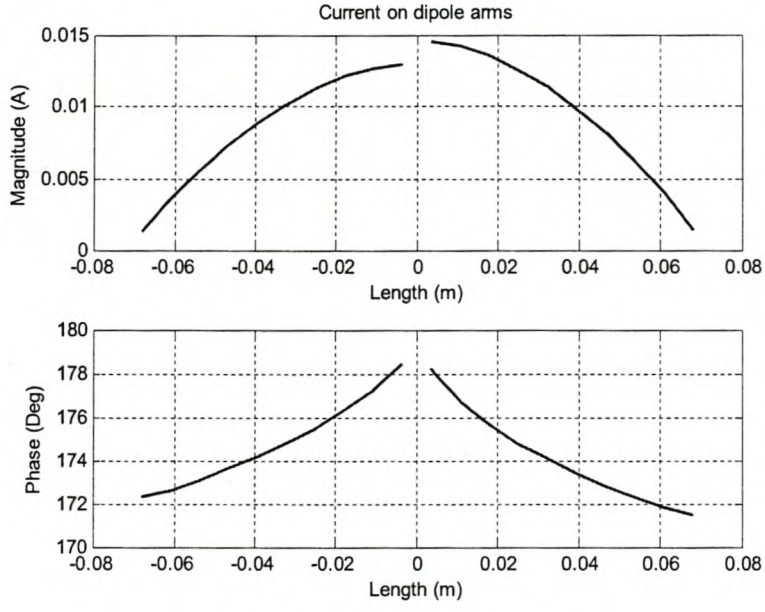

Figure 2-4 Current on Dipole arms

The physical asymmetry, presented by the coaxial line, creates stronger coupling from the one dipole arm to the feed line compared to the coupling between the other arm

Stellenbosch University http://scholar.sun.ac.za

and the feed line. The impedance to ground differs, and hence different currents flow on the two.

This effect may be modeled as shown in Figure 2-5.

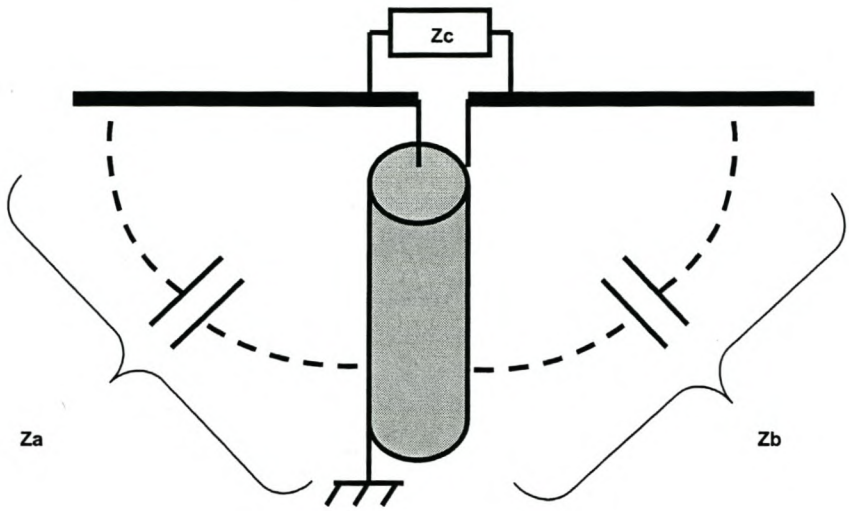

Figure 2-5 Practical Dipole with feed schematic representation of impedances.

Za and Zb represent the coupling of the antenna to the coaxial line and Zc the differential input impedance of the antenna. A network model of Figure 2-5 is shown in Figure 2-6.

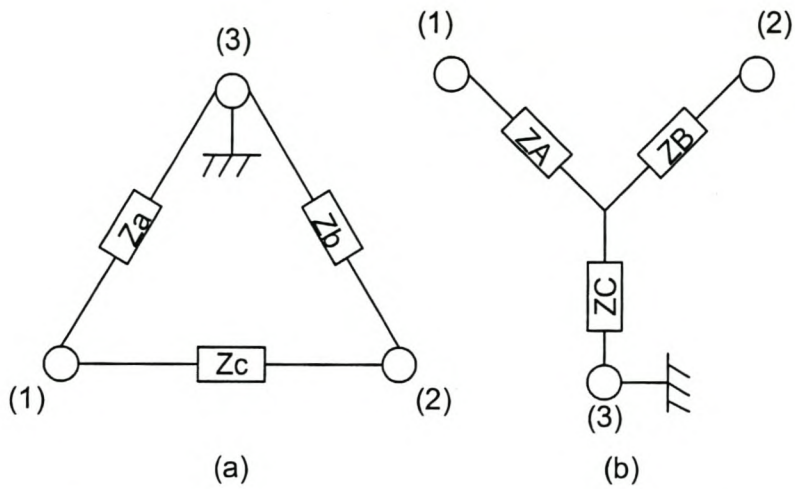

Figure 2-6 Two network models of generalized Baluns. (a) Delta Model (b) Y Model

Stellenbosch University http://scholar.sun.ac.za

We can relate the element values defined in Figure 2-6 to the common and differential mode impedance with the following equations

$$Z_{dif} = Z_c // (Z_a + Z_b) \tag{2.1}$$

and

$$Z_{com} = Z_a // Z_b \tag{2.2}$$

Figure 2-7 explains the concept of a differential and common mode feed.

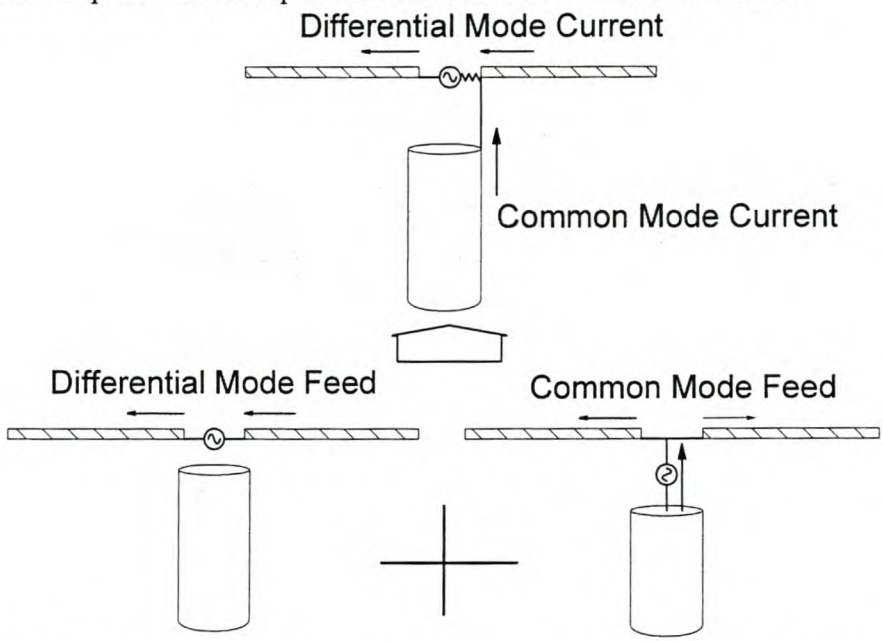

Figure 2-7 Schematic diagram explaining differential and common mode feeds.

2.2 Balun Families

From the model in Figure 2-6 the physical factors that produce the asymmetry can easily be seen. In Figure 2-6 (a), Za and Zb are related to the geometry between the feed line and the antenna, and Zc the antenna's ideal (no feed line) differential impedance. In Figure 2-6 (b), ZC represents the ability of the system to choke the common mode current and ZA and ZB the transformed differential impedance of the system. With these two models in mind, two families of baluns can be defined: The **Symmetrical** balun family and the **Choke** balun family. These definitions are of course interrelated but are introduced only to explain the operation of baluns.

Another balun family, which falls into a totally different class of operation, is the **anti-phase** type. All the investigated baluns fall into one of these families for an explanation of their operation and is explained in the following bullets.

Stellenbosch University http://scholar.sun.ac.za

- The symmetrical baluns produce balance by having a definable point feed and then forcing Za and Zb to be equal, in other words, creating a physically symmetric structure.
- Choke baluns add a series choking impedance in the common mode current path. From equation (2.2) we observe that all antenna/feed line systems have a common mode choking impedance which is dependant on the physical dimensions of the system.
- Anti-phase baluns split the input signal in two, where the two paths to the output have a 180 degree phase difference.

2.3 Performance characteristics

Most published work presents impedance matching as the only measure to characterize the performance of baluns. This says nothing about the balun's main function, which is balance. Matching is an important criterion which defines the ability of the balun to transfer the power from the transmission line to the antenna. For this thesis impedance matching information will be presented in the form of input impedance and the *log* of the magnitude of S_{11}.

To characterize the balance performance of the balun, the balun ratio (BR) is defined. The BR is the ratio of differential mode current to common mode current on the antenna. Ideally all the current must flow in the differential mode, giving a BR of infinity. The BR is mathematically defined by

$$BR = 20\log\left|\frac{I_{dif}}{I_{com}}\right| \tag{2.3}$$

where I_{dif} is the differential mode current and I_{com} is the common mode current.

Stellenbosch University http://scholar.sun.ac.za

Chapter 3. Computation of Balun Performance

The key results displayed in this thesis are obtained by computer computation. Selected baluns impedance response were also measured to verify the computed results. The reason computation is used as the primary result and not measurements, is because of the versatility and low cost of computations where dimensions can easily be changed to study the effects of parameter variation on the response without manufacturing a new balun. The computation package used is FEKO [1], and the key results obtained from computations are balance performance and impedance. All the computational models are checked for convergence to ensure that the results have converged.

3.1 FEKO

The program, FEKO, is based on the Method of Moments where electromagnetic fields are obtained by first calculating the electric and magnetic surface and line currents. Once the current distribution is known, further parameters can be obtained. FEKO can be used for various types of electromagnetic field analyses involving objects of arbitrary shapes.

One big advantage FEKO has over other electromagnetic magnetic computation packages is that it has a text editor for defining the dimensions and computation parameters. This makes it very convenient for changing parameters.

3.2 Data Processing

FEKO saves specified currents on segments in an output file. These currents are saved in vector format. The FEKO output files are loaded into MATLAB where the currents are extracted and processed to obtain common and differential mode currents, and common and differential mode impedances. With this data, the performance characteristics of the baluns can be calculated. The following bullets explain the procedure in more detail. See Figure 3-1.

Stellenbosch University http://scholar.sun.ac.za

- FEKO computation is set up to compute currents on certain segments of the structure. The segments of interest include a dummy wire across the feed point and the feed points of the antenna under investigation. These are currents I_1, I_2 and I_s in Figure 3-1. The dummy segment across the feed points is a wire segment loaded with very high impedance so that the ratio of current flowing on the segment compared to the antenna arms is negligible. The purpose of the dummy segment is to use the measured current to calculate the voltage across the feed point which is needed to calculate the impedances. (For the Bazooka and Quarter wave balun the dummy segment is not required since the excitation voltage can be used directly.)
- The FEKO output file is loaded into MATLAB and the currents are extracted. The common and differential mode current is then calculated with the following equations.

$$I_{com} = I_2 - I_1 \tag{3.1}$$

$$I_{dif} = \frac{(I_1 + I_2)}{2} \tag{3.2}$$

- The voltage across the feed point is determined by

$$V = I_s R \tag{3.3}$$

where $R = 10^8 \Omega$

- The common and differential mode impedance is calculated with the following equations.

$$Z_{com} = \frac{V}{I_{com}} \tag{3.4}$$

$$Z_{dif} = \frac{V}{I_{dif}} \tag{3.5}$$

- The next step is to determine the Balun Ratio which is defined by

$$BR = 20 \log \left| \frac{I_{dif}}{I_{com}} \right| \tag{3.6}$$

Stellenbosch University http://scholar.sun.ac.za

- The input impedance of a transmission line/balun/antenna system is predicted from the response of an ideally fed (no feed line), identical antenna. This enables the designer to get an idea of how the system's (transmission line/balun/antenna) input impedance response will behave if the ideal input impedance of the antenna is known. To be able to predict the response of the system, the balun's differential response has to be extracted. This is done with the following equation.

$$Z_{bal} = \frac{1}{\left(\frac{1}{Z_{difBAL}} - \frac{1}{Z_{difNO}}\right)} \tag{3.7}$$

where

Z_{bal} is the balun's differential impedance

Z_{difBAL} is the differential impedance of the feed line/balun/antenna system

Z_{difNO} is the differential impedance of the antenna alone

- The balun's response is then used to predict the response of the dipole and the bow-tie in the feed line/balun/antenna system. The following equation is used to predict the response.

$$Z_{dif} = \frac{1}{\left(\frac{1}{Z_{bal}} + \frac{1}{Z_{difNO^{\bullet}}}\right)} \tag{3.8}$$

where

Z_{dif} is the predicted differential impedance of the dipole or the bow-tie

Z_{bal} is the balun differential impedance calculated in the previous step

$Z_{difNO^{\bullet}}$ is the ideal differential impedance of the dipole or bow-tie. (Test antennas used)

Stellenbosch University http://scholar.sun.ac.za

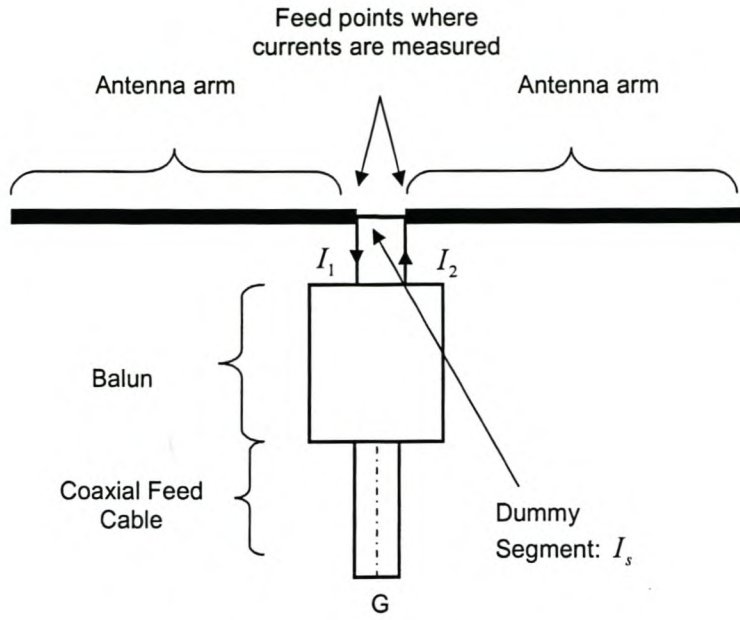

Figure 3-1 Computation Parameters and Results

3.3 Wu-King Feed line

The computations have to model the practical problem as closely as possible. Since feed lines play an important role for baluns in practice, a way had to be devised to model these infinitely long lines. Without the feed lines in the computation, all tested baluns would perform perfectly in the balance criteria because there is no path for the common mode current to flow. To add an infinitely long wire segment in the computation is not an option since this is impractical.

T.T. Wu and R.W.P. King [2] developed a way to suppress all backward travelling waves on finite length dipole antenna arms by loading the arms with an impedance profile. This profile is a function of axial coordinate z and is given by

$$Z^i(z) = \frac{60\psi}{h - |z|} \tag{3.9}$$

where h is the length of the antenna arm and ψ is the complex expansion parameter. The complex expansion parameter is well approximated by

$$\psi_{re} = 2\left[\ln\left(\frac{2h}{a}\right) - 1.65\right] \tag{3.10}$$

Stellenbosch University http://scholar.sun.ac.za

where a is the radius of the antenna arm [3].

Taking one Wu-King loaded arm and using it as a feed line is an excellent way to model the feed line in a computation. Looking into this loaded line gives the appearance of an infinitely long line for local effects and thus a current path for the common mode current to flow while at the same time keeping the computational volume small.

3.4 Test Antennas

Test antennas play an equally important role as the feed line does when it comes to characterizing baluns. A distributed load is required to investigate the asymmetry produced by the feed line because with a lumped element load connected over the balun, the currents will always be perfectly balanced.

Three antennas are used to investigate the balun responses. The Wu-King Loaded Infinite Dipole, Half Wave Dipole and a Ninety Degree Half Wave Bow-Tie antenna. The reasons for these choices are explained in the next sections together with the input impedance of the antenna in both a symmetrical and asymmetrical system. Figure 3-2 shows the models for the asymmetrical and symmetrical scenarios.

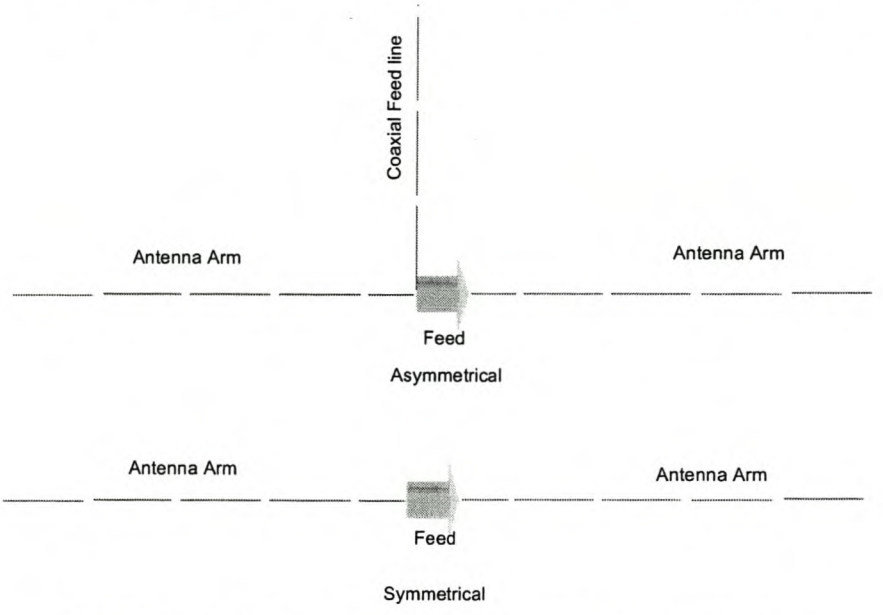

Figure 3-2 Models of the antennas fed asymmetrical and symmetrical.

Stellenbosch University http://scholar.sun.ac.za

3.4.1 Wu-King Loaded Infinite Dipole

This antenna is chosen for its wide bandwidth. The response is reasonably flat over a large frequency band which makes it easier to visualize the balun response without superimposing the effect of the antenna response. The arms of the antenna give good coupling to the feed line to exploit the asymmetry on condition that they are substantially longer than the balun itself.

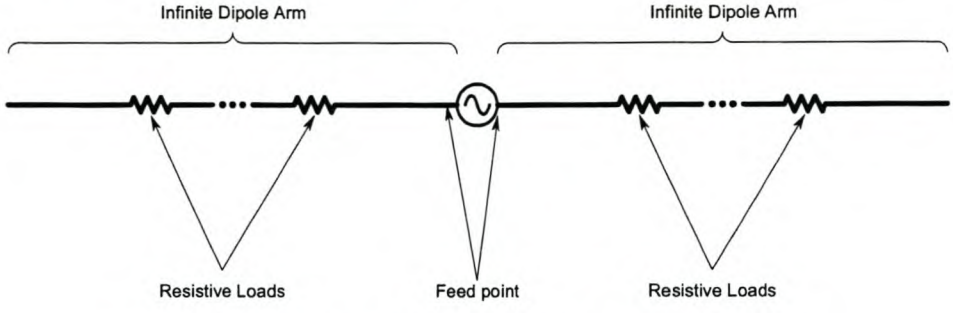

Figure 3-3 Schematic of Wu-King Loaded Infinite Dipole Antenna

The design of this antenna is done with the help of a FEKO computation applet. Table 3-1 displays the applet inputs.

Data for Infinite Dipole Applet		
Inputs	**Value**	**Dimension**
Length of Arm	0.5	m
Number of Loads per Arm	20	
Radius of Antenna	0.55	mm
Length of Loads	4	mm
Feed Gap	3.4	mm
Frequency Band	0.8 – 2.4	GHz

Table 3-1 Inputs for Infinite Dipole Applet

The applet produces a FEKO output file with the currents on all the segments stored in it. These can be converted to obtain the input impedance of the antenna. The input values in Table 3-1 were obtained after a few iterations, maximizing the flatness of the impedance response over the frequency band. One guideline in designing this antenna is to choose the wire sections between the loads not to be near resonance in the frequency band of interest. Figure 3-4 shows the input impedance of the antenna fed with a feed line and without a feed line.

Stellenbosch University http://scholar.sun.ac.za

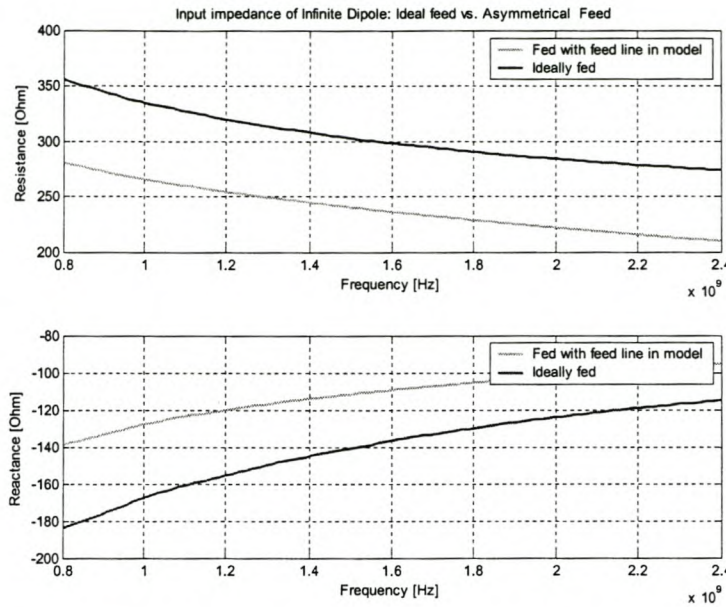

Figure 3-4 Ideal and with feed line input impedance of Infinite Dipole

3.4.2 Half Wave Dipole

This antenna is chosen because it is the most popular, narrow band antenna and it requires a balun for proper operation. The design is very simple with only two design parameters; the radius of the antenna and the feed gap with the length fixed by the centre frequency. Table 3-2 presents the design data.

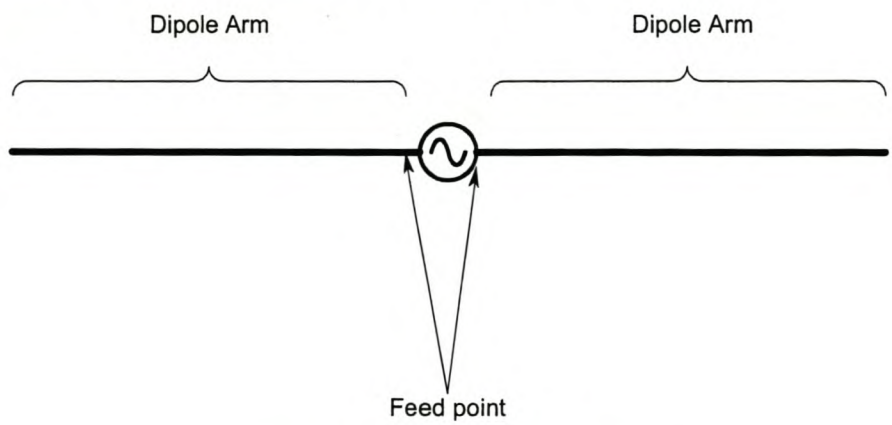

Figure 3-5 Schematic of Half Wave Dipole

Design Data for Dipole		
Inputs	**Value**	**Dimension**
Length of Arm	47	mm
Radius of Antenna	0.55	mm

Stellenbosch University http://scholar.sun.ac.za

Feed Gap	3.4	mm
Frequency Band	0.8 – 2.4	GHz

Table 3-2 Design data for Half Wave Dipole

Figure 3-6 shows the input impedance of the antenna terminated with a feed line and without the feed line.

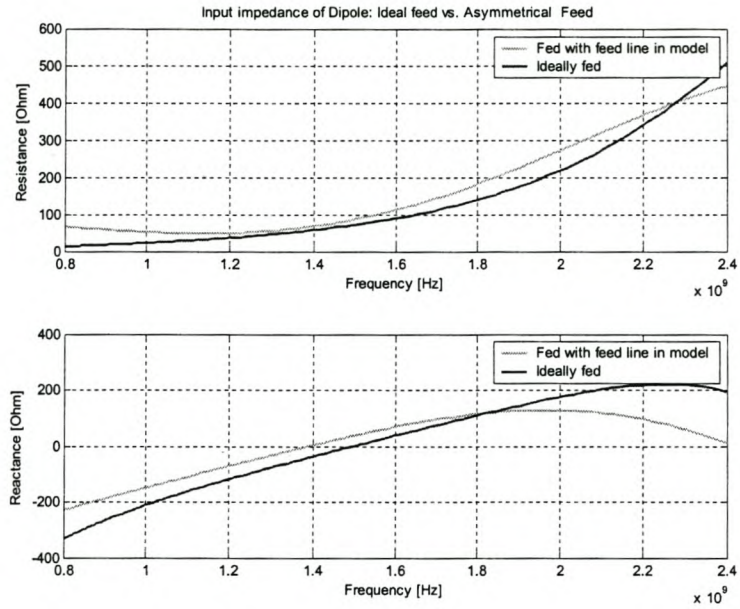

Figure 3-6 Ideal and with feed line input impedance of Dipole

3.4.3 Ninety Degree Half Wave Bow-Tie

The Bow-Tie antenna is also a popular antenna that requires a balun and has a wide bandwidth. The design is straight forward with the name giving away most of the dimensions. Figure 3-7 shows a schematic view of the Bow-Tie while Table 3-3 presents the design data.

Stellenbosch University http://scholar.sun.ac.za

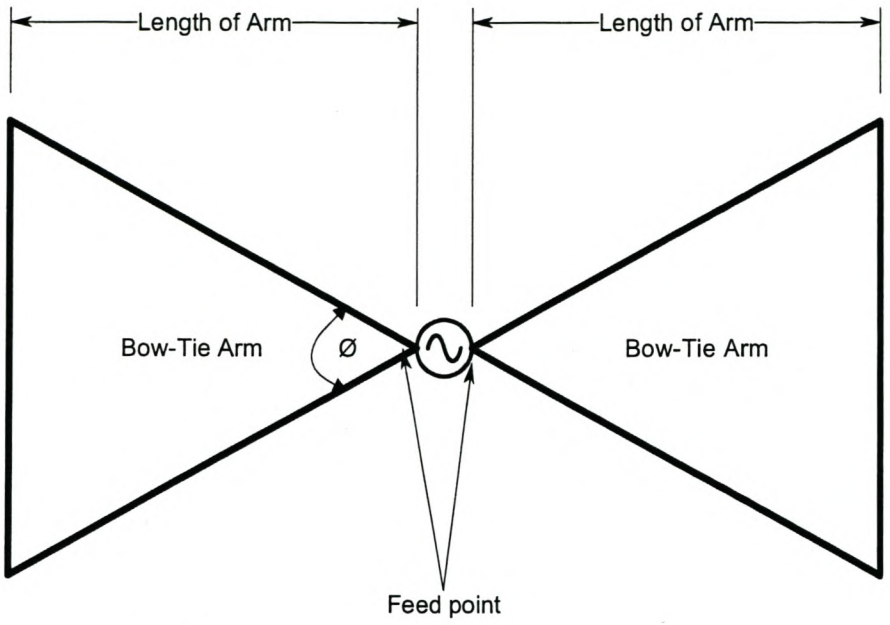

Figure 3-7 Schematic of Ninety Degree Half Wave Bow-Tie

Design Data for Bow-Tie		
Inputs	**Value**	**Dimension**
Length of Arm	47	mm
Flare Angle Ø	90	Deg
Feed Gap	3.4	mm
Frequency Band	0.8 – 2.4	GHz

Table 3-3 Design data for Ninety Degree Half Wave Bow-Tie

Figure 3-8 shows the input impedance of the antenna terminated with the feed line and without the feed line.

Stellenbosch University http://scholar.sun.ac.za

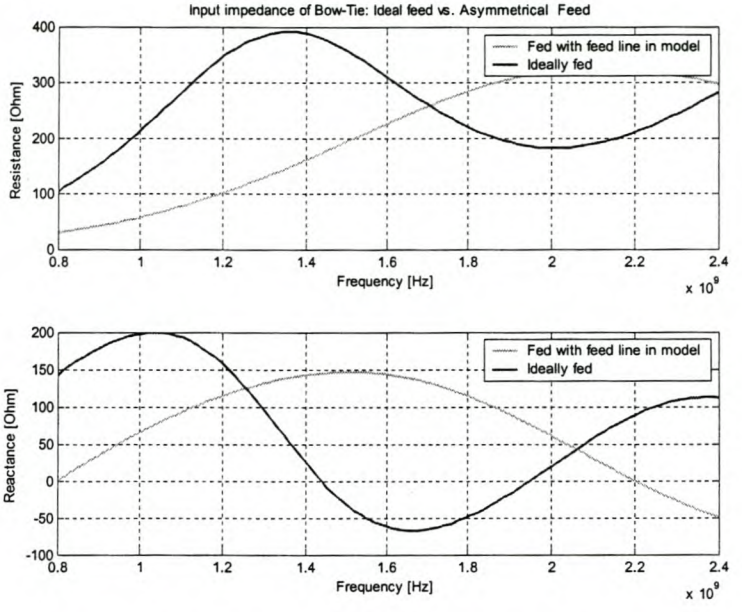

Figure 3-8 Ideal and with feed line input impedance of Bow-Tie

3.4.4 Balun Ratios of Test Antennas

An antenna/feed line system can be modeled by either a delta or a Y model as explained in Chapter 1. From the model a differential and common mode impedance can be calculated, and thus also a Balun Ratio. Figure 3-9 shows the balun ratios of the antenna/feed line system without the baluns added. This can be compared to results presented in Chapter 5. to observe if the balun is operating as a balun or not.

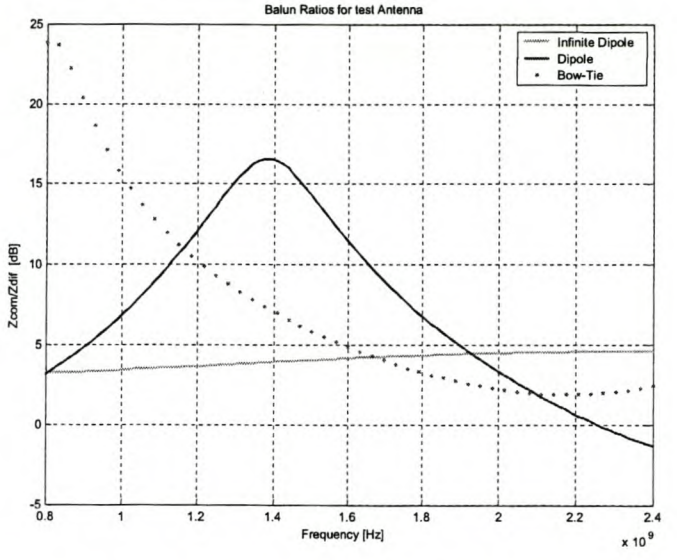

Figure 3-9 Balun Ratio of test antennas terminated with a transmission line model.

Stellenbosch University http://scholar.sun.ac.za

Figure 3-10 shows the percentage common to differential mode current calculated at the feed point on the three test antennas.

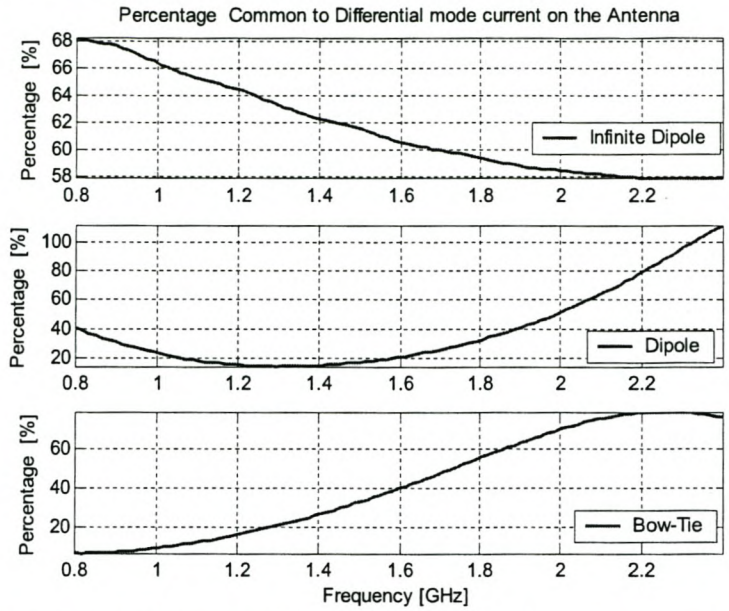

Figure 3-10 Percentage common to differential mode current for the 3 test antennas terminated with a transmission line

Stellenbosch University http://scholar.sun.ac.za

Chapter 4. Balun Measurements

Measurement is the accepted method of characterizing the operation of the device under test. Yet, not many people measure balun performances correctly. The most popular techniques measure only the impedance frequency response of the balun and not the balance property of the balun. This chapter investigates the techniques available and presents a newly proposed technique.

4.1 Back to back

This technique is the most popular and also the worst. Two identical baluns are connected back to back so that the balanced ports connect to each other in the middle. The two unbalanced ports can then conveniently be connected to a network analyzer where the s-parameters can be measured. The setup being reciprocal, either S_{11} and S_{21} or S_{22} and S_{12} are the results obtained by this technique. No information about balance is acquired with this technique.

4.2 Combined Even and Odd mode S – parameters

New measurement hardware using multi ports, [4], makes it possible to measure mixed mode S-parameters. The hardware is a four port test set for network analyzers which enables the user to connect all four ports of a general balun to the network analyzer and measure the s-parameters for the four port system. The theory of mixed mode parameters, mixed mode s-parameter conversion from the measured s-parameter and the extraction of the common and differential mode impedances for the device under test is derived and discussed in [5]. [4] explains the detail of the physical measurement.

The method is useful to gain an idea of the balun's balance performance and gives good results for the balun's impedance response. It is however impossible to obtain the balun/antenna system's balance performance using this method because all four

Stellenbosch University http://scholar.sun.ac.za

ports of the balun under test are connected to the network analyzer. This method also only tests the common mode choking properties of the balun and not the symmetry properties.

4.3 Measurement system proposed by Palmer and Van Rooyen, [6]

A technique to measure broadband balanced loads with a network analyzer is presented in [6]. The method uses a measurement jig shown in Figure 4-1. The two ports of the network analyzer are connected to the two SMA connectors, in Figure 4-1, and the balanced load is connected to the two centre conductors coming out of the semi-rigid coaxial cable. This method allows one to obtain the balanced load's pi equivalent network values which can be used to calculate the common and differential mode impedances once S_{11} and S_{21} are measured.

This method can also be used to measure balun/antenna systems. Instead of directly connecting an antenna to the jig, a balun/antenna system can be connected. This setup measures the common and differential mode impedances of the whole balun/antenna system. Together with a measurement of the antenna alone, the balun's common and differential mode impedances can be extracted. This is a very powerful technique since information on both the balance performance and the impedance matching is obtained. This technique is promising in theory but has as yet not been tested.

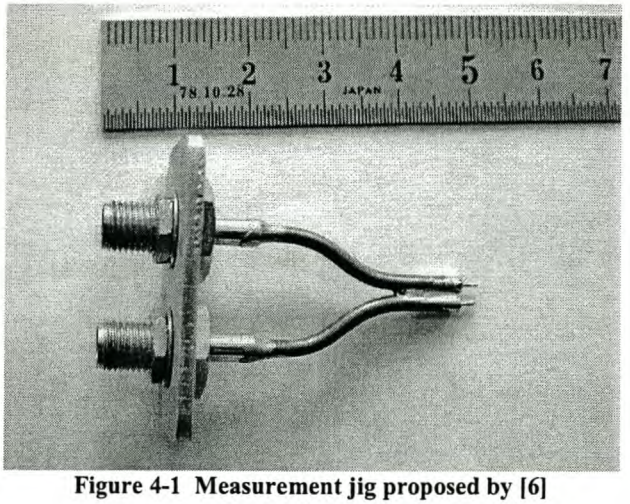

Figure 4-1 Measurement jig proposed by [6]

Figure 4-2 shows how the technique could possibly applied to balun measurements. Practically the balun/transmission line part will have to be folded onto the jig and grounded at their respective grounds. This is done to avoid unwanted asymmetry and

Stellenbosch University http://scholar.sun.ac.za

to get the system as accurate as possible. A drawback of implementing the jig like this is that only shielded or baluns with ground planes can be measured with it.

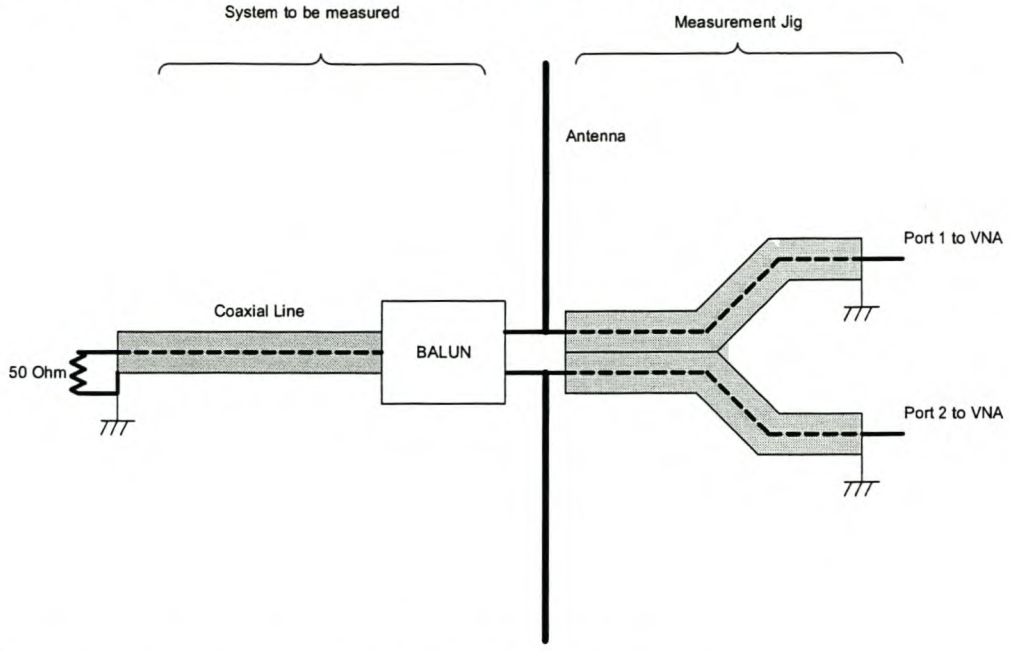

Figure 4-2 Proposed technique applied to balun measurements

4.4 Other Techniques

4.4.1 Balance Comparator

This technique requires a complicated measurement system. [7] shows the construction with dimensions and gives a thorough explanation of the operation of this jig. The jig together with a signal generator and a receiver measures only the balance quality of the balun under test. It is assumed that the differential balun impedance is known because the measurement system has to be matched with a lumped element resistor to the balun.

4.4.2 Using VNA's, discussed in [7]

The network analyzer method, thoroughly explained in [7], uses a simple measurement jig. The method measures the balance quality of the balun but not the impedance response of the balun. The method is questionable because it only gives an indication of the balun on its own and not of the balun in the system (with antenna)

Stellenbosch University http://scholar.sun.ac.za

and as with the mixed mode s-parameter method only gives performance characteristics of the choking properties and not of the symmetry properties.

4.5 Comparison

Table 4-1 summarizes the results available from various measurement techniques.

Method	Test		
	Balanced		Impedance
	Choking	Symmetry	
Back to back	No	No	Yes
Mixed mode S-parameters	Yes	No	Yes
System proposed by Palmer & Van Rooyen [6]	Yes	Yes	Yes
Balance comparator	Yes	No	No
Network analyzer	Yes	No	No

Table 4-1 Results available for various measurement techniques.

Stellenbosch University http://scholar.sun.ac.za

Chapter 5. Analysis of Popular Baluns

This chapter analyzes existing baluns with the theory developed in the previous chapters. The analysis of each balun is divided into two parts: Principle of operation and design. Table 5-1 lists the baluns that are considered.

Balun	Bandwidth	Family
Bazooka	Narrow band	Choke
Quarter wave	Narrow band	Choke /Symmetric
Marchand	Wide band	Symmetric/Choke
Tapered line	Wide band	Choke/ Symmetric?
Double Y	Wide band	Choke /Symmetric?
"Slot line"	Wide band	Choke?
"Log-periodic"	Wide band	Choke /Symmetric/Anti-phase

Table 5-1 Investigated Baluns sorted into families.

5.1 The Sleeve or "Bazooka" Balun

Popular in textbooks, for this balun the coaxial feed line is covered by a coaxial shield of a quarter wave length at the centre frequency. At a quarter wave length away from the antenna feed point, the outer coaxial shield is shorted to the feed lines' coaxial shield. Figure 5-1 shows a photograph of the balun terminated with a dipole antenna while Figure 5-2 shows the schematic diagram of the balun.

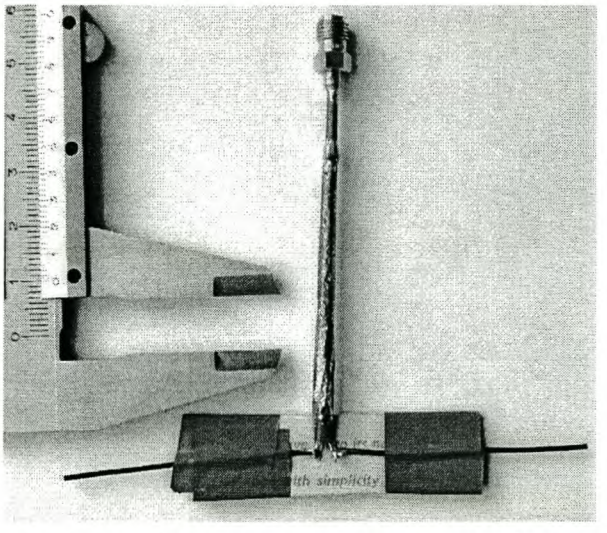

Figure 5-1 Photograph manufactured balun terminated with a Dipole

Stellenbosch University http://scholar.sun.ac.za

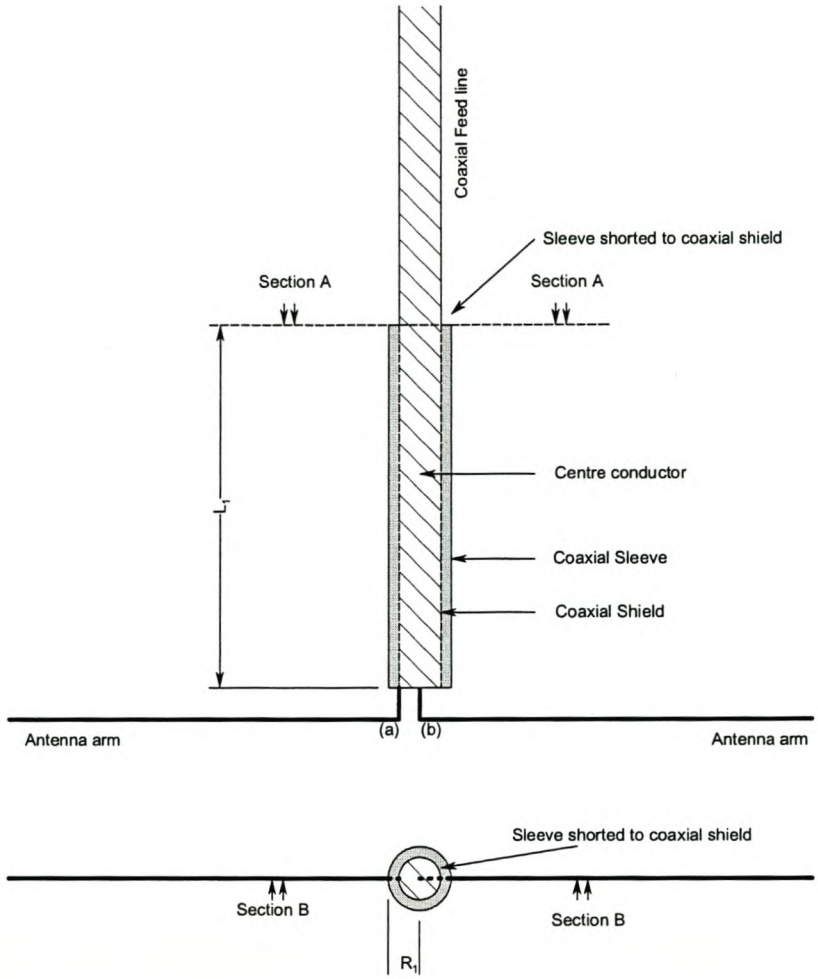

Figure 5-2 Schematic diagram of the sectioned front and top view of the Bazooka Balun

5.1.1 Principle of Operation: "Bazooka" Balun

This balun falls in the choke balun family. The added quarter wave section introduces a series impedance (choke) into the common mode current path. At the centre frequency this impedance is close to infinity, forcing balance in the system. The bandwidth where the balun will balance the system is thus limited to that of a quarter wave transformer. Z_a' and Z_b' are not equal in this case. (The coupling from the one arm of the antenna to ground and the other arm of the antenna to ground differs.) Figure 5-3 shows the equivalent network model for the balun. The input impedance for the system is defined as

$$Z_{in} = Z_{ant} // Z_{baz}'//(Z_a''+Z_b'') \qquad (5.1)$$

Stellenbosch University http://scholar.sun.ac.za

where Z_{baz}', Z_a'' and Z_b'' is the impedances formed by transforming the Y section to a delta. The parallel combination of $Z_{baz}'//(Z_a''+Z_b'')$ has very little effect on the differential mode impedance. Mathematically we can explain this as follows: Z_{baz} has a quarter wave transformers response. Z_a' and Z_b' are high impedances with some variation over the band. Transforming the Y model to a delta model will give a high, flat response for Z_{baz}'. Z_a'' and Z_b'' will have high values with the effects of the quarter wave transformer visible in the response. The parallel combination of these two factors gives a high response over the band compared to Z_{ant} and can almost be neglected.

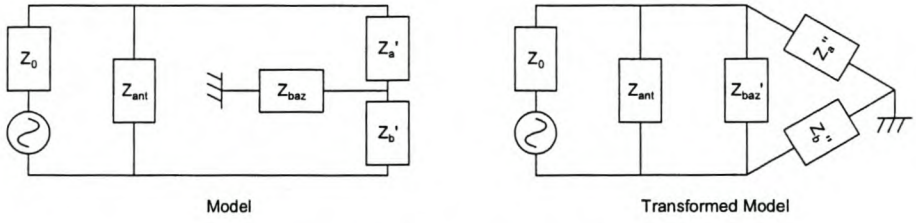

Figure 5-3 Network model

Design: "Bazooka" Balun

The variable parameter in the balun is the radius of the external shield once the centre frequency is known. This parameter has little effect on the bandwidth of the system so any convenient radius can be chosen.

5.2 Quarter wave Balun

The quarter wave balun is probably the most popular balun because of its trivial design, easy manufacturing and good performance. Figure 5-4 shows a photograph of the balun terminated with a dipole antenna.

Stellenbosch University http://scholar.sun.ac.za

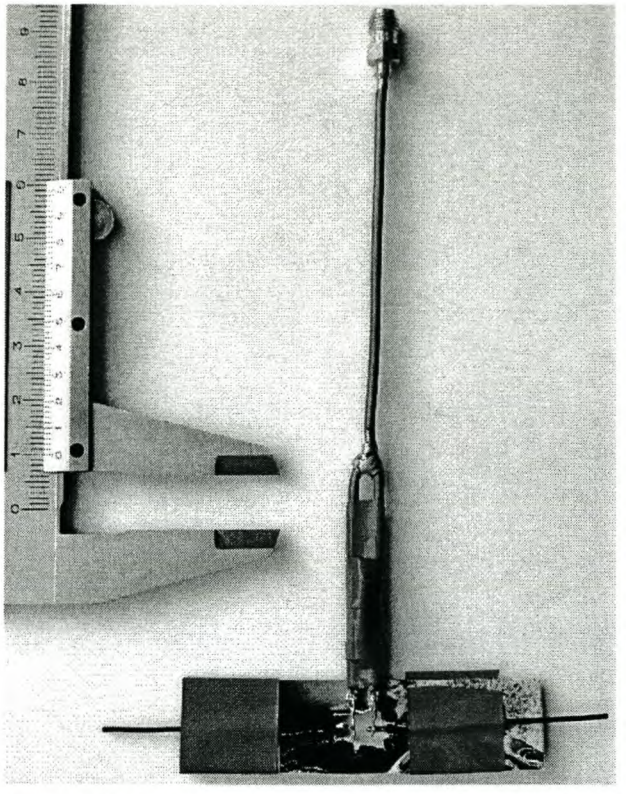

Figure 5-4 Photograph of manufactured balun with dipole.

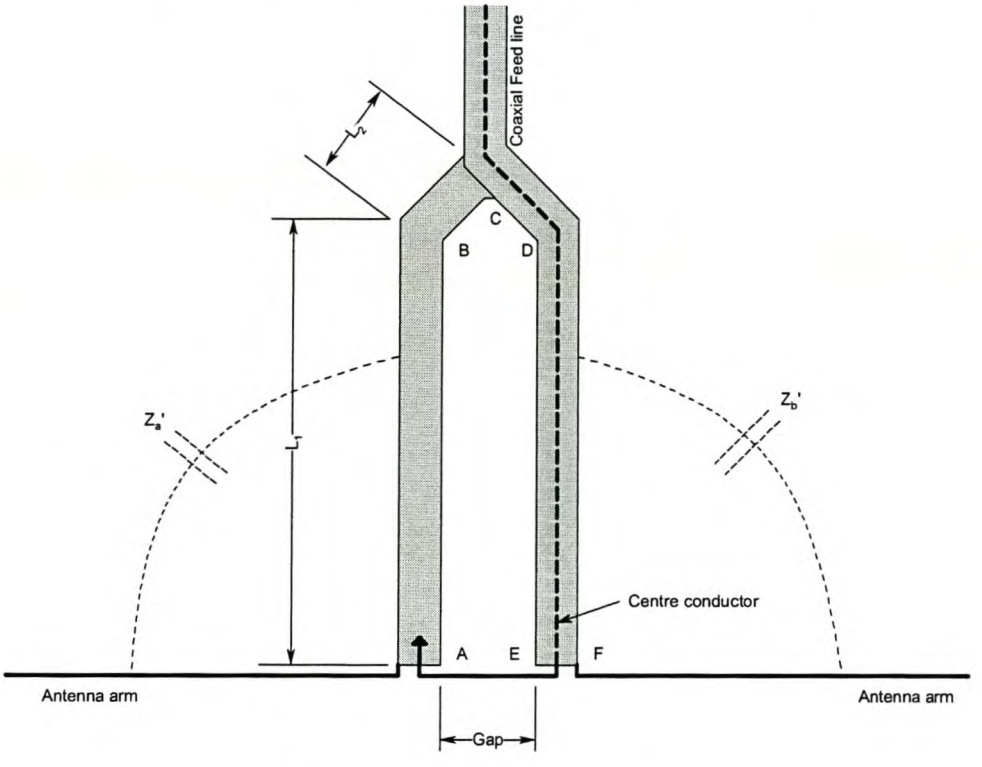

Figure 5-5 Schematic diagram of Quarter wave Balun

Stellenbosch University http://scholar.sun.ac.za

5.2.1 Principle of Operation: Quarter wave Balun

Two aspects of the quarter wave balun should be investigated: The balun principle and the effect of the balun on the differential mode impedance of the system. Figure 5-5 presents the schematic diagram of the balun. The balun is part of the symmetrical balun family, thus creating a symmetrical structure(with definable point source) to feed the antenna. Z_a' is always equal to Z_b'. Common mode current is never generated and there is no need for any common mode choking. In creating the symmetrical structure, a parallel impedance consisting of the loop ABCDEF is added in the system. To obtain the same input impedance as before the addition of the balun, the loop impedance should be as high as possible, preferably over an infinite bandwidth. Choosing the length of the added balun structure to be a quarter wave length at the centre frequency, approximated this impedance criteria, as at the centre frequency the shorted quarter wave section will become an open circuit. A drawback of the quarter wave section is that if the frequency shifts from the centre frequency, the impedance drops rapidly and starts interfering with the system input impedance. Figure 5-6 shows the equivalent circuit for the quarter wave balun terminated with an antenna. The system input impedance is given by

$$Z_{in} = Z_{ant} // Z_{qw} \tag{5.2}$$

The parallel impedance formed by Z_a' and Z_b', which represents the coupling from the antenna arms to ground, can be neglected since it is very high compared to the antenna impedance over the frequency band . Z_{ant} is the antenna input impedance for an ideally fed antenna with no feed cable. The delta in Figure 5-6 can be transformed to a Y. In this model the balun has a series impedance in the common mode current path, although no current will flow there because Z_a'' and Z_b'' are equal.

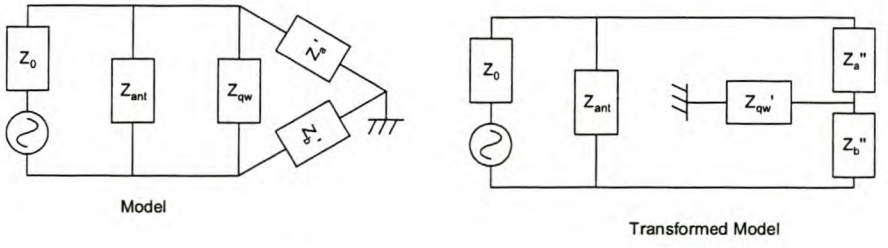

Figure 5-6 Network model of quarter wave balun

Stellenbosch University http://scholar.sun.ac.za

Design: Quarter wave Balun

The design is simple as the loop length must be resonant at the centre frequency. The gap AE defined in Figure 5-5, is the only variable as the equivalent arm width, EF, is not a sensitive parameter. Computations show as expected from a transmission line model, that a wider gap gives a higher impedance for the quarter wave section at resonance.

5.3 Planar Marchand Balun [8, 9]

This balun was proposed in 1944 by Nathan Marchand and was one the first wide band baluns manufactured [8]. The classic Marchand balun is realized in a coaxial environment. It was only when planar topologies became popular that the planar version was implemented. Since the balun principle for the two topologies are the same, both in the symmetrical and choke family, the planar version is implemented as it is easier to simulate. Figure 5-7 shows a photograph of the balun.

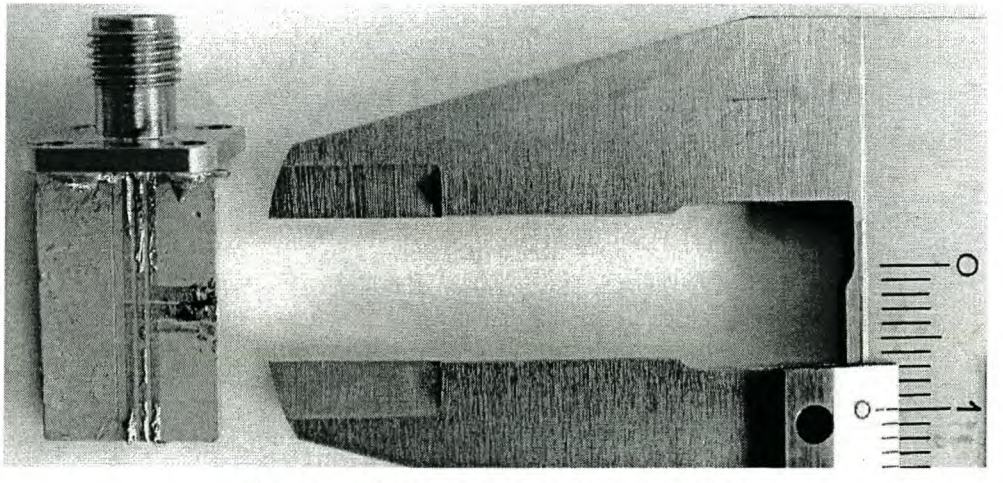

Figure 5-7 Photograph of manufactured balun.

5.3.1 Principle of Operation: Marchand Balun

The coaxial topology is used to explain the operation of the balun. Figure 5-8 shows the first step in the development of the Marchand balun. A basic transition from coaxial to a balanced twin wire is placed inside a shielded box. The shielding box should enclose all internal currents. To explain the operation of this network, currents must be traced. The criterion is that I_1 and I_2 should be equal in magnitude and opposite in phase.

Stellenbosch University http://scholar.sun.ac.za

Current I_1 flows from the centre conductor to the one conductor of the balanced twin wire. Current I_2 flows from the other conductor of the balanced line either on the inside, I_3, of the coaxial line or on the outside, I_4, of the coaxial line. Since the coaxial line is extended a quarter wavelength (BC) into the box, I_4 sees a very high impedance at the centre frequency and all the current flow in I_3. The network is thus perfectly balanced at one frequency where the extended coax is a quarter wavelength.

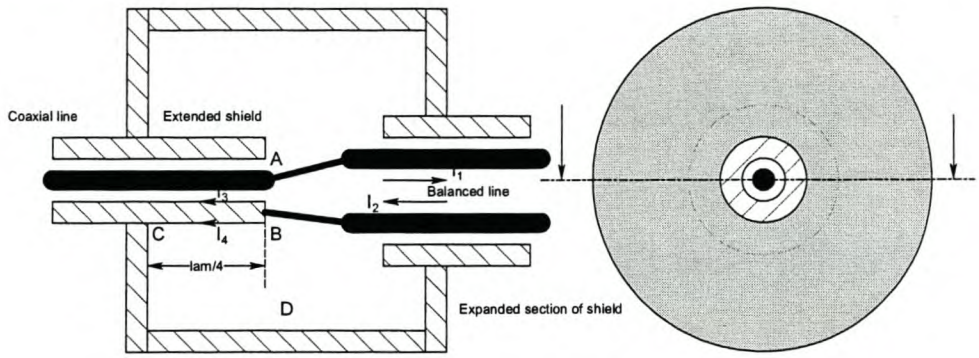

Figure 5-8 Cross section of a single frequency transformer

Figure 5-9 is the distributed element equivalent of Figure 5-8.

where

$$L = jZ_o' \tan\theta \tag{5.3}$$

and Z_o is the characteristic impedance of the coaxial line and Z_o' is the characteristic impedance of the box with respect to outer conductor.

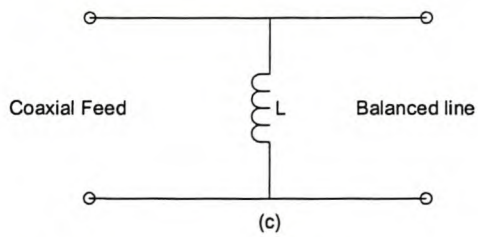

Figure 5-9 Distributed element equivalent circuit of Figure 5-8

Figure 5-10 shows the next stage of the balun development. A solid stub connected to the centre conductor of the coaxial line is added. The stub is the same length and outer radius as the extended shield. This introduces an impedance from A to D (Figure 5-8) equal to the impedance from B to D (Figure 5-8). Change in frequency will now only introduce a phase error with perfectly balanced magnitude. Figure 5-11 is the distributed element equivalent of Figure 5-10. Notice how the stub doubles the inductance.

Stellenbosch University http://scholar.sun.ac.za

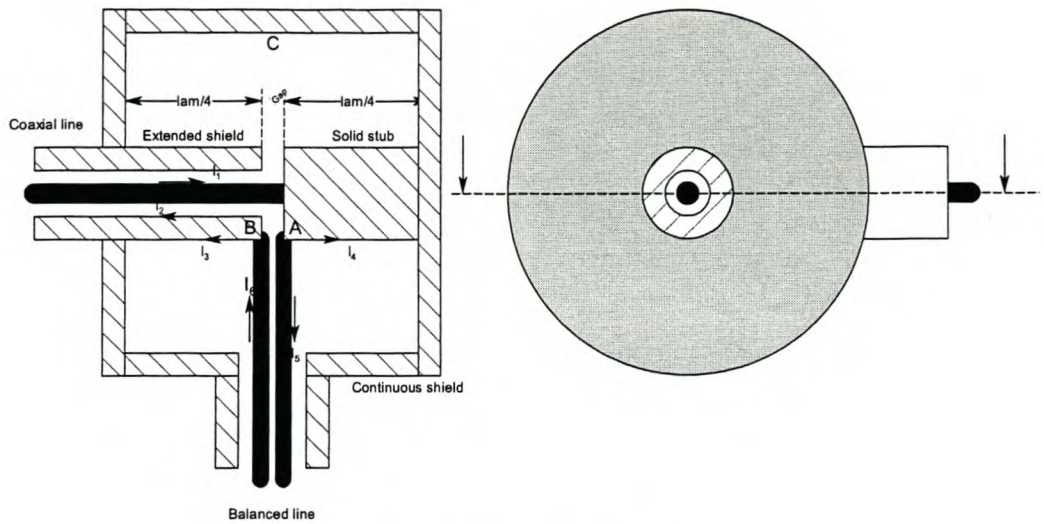

Figure 5-10 Second stage of development

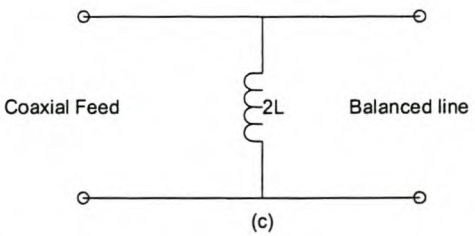

Figure 5-11 Distributed element equivalent circuit of Figure 5-10

To correct the phase error and complete the balun, the solid stub is replaced with an open circuited coaxial stub shown in Figure 5-12.

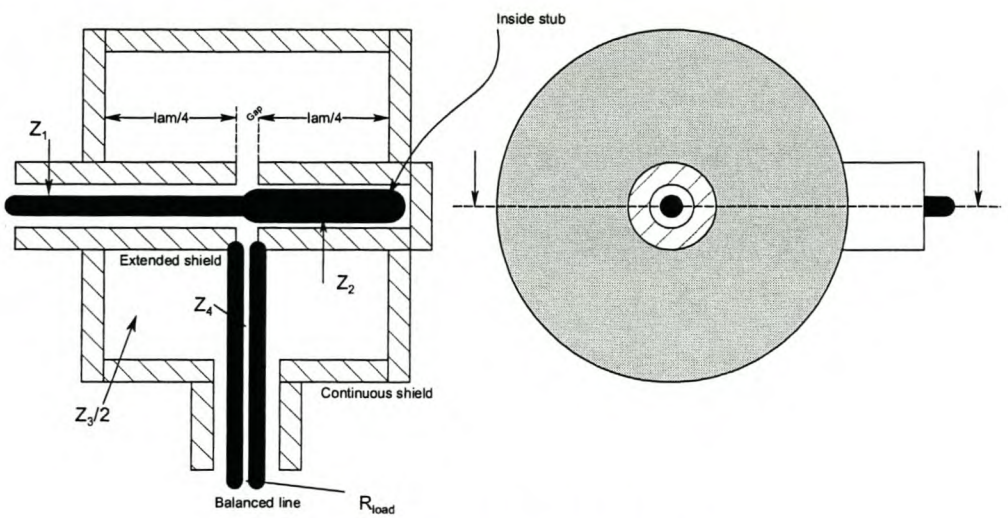

Figure 5-12 Coaxial Marchand Balun

Stellenbosch University http://scholar.sun.ac.za

Figure 5-13 shows the final distributed element equivalent circuit. It is a second order model which gives it high pass filter properties, translated to a band pass filter when realized with quarter wave transformers. The Marchand balun is also implemented for higher orders. A detailed description of the coaxial Marchand is given in [10]

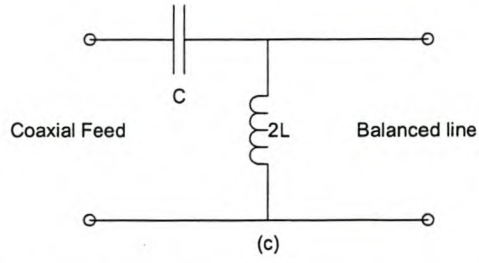

Figure 5-13 Distributed element equivalent circuit of Figure 5-12

The element values are given by

$$L = jZ_{o'} \tan\theta \tag{5.4}$$

and

$$C = jZ_{oe} \cot\theta \tag{5.5}$$

where Z_o is the characteristic impedance of the coaxial line, $Z_{o'}$ is the characteristic impedance of the box with respect to outer conductor and Z_{oe} is the characteristic impedance of the stub with respect to the shield around it.

5.3.2 Principle of Operation and Design of the Planar Marchand Balun

The planar Marchand balun can be implemented in any of the planar technologies. This design implements the balun with micro strip coupled lines. A comparison between the coaxial version and the planar version's model is made as starting point to show that they are equivalent.

Figure 5-14 shows a section of coupled micro strip line, its equivalent circuit and two network properties. The characteristic impedance and coupling coefficient of the coupled line is given by

$$\begin{aligned} Z_{oc} &= \sqrt{Z_{oe}Z_{oo}} \\ k &= \frac{Z_{oe} - Z_{oo}}{Z_{oe} + Z_{oo}} \end{aligned} \tag{5.6}$$

Stellenbosch University http://scholar.sun.ac.za

and are related to the network equivalent circuit elements by

$$Z_1 = \frac{Z_{oc}}{\sqrt{1-k^2}}$$
$$Z_2 = Z_{oc}\frac{\sqrt{1-k^2}}{k^2} \qquad (5.7)$$
$$n = \frac{1}{k}$$

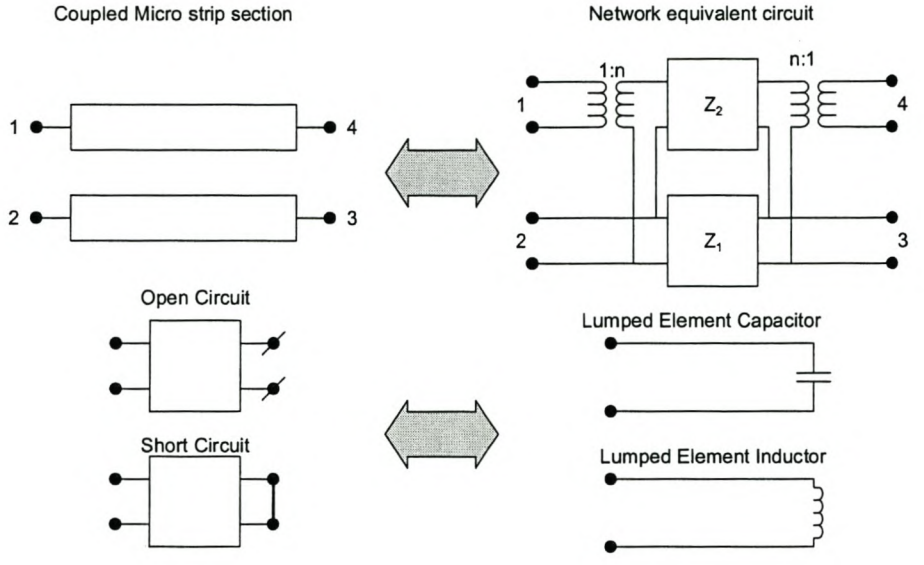

Figure 5-14 Basic Network Forms [11]

With this information the distributed element equivalent circuit of the planar Marchand, shown in Figure 5-15 is derived graphically in Figure 5-16.

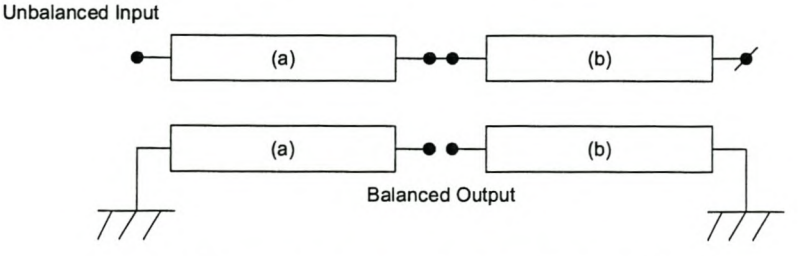

Figure 5-15 Coupled line model of planar Marchand Balun

Stellenbosch University http://scholar.sun.ac.za

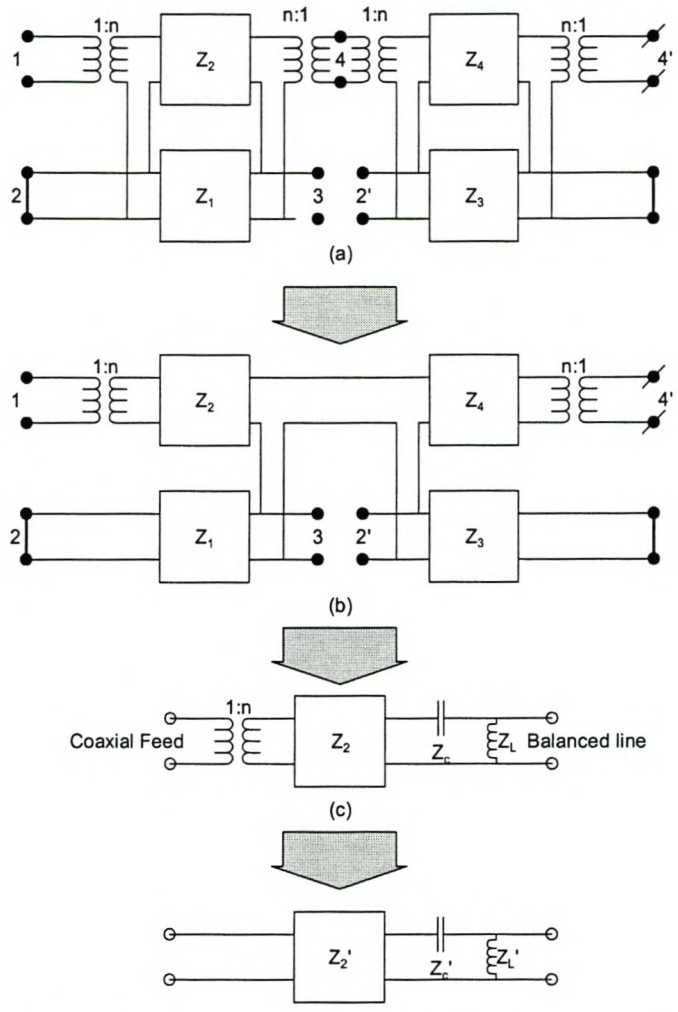

Figure 5-16 Derivation of network model of planar Marchand Balun

This model is essentially the same as the model for the coaxial Marchand. The element values defined in Figure 5-16 are specified by the following equations.

$$Z_2' = \frac{Z_2}{n^2} \tag{5.8}$$

$$Z_L' = \frac{Z_1 + Z_3}{n^2} \tag{5.9}$$

$$Z_C' = \frac{Z_4}{n^2} \tag{5.10}$$

Stellenbosch University http://scholar.sun.ac.za

The network model in Figure 5-16 explains only the impedance frequency response of the balun. By adding an antenna to the balun the symmetry can be explained. Figure 5-17 shows the system's network model. Coupling from the arms to the balun and feed line, represented by Z_a' and Z_b', is almost equal when looking at the coupled line model in Figure 5-15 and especially in the coaxial Marchand shown in Figure 5-12. The coaxial version's internal structure can be modeled as a perfect point source, with a symmetrical external shield. This will bring perfect balance to the system. For the planar version, the internal and external parts are not shielded from each other and can thus only be approximated by a point source with a symmetrical outer. The planar version's balance is not expected to be perfect because of this approximation.

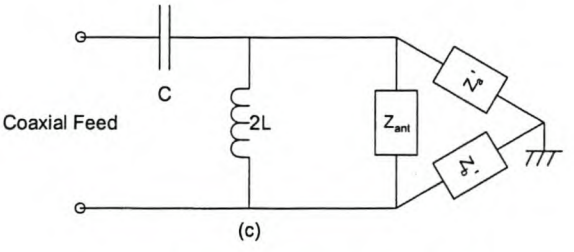

Figure 5-17 Network model of system

Design: Marchand Balun

The capacitance, inductance and unit element values (Figure 5-17) can be calculated to fit a Chebyshev, Butterworth or any other filter response, using the technique explained in [12]. The synthesis of the balun is summarized by the following bullets.

- L, C and the unit element are obtained using filter design techniques. [12]
- The coupled line parameters are determined by the following equations.

$$k = \sqrt{\frac{Z_L'}{Z_2' + Z_C' + Z_L'}}$$
$$Z_{ac} = \frac{Z_2'}{\sqrt{1-k^2}} \qquad (5.11)$$
$$Z_{ac} = \frac{Z_C'}{\sqrt{1-k^2}}$$
$$R' = Rk^2$$

where R is the load impedance and

Stellenbosch University http://scholar.sun.ac.za

$$Z_{ac}^{\ 2} = Z_{oe}^{\ a} Z_{oo}^{\ a}$$
$$Z_{bc}^{\ 2} = Z_{oe}^{\ b} Z_{oo}^{\ b} \qquad (5.12)$$

- Coupled line dimensions are determined using curves or CAD tools. To obtain the tight coupling required, a second set of coupled lines are added on the opposite side. These extra coupled lines are connected to the initial coupled line with air bridges.

Figure 5-18 shows the dimensions of the designed balun. The substrate has an ε_r = 10.2 and a thickness of 0.635 mm.

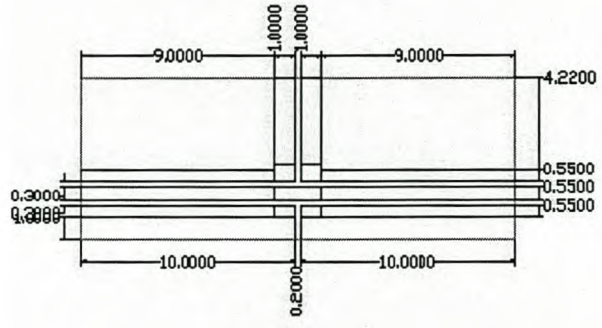

Figure 5-18 Dimensions of designed and manufactured Marchand Balun

5.4 Double Y Balun [13, 14 & 15]

The double Y balun is based on the double Y junction, which is a complex transition from an unbalanced to balanced transmission line. This balun has only been realized in a planar environment. Any of the planer topologies can be used. For this project the coplanar waveguide-finite-ground-plane to coplanar strip-line topology is investigated.

5.4.1 Principle of Operation: Double Y Balun

To obtain a network model, we trace the currents. Figure 5-19 shows the double Y junction with the equivalent model for it. The influence of the junction itself is neglected in the network model.

Stellenbosch University http://scholar.sun.ac.za

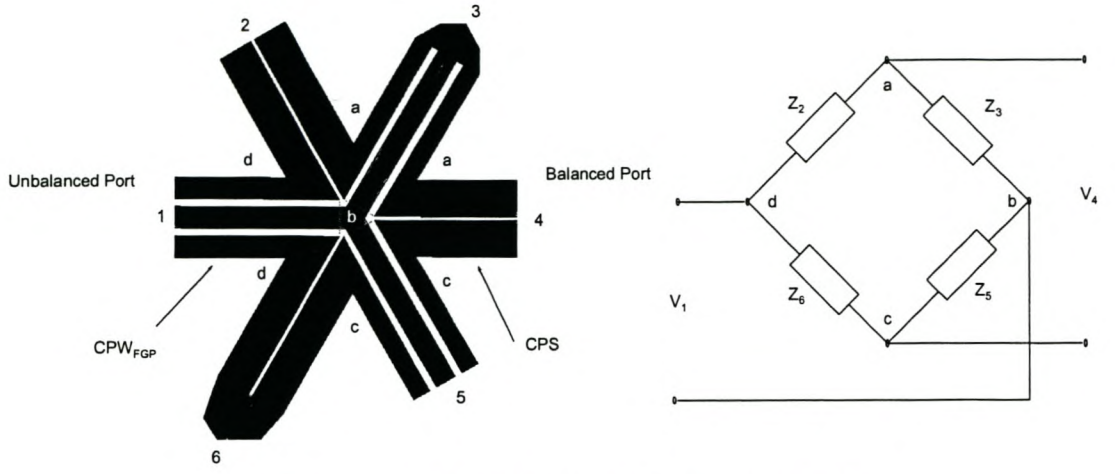

Figure 5-19 Diagram of Double Y junction with equivalent circuit

In making the bridge symmetric, the impedances simplify to $Z_2 = Z_5 = Z_a$ and $Z_3 = Z_6 = Z_b$. The impedance matrix of the equivalent circuit is defined as

$$Z = \begin{bmatrix} Z_A & Z_B \\ Z_B & Z_A \end{bmatrix} \tag{5.13}$$

where

$$\begin{aligned} Z_A &= \frac{(Z_a + Z_b)}{2} \\ Z_B &= \frac{(Z_b - Z_a)}{2} \end{aligned} \tag{5.14}$$

If the load impedance is real, the input impedance is expressed by

$$\begin{aligned} R_{in} &= Z_o \frac{\left[\frac{1}{2}(X_a + X_b)\right]^2}{\left[\frac{1}{2}(X_a + X_b)\right]^2 + (Z_o^2 - X_a X_b)} \\ Z_{in} &= \frac{1}{2Z_o}(X_a - X_b)(Z_o - R_{in}) \end{aligned} \tag{5.15}$$

Thus, if Z_a and Z_b fulfill the following condition (5.16), the input impedance is real and frequency independent.

$$X_a X_b = Z_o^2 \tag{5.16}$$

Stellenbosch University http://scholar.sun.ac.za

This condition is fulfilled because the bridge has short and open circuits with the same lengths alternately, producing an all pass network. This explains the impedance behavior of the balun, but says nothing about the balance. Analyzing the equivalent circuit, we find no series impedance in the common mode current path. Looking at the physical structure, there is some symmetry placing the double y balun in the symmetric balun family.

Design: Double Y Balun

The design for the balun is trivial compared to laying it out for construction. The two types of transmission line dimensions are the only parameters to be designed and can be done with design curves or CAD packages. Air bridges should be added at the transition, connecting the grounds of the CPW_{FGP}. Table 5-2 presents the parameters for the transmission lines and substrate obtained for this design. Since the structure is frequency independent, the transmission line lengths can be made any convenient length.

Substrate		CPS[mm]			CPW_{FGP} [mm]			
ε_r	h [mm]	W	G	L	W_O	G	W_C	L
9.8	0.635	0.2	0.02	1	0.1	0.04	0.12	0.996
		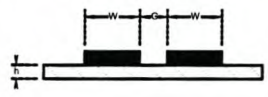			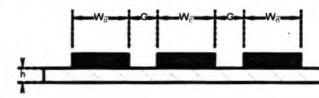			

Table 5-2 Transmission line dimensions for CPS - CPW_{FGP} Double Y Balun

5.5 Tapered-line/Split Coaxial Balun [16 & 17]

The tapered line balun is the planar version of the split coaxial balun. Basically, it is two planar transmission lines of different impedance connected together with an impedance taper. The two planar transmission lines are of different topology, with the one an unbalanced topology and the other balanced. Figure 5-20 shows a photograph of the balun.

Stellenbosch University http://scholar.sun.ac.za

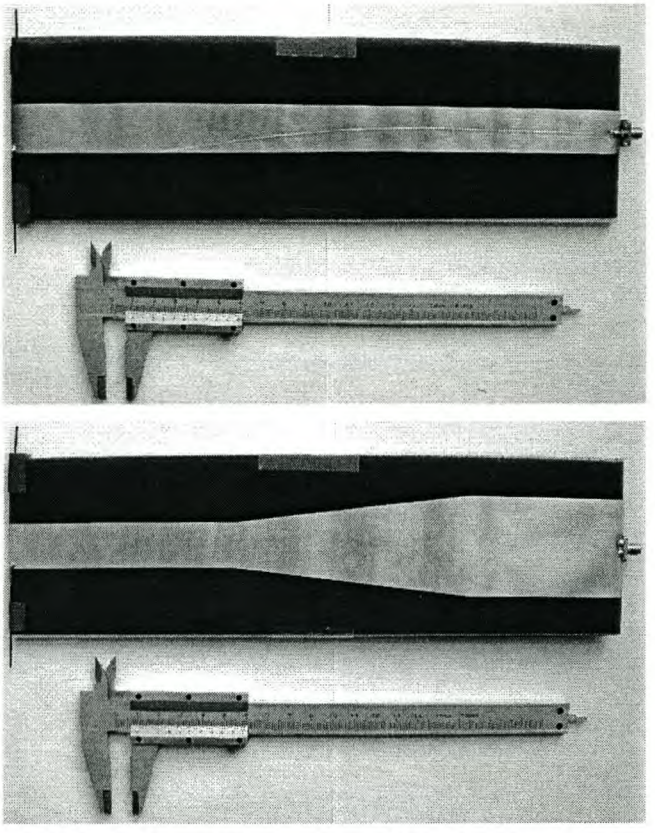

Figure 5-20 Photograph manufactured balun terminated with a Dipole (Top and bottom view).

5.5.1 Principle of Operation: Tapered-line

Looking at the impedance aspect there are a number of techniques available for designing impedance tapers, with a few popular ones discussed in [18], and [16] reporting a 100:1 bandwidth balun using a Chebyshev taper. Impedance matching is thus not a problem with the availability of literature. The balun principle is not as trivial though. The balun is part of the symmetrical balun family, if indeed it is a balun at all. For the balun to be a symmetric balun coupling between the two antenna arms and the balun/feed line should be equal. This is not true if the physical structure shown in Figure 5-22 is inspected. The orientation of the antenna also plays an important role in the symmetry of the system, although no orientation can give reasonable symmetry. From a common mode choke perspective; [16] claims that the taper angle is directly proportional to the common mode choking impedance. The reasoning behind this theory is that the taper will force the currents to stay on the top of the microstrip ground plane and not flow on the bottom. Intuitively this does not make sense because there is nothing to prevent the electromagnetic fields from curling around to the bottom of the ground plane, creating currents. This was investigated in the computations with little success

Stellenbosch University http://scholar.sun.ac.za

in the improvement of the common mode choking impedance. Figure 5-21 shows a simplified network model for the balun. The impedance transformer represents the impedance transforming properties of the taper and Z_a' and Z_b' is the new coupling impedance from the antenna arm to the feed line/balun. Intuitively this balun should give worst results than a normally fed antenna system because of the highly asymmetrical structure with very little common mode current choking.

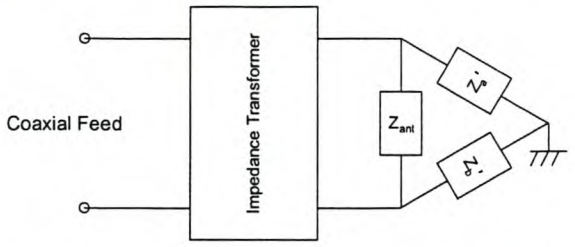

Figure 5-21 Network Model of Tapered-line Balun

Design: Tapered-line

The design of this balun is in the design of the taper. As mentioned earlier, [18] has detailed descriptions of the design of popular tapers. The antenna should be terminated horizontally as shown in Figure 5-20. Figure 5-22 shows the dimensions of the designed balun. A piece of foam($\varepsilon_r \approx 1$), 0.45 mm thick, is used as substrate.

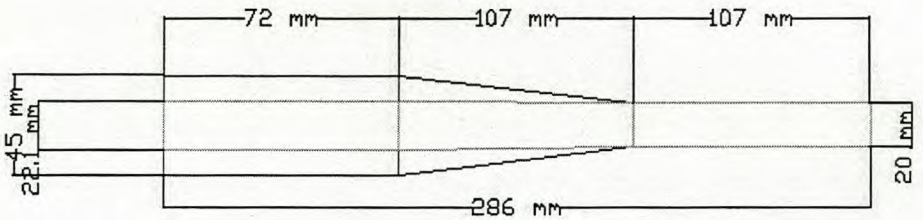

Figure 5-22 Dimensions of designed Tapered line balun

5.6 "Log-periodic" Balun [19]

This balun is not studied in the same detail as the previous baluns. A few remarks on the operation and performance will only be made. The Log–Periodic balun is a anti-phase balun, which falls in the class of popular baluns using combiners and dividers. Other baluns that falls into this class are the 180 degree hybrid and Magic T baluns. A schematic diagram of the balun is shown in Figure 5-23.

Stellenbosch University http://scholar.sun.ac.za

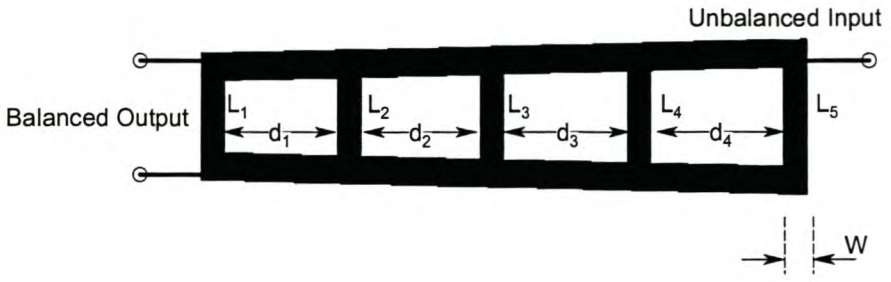

Figure 5-23 Schematic diagram of the "Log-periodic" Balun

5.6.1 Principle of Operation: "Log-periodic" Balun

This balun is not much more than a power divider designed for a wide bandwidth with a physically symmetrical structure. The "Log-periodic" structure is inherited from the "Log-periodic" antenna explained in [20]. In essence these baluns operate by splitting, the input signal into two, where the two paths have a difference of 180 degrees. The different length of periodic sections gives the 180 degree path difference at different frequencies.

Design: "Log-periodic" Balun

The design is once again simple compared to the circuit board layout with only a few basic equations to determine the length, width and separation of the periodic elements. The design procedure is summarized in [19]

5.7 Coplanar-Slot balun [21]

This balun is also not studied in detail. A few remarks on the operation and performance will only be made.

5.7.1 Principle of Operation: Coplanar-Slot balun

The balun is a basic transition from coplanar waveguide to coplanar stripline. The balance in the system is forced by the addition of a radial slot, which acts as a wide band open circuit. The radial slot forces the electric field to be mainly between the balanced arms of the CPS. Air bridges on the transition plane ensure that the potential on the two ground planes are the same.

Stellenbosch University http://scholar.sun.ac.za

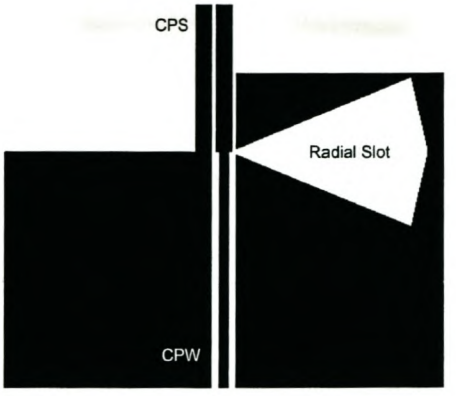

Figure 5-24 Schematic diagram of the Coplanar-Slot Balun

Design: Coplanar-Slot balun

The design of the balun is straight forward once a substrate is found on which CPW and CPS lines of the same impedance can be realized. Transmission line parameters can easily be obtained using curves, equations [21] or CAD software. An impedance transformer can be added to the system on the unbalanced side if desired.

Substrate		CPS[mm]			CPW_{FGP} [mm]		
ε_r	h [mm]	W	G	L	W	G	L
1	2.5	1.8	0.46	37.5	0.92	0.9	37.5
		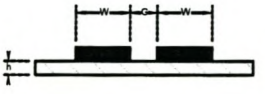			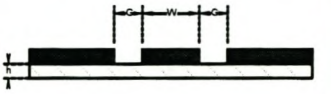		

Table 5-3 Dimensions of the Slot-line balun

Stellenbosch University http://scholar.sun.ac.za

Chapter 6. Computational Results

The results are divided into three sections: currents, impedances and antenna influence on balun performance. The first section presents the following results.

- Comparison of the two antenna arm currents. (magnitude & phase)
- The balun ratio for the balun terminated with an infinite dipole.

The second section is titled Impedance, and displays the following results:

- Feed impedance response of the balun terminated with the infinite dipole.
- The differential and common mode impedance computed from currents on the infinite dipole arms at the feed point.

The third section presents the balun ratios for the balun terminated with all three test antennas to see the effect finite antennas have on the balun's performance.

For the four baluns that were manufactured, there is a fourth section which deals with the validation of the computational model. A comparison between the computed and measured feed impedance or $|S_{11}|$ is presented.

6.1 The Sleeve or "Bazooka" Balun

6.1.1 Balun Construction: "Bazooka" Balun

Figure 6-1 shows the computational model used in FEKO, while Figure 6-2 shows the detailed view of the feeding section.

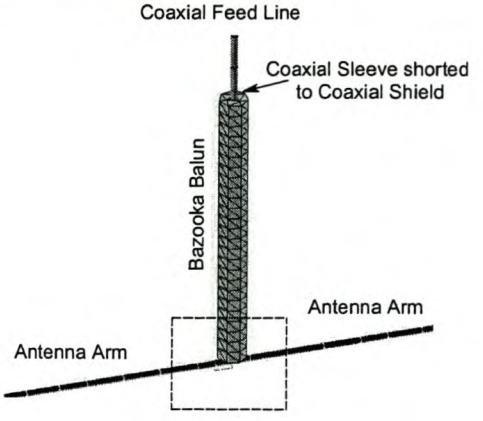

Figure 6-1 Computational model

Stellenbosch University http://scholar.sun.ac.za

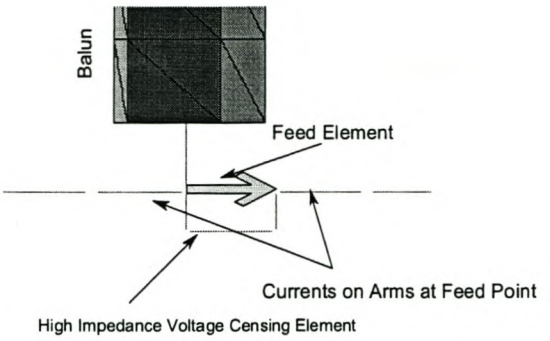

Figure 6-2 Detailed view of the feed section for Figure 6-1

6.1.2 Currents: "Bazooka" Balun

Figure 6-3 presents the arm currents calculated at the feed point and balun ratio for the bazooka balun terminated with the infinite dipole. Notice that the currents are only balanced around the centre frequency. This explains the peak in the balun ratio response at that frequency. The balun ratio bandwidth is 11 % around the centre frequency.

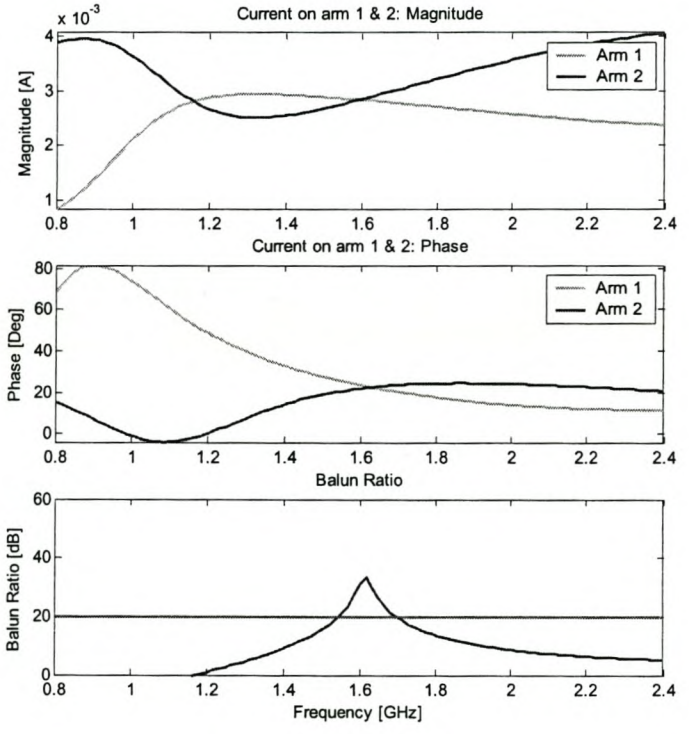

Figure 6-3 Currents on Infinite Dipole Arms (Magnitude & Phase) and Balun Ratio for Infinite Dipole

Stellenbosch University http://scholar.sun.ac.za

6.1.3 Impedance: "Bazooka" Balun

Figure 6-4 presents the feed impedance and differential and common mode impedance calculated from currents (At feed point) on infinite dipole arms. The balun has little effect on the feed impedance as expected from the theory. The effect of the quarter wave line can be seen in the common mode impedance.

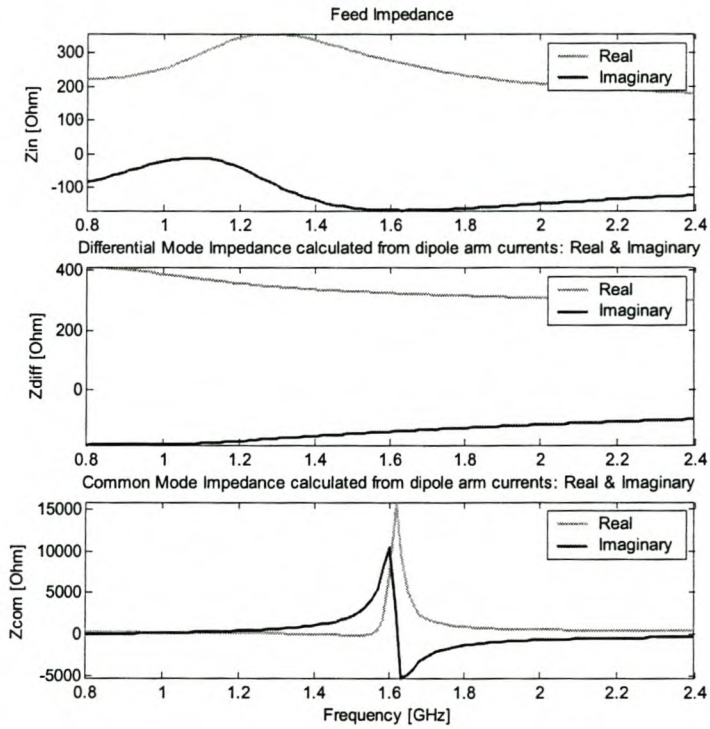

Figure 6-4 Feed Impedance and Differential and Common Mode Impedance Calculated from Currents on Infinite Dipole Arms (At Feed Point)

6.1.4 Antenna Type Influence on Balun Performance: "Bazooka" Balun

Figure 6-5 presents the Balun Ratios for the Three test antennas to show how the different antennas influence the balun performance. Refer to *Appendix B* for the currents and impedance results of the dipole and bow-tie antennas terminated with the various baluns.

Stellenbosch University http://scholar.sun.ac.za

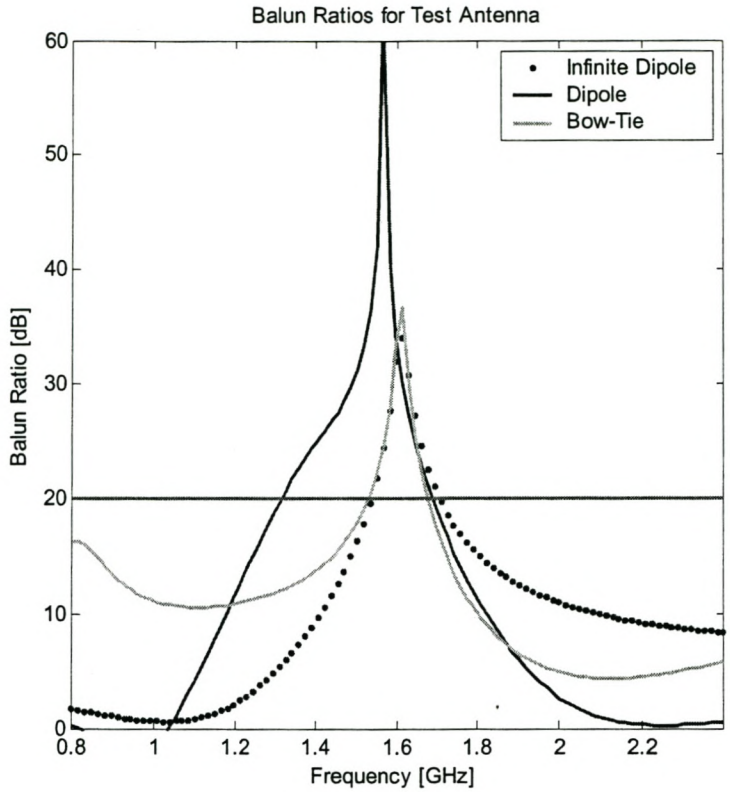

Figure 6-5 Balun Ratios for the Three test antennas

6.1.5 Validation of Model: "Bazooka" Balun

Figure 6-6 presents the measured and computed $|S_{11}|$ for the balun terminated with the half wave dipole antenna. The measurement is done on a HP 8753 network analyzer with a standard one port calibration.

Stellenbosch University http://scholar.sun.ac.za

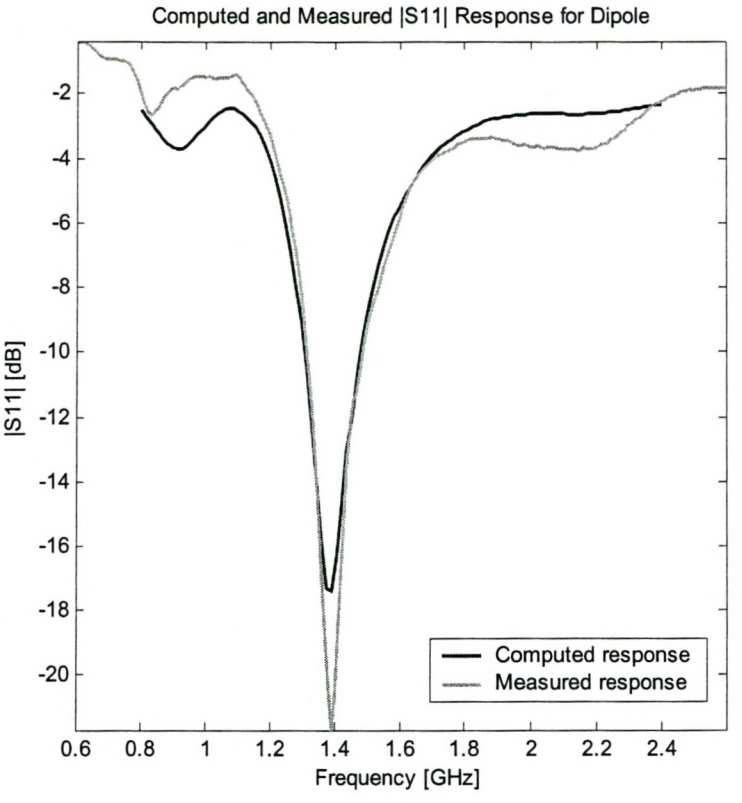

Figure 6-6 Measured and Computed $|S_{11}|$

6.2 Quarter wave Balun

6.2.1 Balun Construction: Quarter wave Balun

Figure 6-7 shows the computational model used in FEKO, while Figure 6-8 shows the detailed view of the feeding section.

Stellenbosch University http://scholar.sun.ac.za

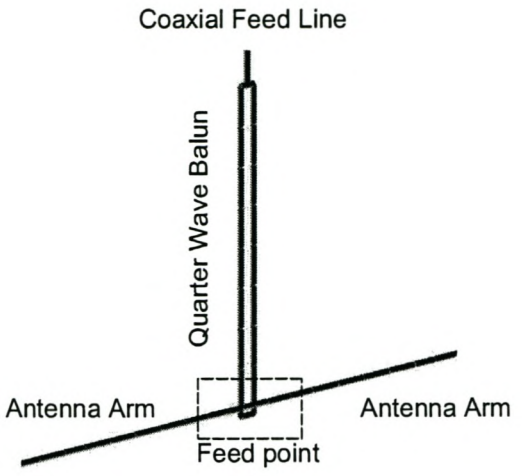

Figure 6-7 Computational model

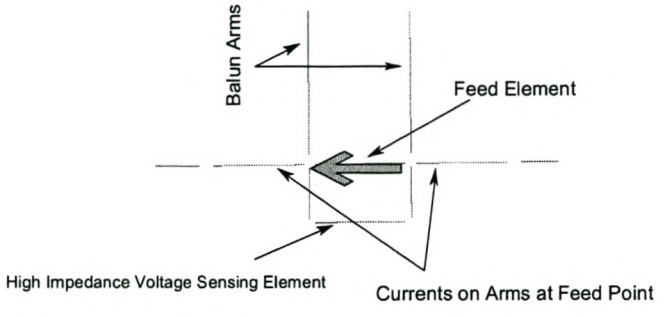

Figure 6-8 Detailed view of the feed section for Figure 6-7

6.2.2 Currents: Quarter wave Balun

Figure 6-9 presents the arm currents calculated at the feed point and balun ratio for the quarter wave balun terminated with the infinite dipole. The currents on the two arms are perfectly balanced and coincide on the figure. The balun ratio is infinite over the whole band because of the balanced currents.

Stellenbosch University http://scholar.sun.ac.za

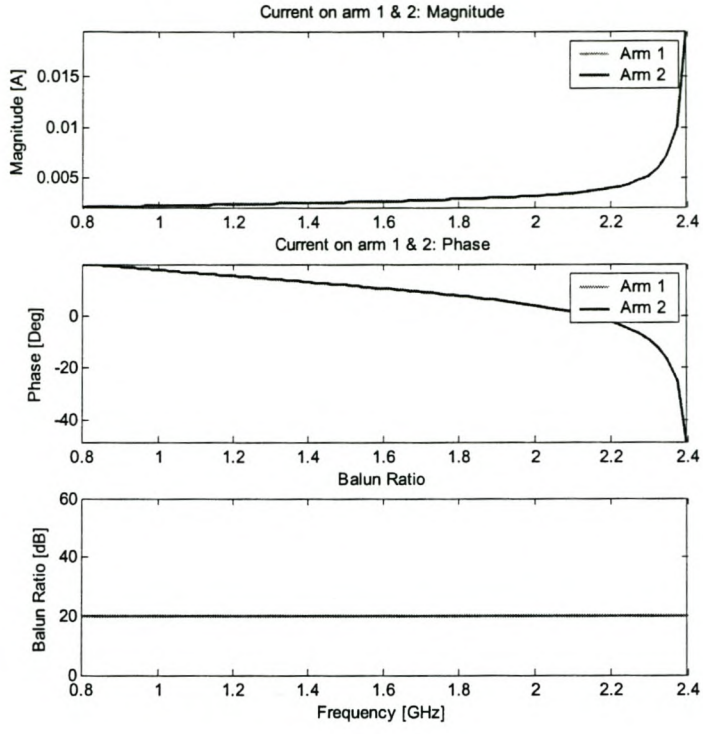

Figure 6-9 Currents on Infinite Dipole Arms (Magnitude & Phase) and Balun Ratio for Infinite Dipole.

6.2.3 Impedance: Quarter wave Balun

Figure 6-10 presents the feed, differential and common mode impedance calculated from currents on infinite dipole arms. Notice the effect of the parallel combination of the quarter wave loop and the antenna input impedance on the feed impedance. The common mode impedance is infinite over the band as expected.

Stellenbosch University http://scholar.sun.ac.za

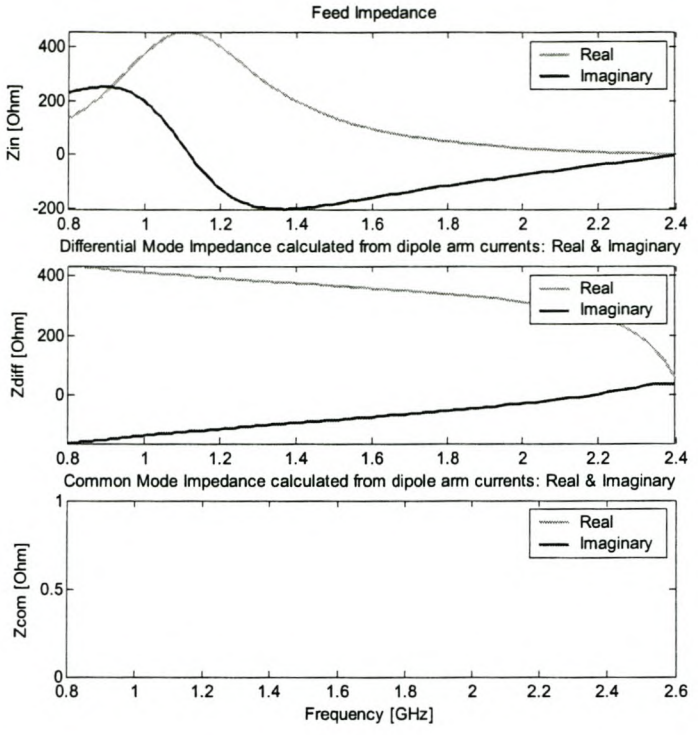

Figure 6-10 Feed Impedance and Differential and Common Mode Impedance Calculated from Currents on Infinite Dipole Arms (At Feed Point)

6.2.4 Antenna Type Influence on Balun Performance: Quarter wave Balun

Figure 6-11 presents the Balun Ratios for the three test antennas to show how the different antennas influence the balun performance. Refer to *Appendix B* for the current and impedance results of the dipole and bow-tie antennas terminated with the various baluns. The balun ratios obtained with the infinite dipole and the dipole is infinite over the band.

Stellenbosch University http://scholar.sun.ac.za

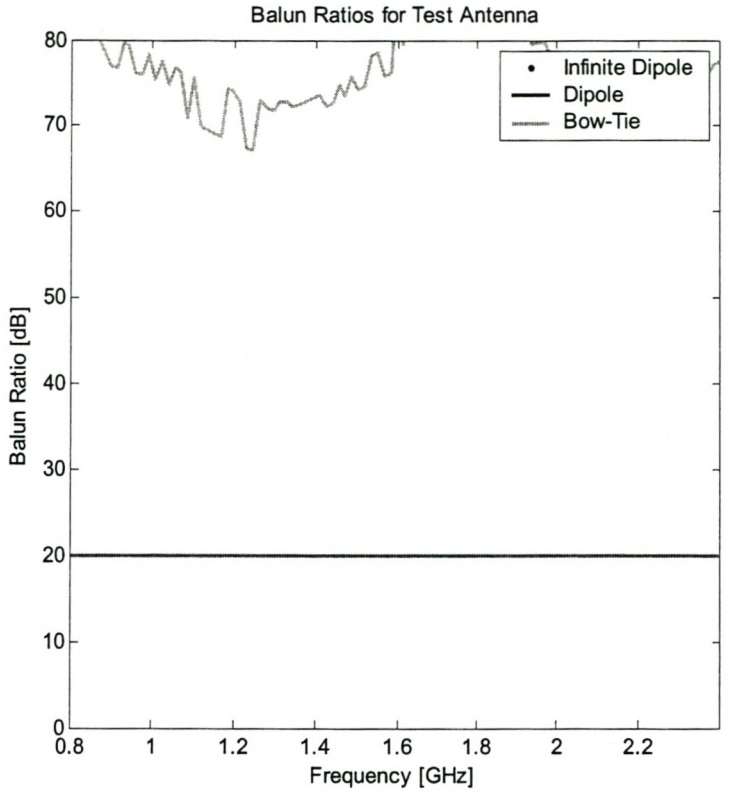

Figure 6-11 Balun Ratios for the Three test antennas

6.2.5 Validation of Model: Quarter wave Balun

Figure 6-12 presents the measured and computed $|S_{11}|$ for this balun terminated with a half wave dipole antenna. The measurement is done on a HP 8753 network analyzer with a standard one port calibration. The extra resonance in the measured data (1.4GHz) could not be explained.

Stellenbosch University http://scholar.sun.ac.za

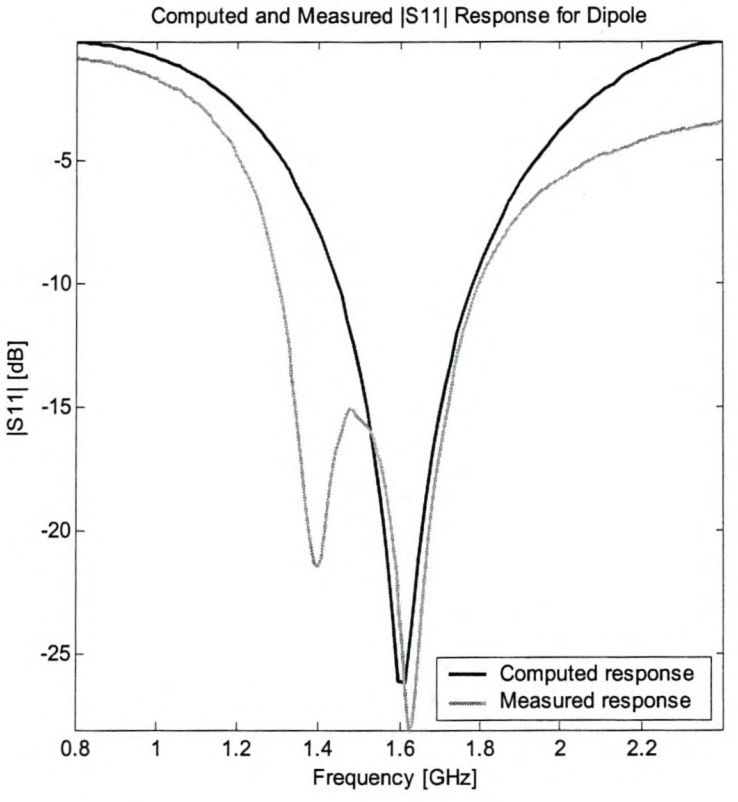

Figure 6-12 Measured and Computed $|S_{11}|$

6.3 Marchand Balun

6.3.1 Balun Construction: Marchand Balun

Figure 6-13 shows the computational model used in FEKO, while Figure 6-14 shows the detailed view of the feeding section. The following computations were done with an ideal configuration to show the wide band properties of the Marchand balun. The SMA connector model, shown in Figure 6-13, was removed from the computational model. In the *validation of model* section, the SMA was added again to be able to make a good comparison with the measured results.

Stellenbosch University http://scholar.sun.ac.za

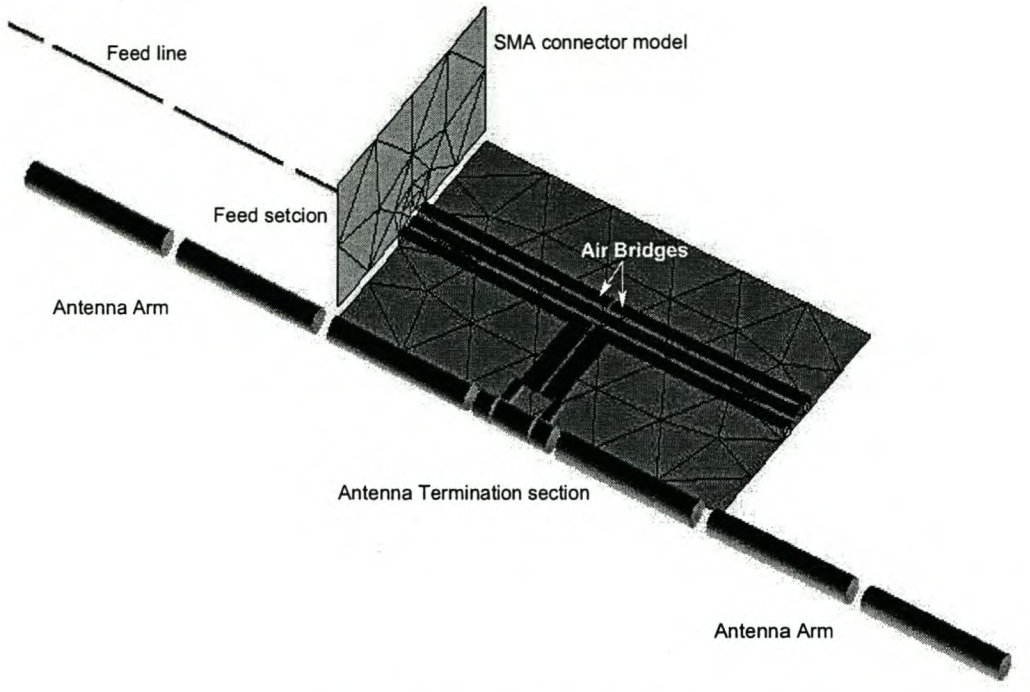

Figure 6-13 Computational model

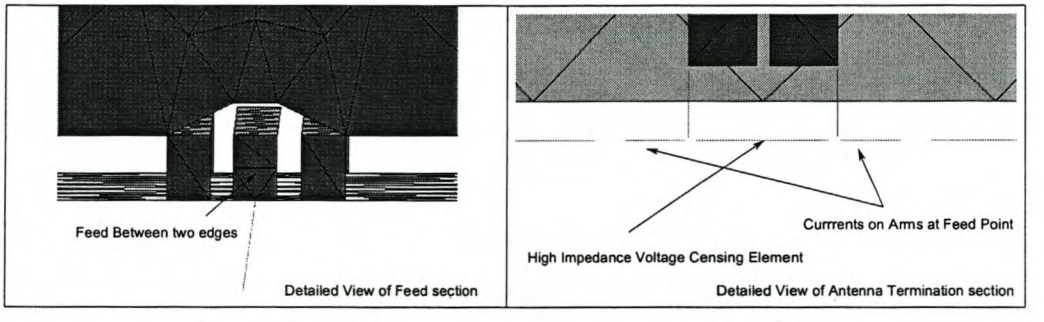

Figure 6-14 Detailed view of the feed section for Figure 6-13

6.3.2 Currents: Marchand Balun

Figure 6-15 presents the arm currents calculated at the feed point and balun ratio for the Marchand balun terminated with the infinite dipole. The results show good balance over the band.

Stellenbosch University http://scholar.sun.ac.za

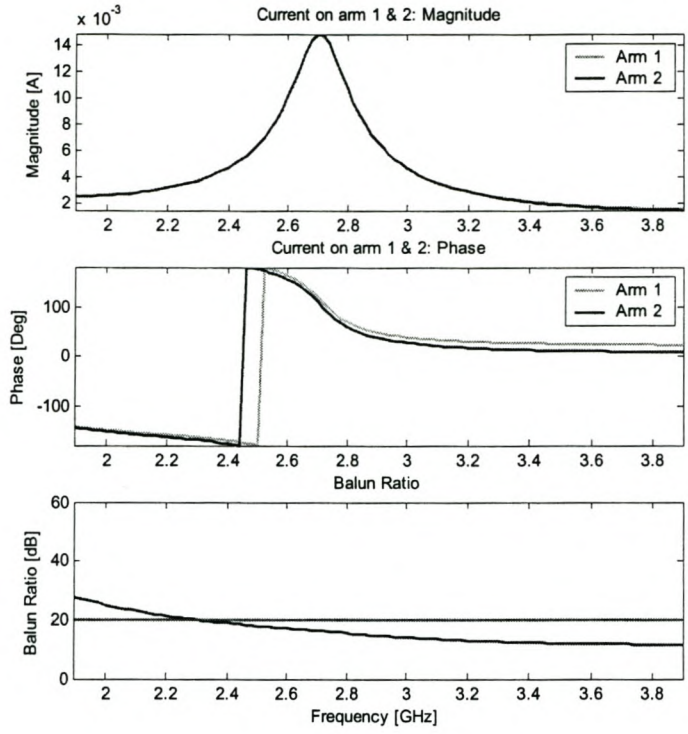

Figure 6-15 Currents on Infinite Dipole Arms (Magnitude & Phase) and Balun Ratio for Infinite Dipole

6.3.3 Impedance: Marchand Balun

Figure 6-16 presents the feed, differential and common mode impedance calculated from currents on infinite dipole arms. The feed impedance of the system is flat over the whole band as expected for a well designed Marchand balun. The impedance transforming property of the balun is also visible from the feed impedance.

Stellenbosch University http://scholar.sun.ac.za

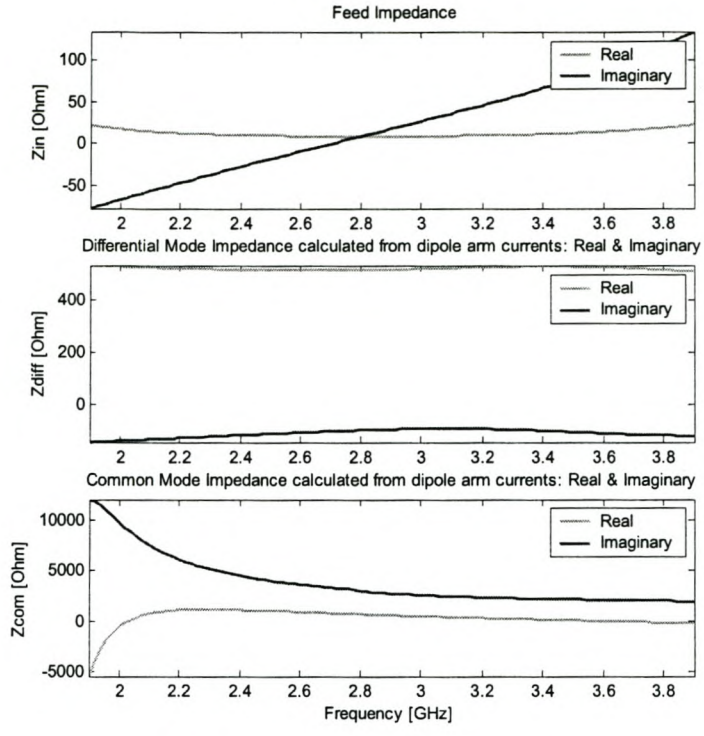

Figure 6-16 Feed Impedance and Differential and Common Mode Impedance Calculated from Currents on Infinite Dipole Arms (At Feed Point)

6.3.4 Antenna Type Influence on Balun Performance: Marchand Balun

Figure 6-17 presents the Balun Ratios for the Three test antennas to show how the different antennas influence the balun performance. Refer to *Appendix B* for the currents and impedance results of the dipole and bow-tie antennas terminated with the various baluns.

Stellenbosch University http://scholar.sun.ac.za

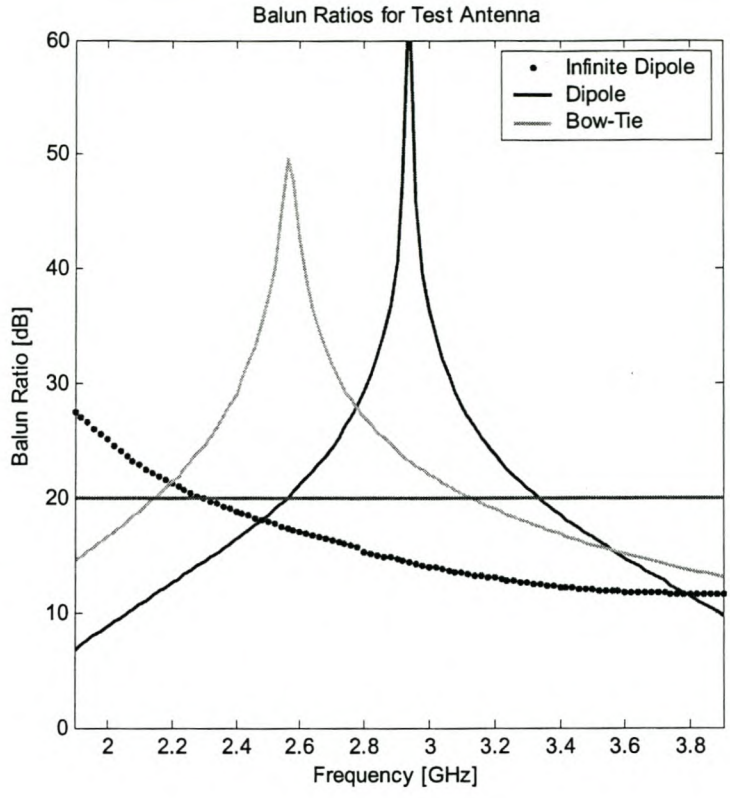

Figure 6-17 Balun Ratios for the Three test antennas

6.3.5 Validation of Model: Marchand Balun

Figure 6-18 presents the measured and computed input impedance for the balun terminated with the half wave dipole antenna. The measurement is done on a HP 8753 network analyzer with a standard one port calibration.

The following results are obtained with the SMA connector added to the computational model, as shown in Figure 6-13. Values obtained by the computation do not hold any importance. What is important is to notice that the computation and the measurement do agree. A hypothesis can be made that the other results such as; differential and common mode impedances and balun ratios obtained by computation, are correct.

Stellenbosch University http://scholar.sun.ac.za

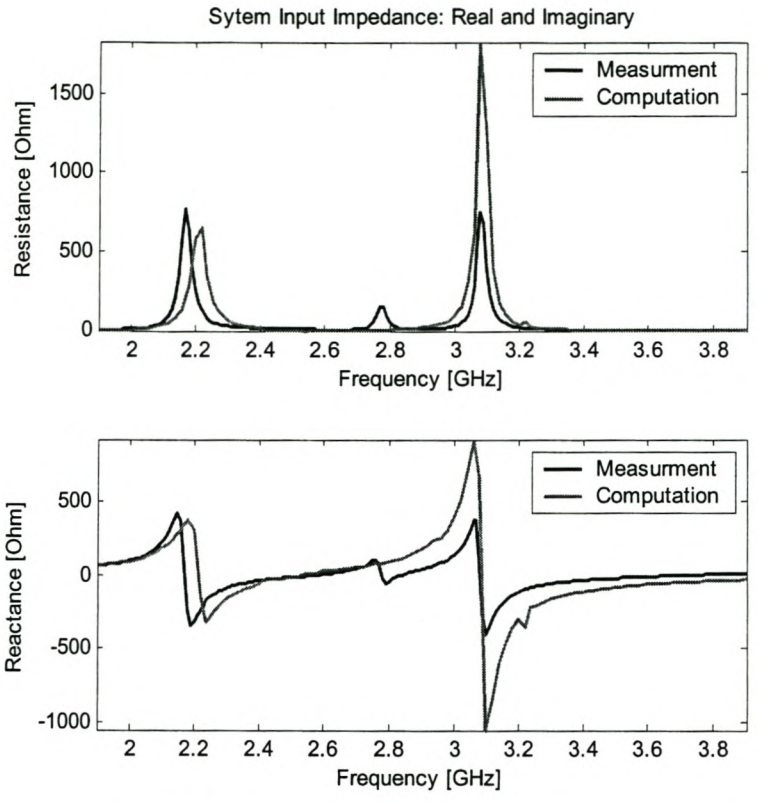

Figure 6-18 Measured and Computed System Input Impedance

6.4 Double Y Balun [13, 14 & 15]

6.4.1 Balun Construction: Double Y Balun

Figure 6-19 shows the computational model used in FEKO, while Figure 6-20 shows the detailed view of the feeding section.

Stellenbosch University http://scholar.sun.ac.za

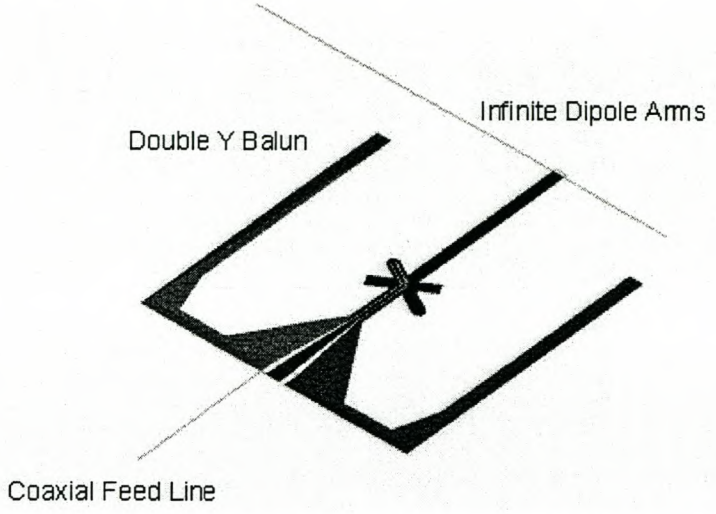

Figure 6-19 Computational model (Detailed view of antenna termination section is the same as for the Marchand Balun)

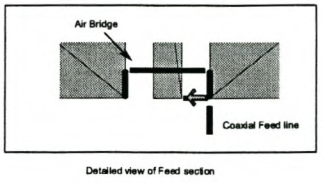

Figure 6-20 Detailed view of the feed section of Figure 6-19

6.4.2 Currents: Double Y Balun

Figure 6-21 presents the arm currents calculated at the feed point and balun ratio for the double Y balun terminated with the infinite dipole. The results show very poor balance over the band.

Stellenbosch University http://scholar.sun.ac.za

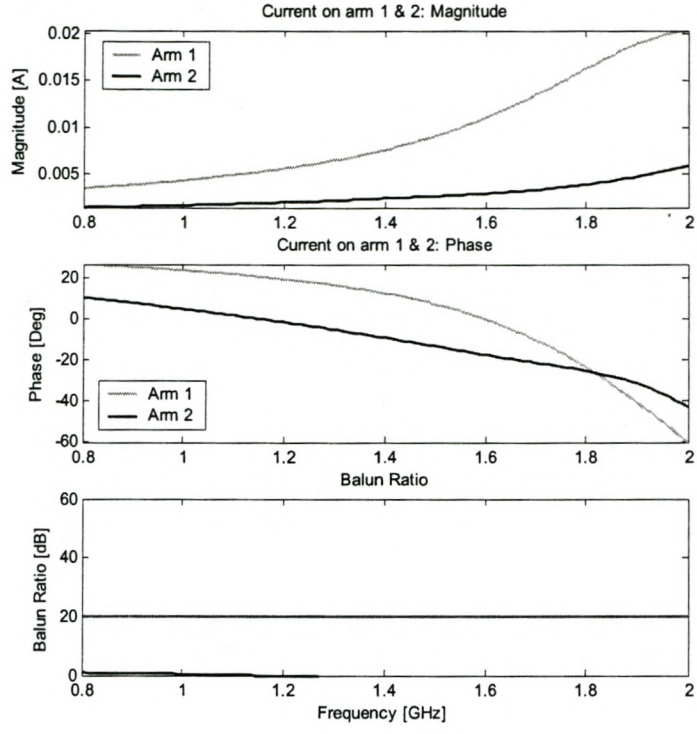

Figure 6-21 Currents on Infinite Dipole Arms (Magnitude & Phase) and Balun Ratio for Infinite Dipole

6.4.3 Impedance: Double Y Balun

Figure 6-22 presents the feed, differential and common mode impedance calculated from currents on infinite dipole arms. The feed impedance of the system is flat over the whole band as expected.

Stellenbosch University http://scholar.sun.ac.za

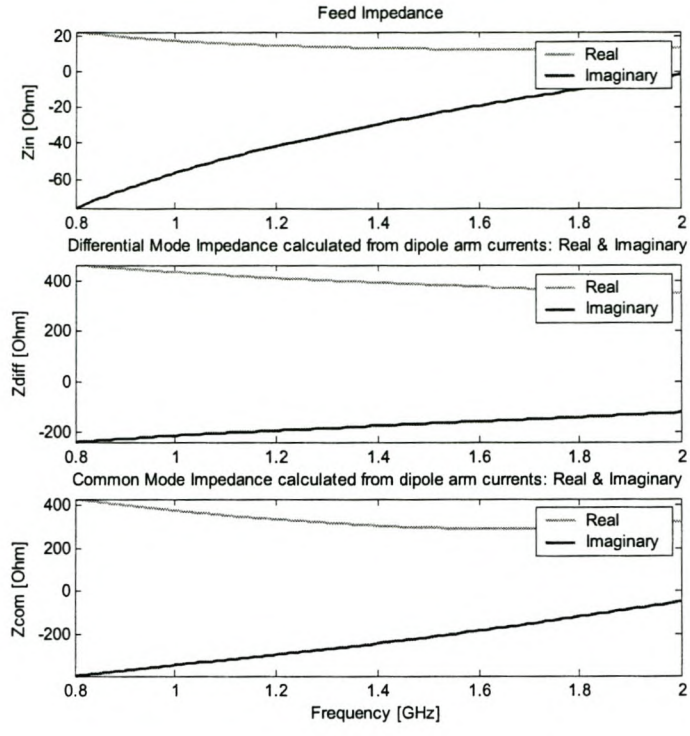

Figure 6-22 Feed Impedance and Differential and Common Mode Impedance Calculated from Currents on Infinite Dipole Arms (At Feed Point)

6.4.4 Antenna Type Influence on Balun Performance: Double Y Balun

Figure 6-23 presents the Balun Ratios for the three test antennas to show how the different antennas influence the balun performance. Refer to *Appendix B* for the currents and impedance results of the dipole and bow-tie antennas terminated with the various baluns.

Stellenbosch University http://scholar.sun.ac.za

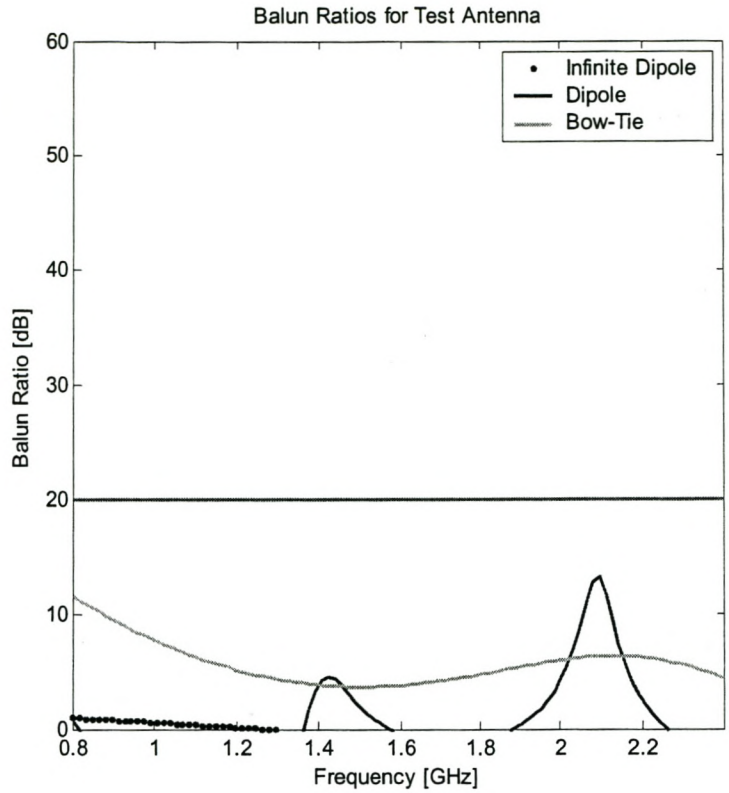

Figure 6-23 Balun Ratios for the Three test antennas

6.5 Tapered-line/Split Coaxial Balun [16 & 17]

6.5.1 Balun Construction: Tapered-line Balun

Figure 6-24 shows the computational model used in FEKO, while Figure 6-25 shows the detailed view of the feeding and antenna terminating section.

Stellenbosch University http://scholar.sun.ac.za

Figure 6-24 Computational model

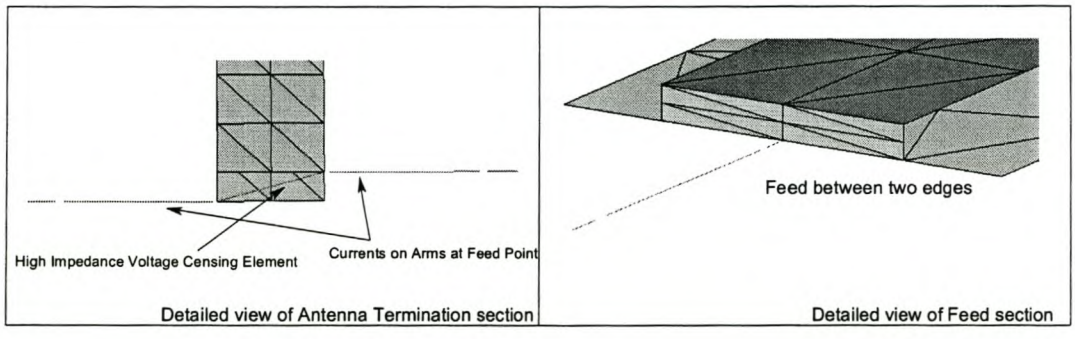

Figure 6-25 Detailed view of the antenna termination and feed section for Figure 6-24

6.5.2 Currents: Tapered-line Balun

Figure 6-26 presents the arm currents calculated at the feed point and balun ratio for the tapered line balun terminated with the infinite dipole. The results show reasonable current balance over the band. The balun ratio is unpredictable and oscillates around 10 dB.

Stellenbosch University http://scholar.sun.ac.za

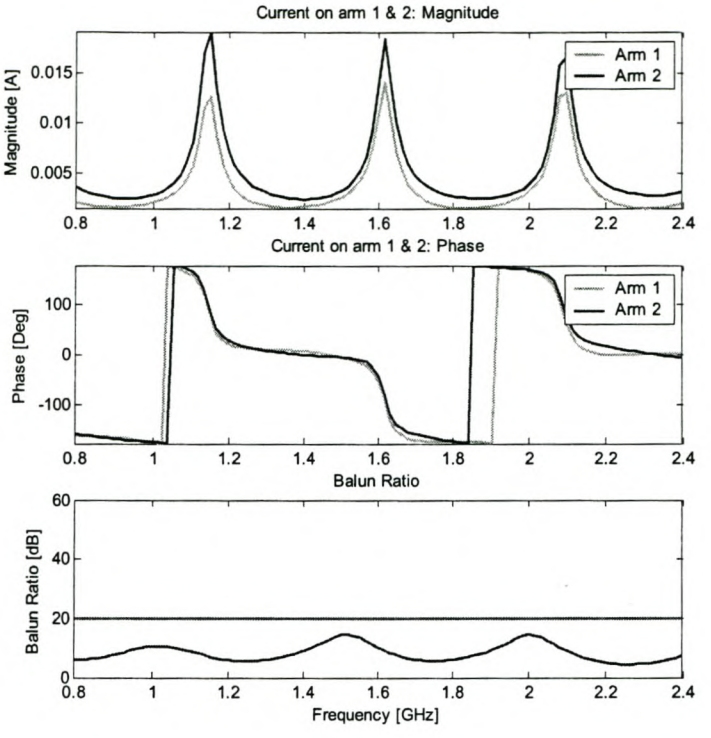

Figure 6-26 Currents on Infinite Dipole Arms (Magnitude & Phase) and Balun Ratio for Infinite Dipole

6.5.3 Impedance: Tapered-line Balun

Figure 6-27 presents the feed, differential and common mode impedance calculated from currents on infinite dipole arms. The length of either the microstrip, taper or balanced line causes resonances in the band. This can be removed by carefully redesigning the lengths mentioned. This does not interfere with the balance investigation. The impedance transforming property can still be seen though.

Stellenbosch University http://scholar.sun.ac.za

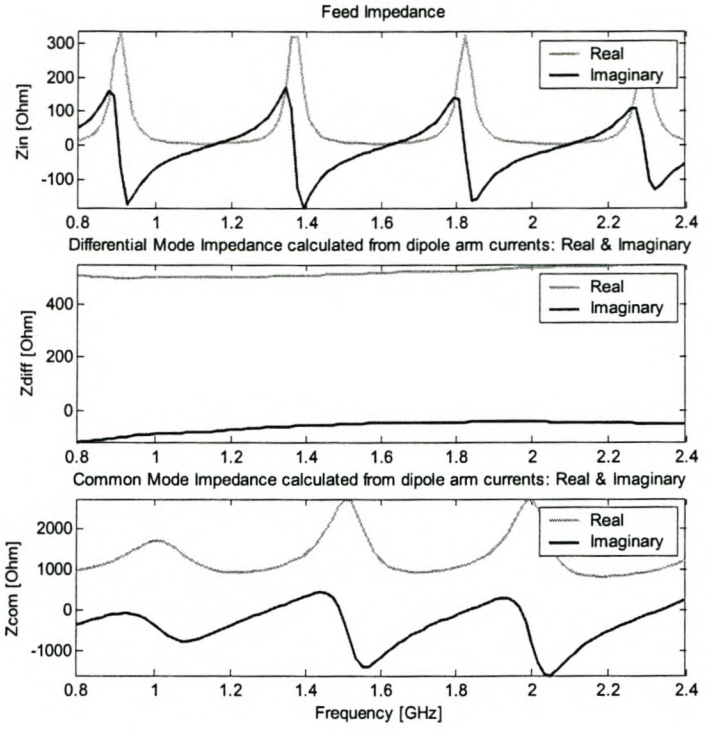

Figure 6-27 Feed Impedance and Differential and Common Mode Impedance Calculated from Currents on Infinite Dipole Arms (At Feed Point)

6.5.4 Antenna Type Influence on Balun Performance: Tapered-line Balun

Figure 6-28 presents the Balun Ratios for the three test antennas to show how the different antennas influence the balun performance. Refer to *Appendix B* for the currents and impedance results of the dipole and bow-tie antennas terminated with the various baluns.

Stellenbosch University http://scholar.sun.ac.za

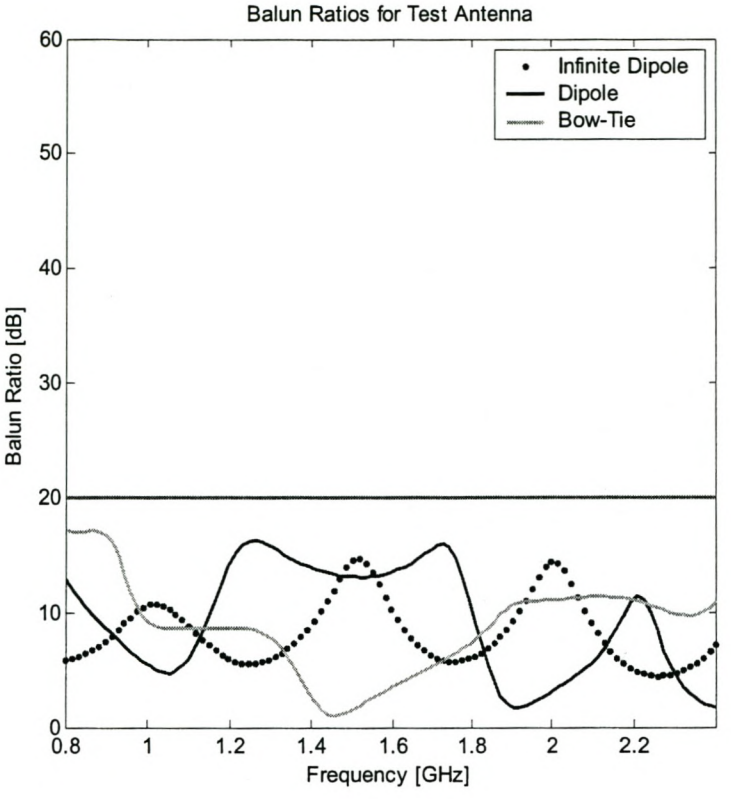

Figure 6-28 Balun Ratios for the Three test antennas

6.5.5 Validation of Model: Tapered-line Balun

Figure 6-29 presents the measured and computed input impedance for the balun terminated with the half wave dipole antenna. The measurement is done on a HP 8753 network analyzer with a standard one port calibration.

Stellenbosch University http://scholar.sun.ac.za

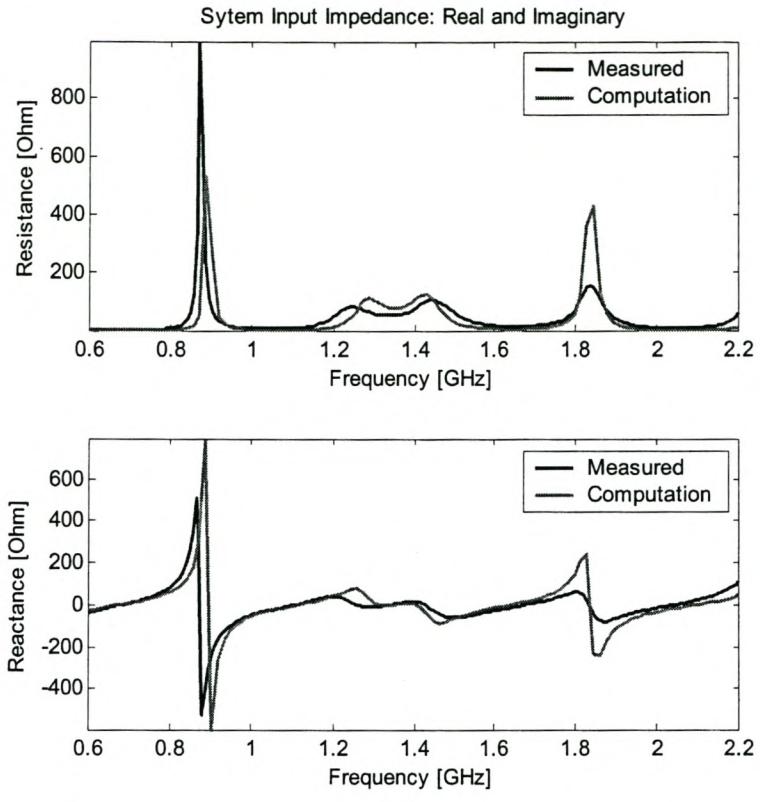

Figure 6-29 Measured and Computed System Input Impedance

6.6 "Log-periodic" Balun [19]

6.6.1 Balun Construction: "Log-periodic" Balun

Figure 6-30 shows the computational model used in FEKO.

Stellenbosch University http://scholar.sun.ac.za

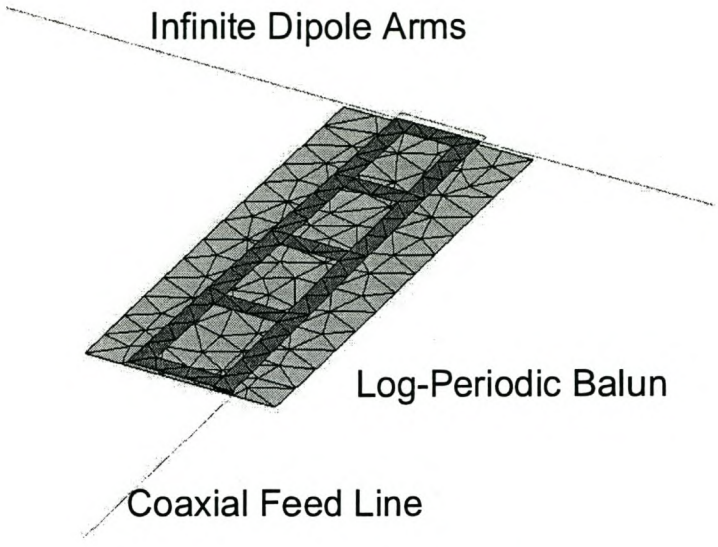

Figure 6-30 Computational model

6.6.2 Currents: "Log-periodic" Balun

Figure 6-31 presents the arm currents calculated at the feed point and balun ratio for the "Log-periodic" balun terminated with the infinite dipole.

Stellenbosch University http://scholar.sun.ac.za

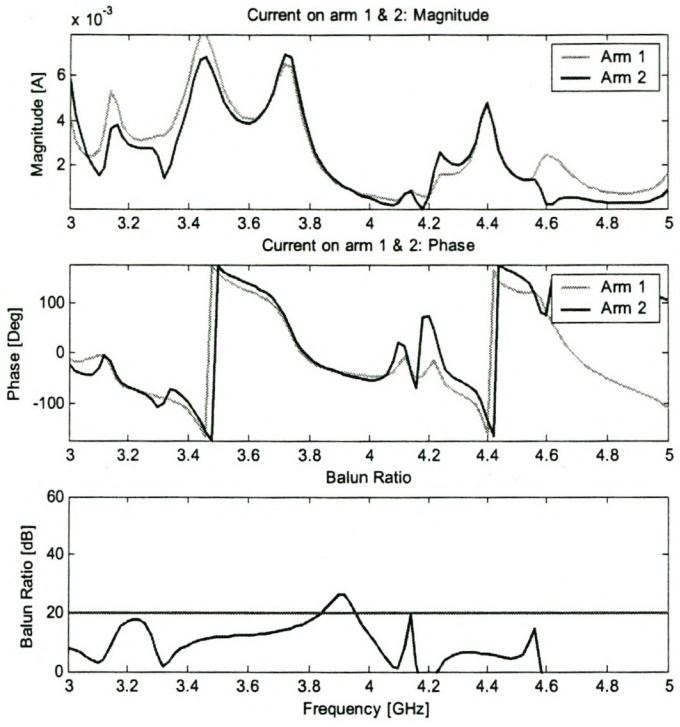

Figure 6-31 Currents on Infinite Dipole Arms (Magnitude & Phase) and Balun Ratio for Infinite Dipole

Stellenbosch University http://scholar.sun.ac.za

6.6.3 Impedance: "Log-periodic" Balun

Figure 6-32 presents the feed, differential and common mode impedance calculated from currents on infinite dipole arms

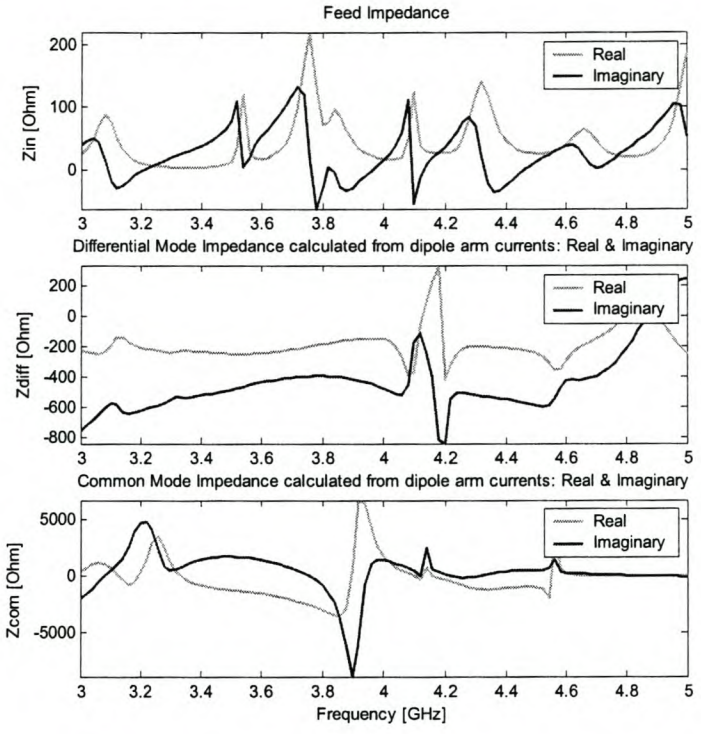

Figure 6-32 Feed Impedance and Differential and Common Mode Impedance Calculated from Currents on Infinite Dipole Arms (At Feed Point)

6.6.4 Antenna Type Influence on Balun Performance: "Log-periodic" Balun

Figure 6-33 presents the balun ratios for the three test antennas to show how the different antennas influence the balun performance. Refer to *Appendix B* for the currents and impedance results of the dipole and bow-tie antennas terminated with the various baluns.

Stellenbosch University http://scholar.sun.ac.za

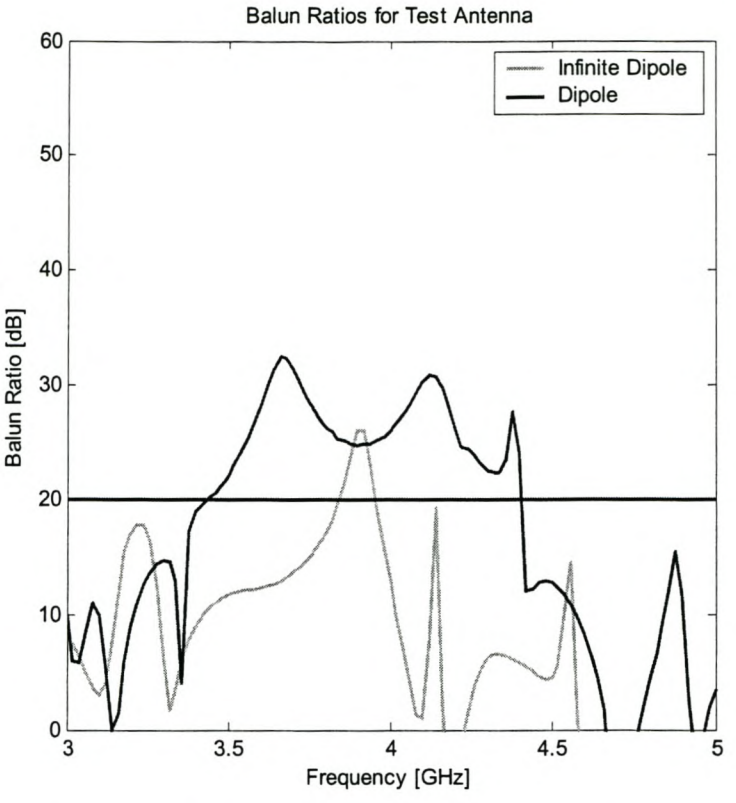

Figure 6-33 Balun Ratios for the Three test antennas

6.7 Coplanar-Slot balun [21]

6.7.1 Balun Construction: Coplanar-Slot balun

Figure 6-34 shows the computational model used in FEKO.

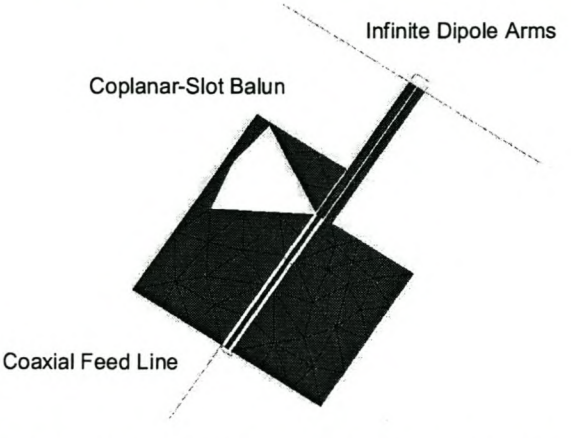

Figure 6-34 Computational model (Detailed view of the feed section is shown in Figure 6-20)

Stellenbosch University http://scholar.sun.ac.za

6.7.2 Currents: Coplanar-Slot balun

Figure 6-35 presents the arm currents calculated at the feed point and balun ratio for the coplanar-slot balun terminated with the infinite dipole.

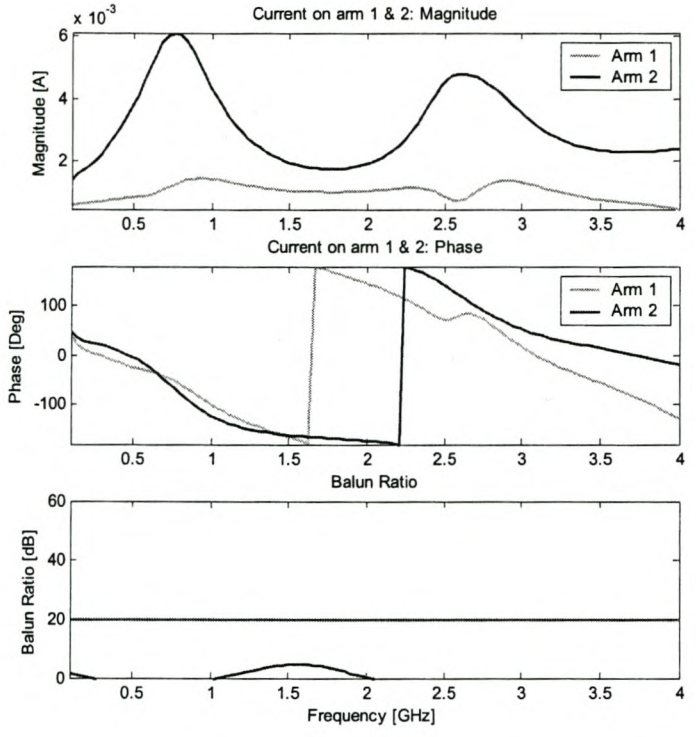

Figure 6-35 Currents on Infinite Dipole Arms (Magnitude & Phase) and Balun Ratio for Infinite Dipole

6.7.3 Impedance: Coplanar-Slot balun

Figure 6-36 presents the feed, and differential and common mode impedance calculated from currents (At feed point) on infinite dipole arms

Stellenbosch University http://scholar.sun.ac.za

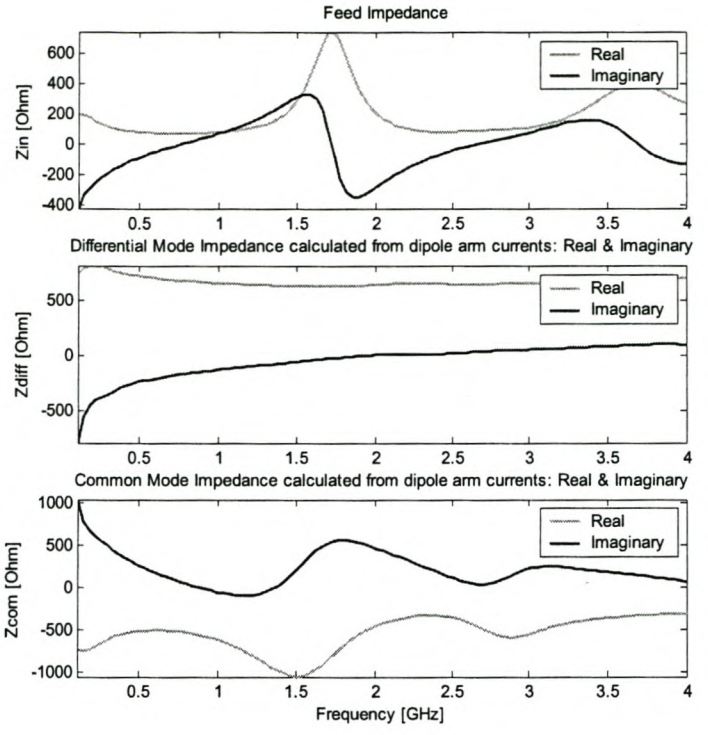

Figure 6-36 Feed Impedance and Differential and Common Mode Impedance Calculated from Currents on Infinite Dipole Arms (At Feed Point)

6.7.4 Antenna Type Influence on Balun Performance: Coplanar-Slot balun

Figure 6-37 presents the balun ratios for the three test antennas to show how the different antennas influence the balun performance. Refer to *Appendix B* for the results of the dipole and bow-tie antennas terminated with the various baluns.

Stellenbosch University http://scholar.sun.ac.za

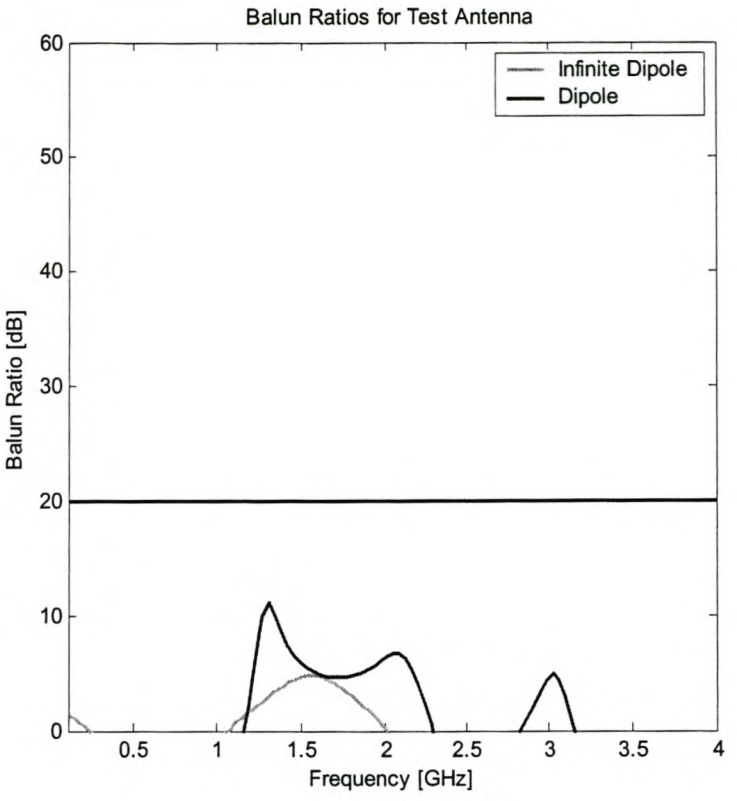

Figure 6-37 Balun Ratios for the Three test antennas

6.8 Using Infinite Dipole Results to Predict Finite Antenna Performance

As discussed in Chapter 3, the results of the infinite dipole are used to predict the response of the finite antennas terminated with the investigated baluns. These results are not expected to be very good since the baluns performance is highly dependant on the antenna terminated to it. The dipole's prediction should be much better than the Bow-Tie prediction because the infinite dipole and dipole look electrically almost the same. This technique is only presented to enable you to get an idea of what the system's response would be.

6.8.1 Bazooka Balun

Figure 6-38 presents a comparison between the predicted Bazooka/Dipole response and the computed Bazooka/Dipole response.

Stellenbosch University http://scholar.sun.ac.za

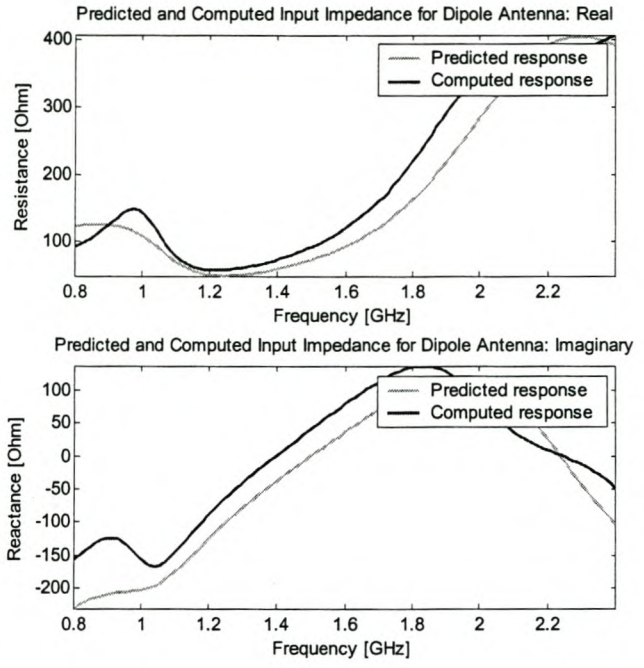

Figure 6-38 Predicted and Computed Input Impedance for Dipole Terminated to a Bazooka Balun

Figure 6-39 presents a comparison between the predicted Bazooka/Bow-tie response and the computed Bazooka/ Bow-tie response.

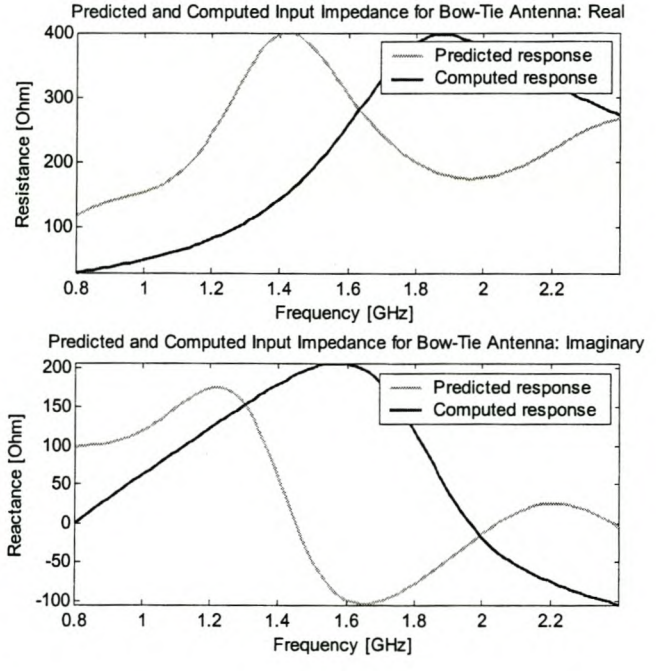

Figure 6-39 Predicted and Computed Input Impedance for Bow-Tie Terminated to a Bazooka Balun

Stellenbosch University http://scholar.sun.ac.za

6.8.2 Quarter Wave Balun

Figure 6-40 presents a comparison between the predicted quarter wave balun /dipole response and the computed quarter wave balun /dipole response.

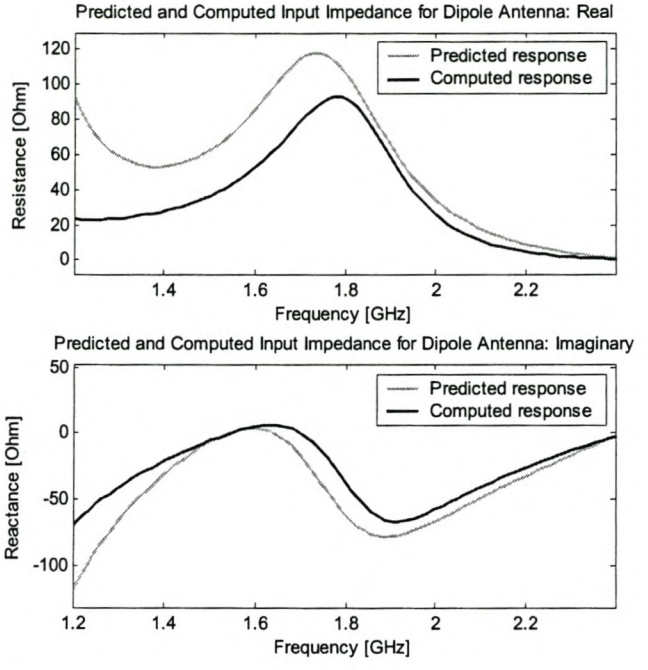

Figure 6-40 Predicted and Computed Input Impedance for Dipole Terminated to a Quarter Wave Balun

Figure 6-41 presents a comparison between the predicted quarter wave balun /bow-tie response and the computed quarter wave balun / bow-tie response.

Stellenbosch University http://scholar.sun.ac.za

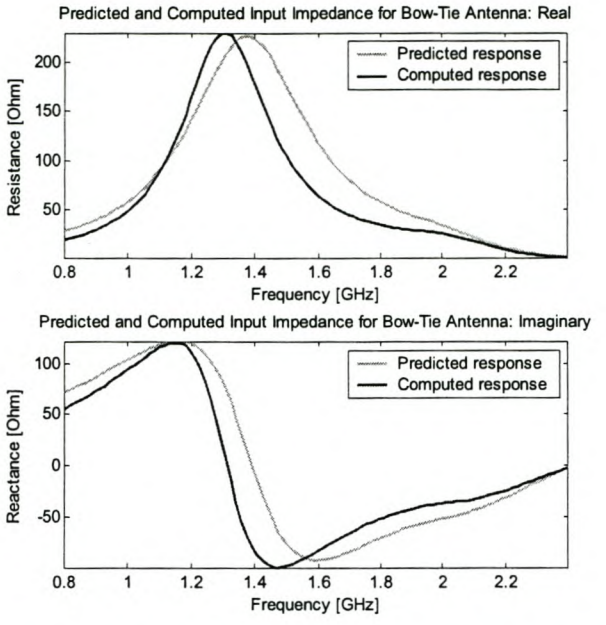

Figure 6-41 Predicted and Computed Input Impedance for Bow-Tie terminated to a Quarter Wave Balun

6.8.3 Marchand Balun

Figure 6-42 presents a comparison between the predicted Marchand balun /dipole response and the computed Marchand balun /dipole response.

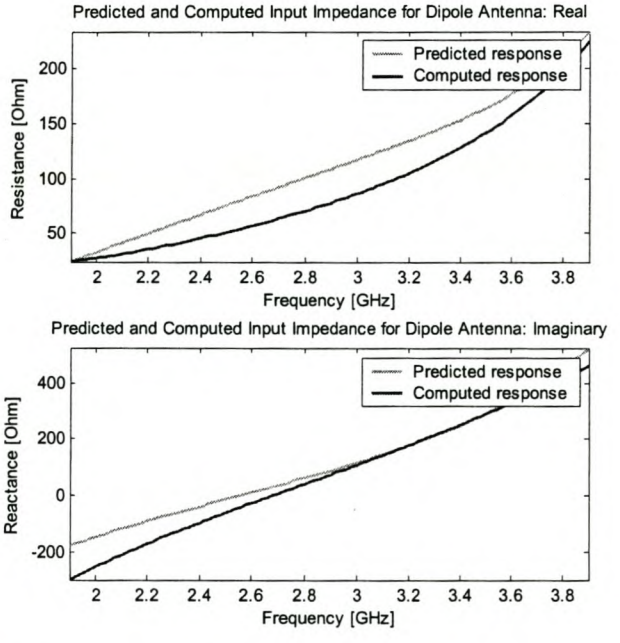

Figure 6-42 Predicted and Computed Input Impedance for Dipole terminated to a Marchand Balun

Stellenbosch University http://scholar.sun.ac.za

Figure 6-43 presents a comparison between the predicted Marchand Balun/Bow-Tie response and the computed Marchand Balun /Bow-Tie response.

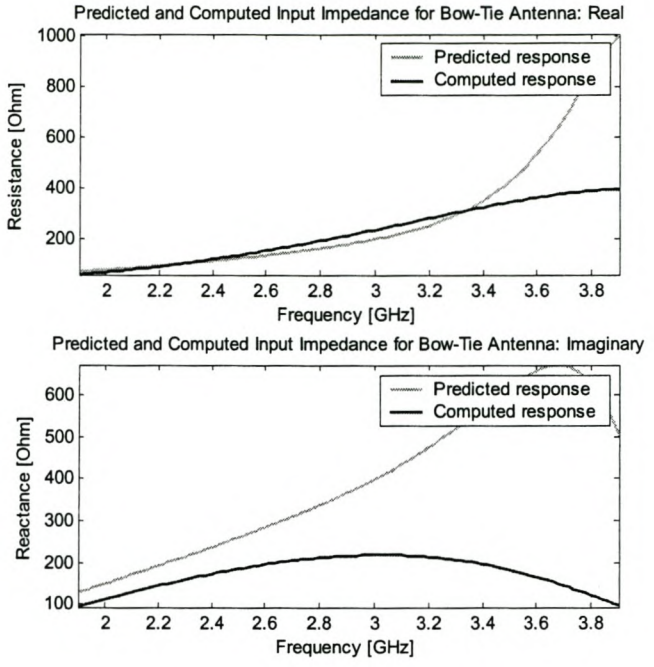

Figure 6-43 Predicted and Computed Input Impedance for Bow-Tie Terminated to a Marchand Balun

6.8.4 Double Y Balun

Figure 6-44 presents a comparison between the predicted double Y balun /dipole response and the computed double Y balun /dipole response.

Stellenbosch University http://scholar.sun.ac.za

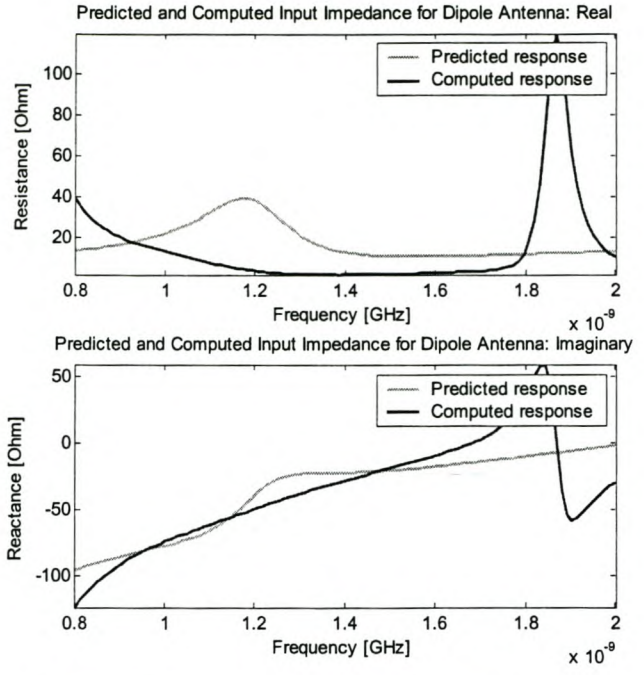

Figure 6-44 Predicted and Computed Input Impedance for Dipole terminated to a Double Y Balun

Figure 6-45 presents a comparison between the predicted double Y balun /bow-tie response and the computed double Y balun /bow-tie response.

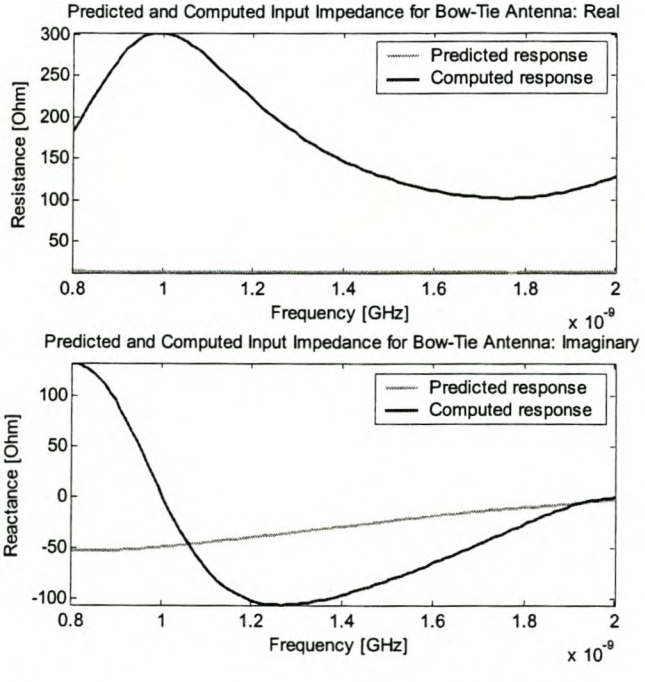

Figure 6-45 Predicted and Computed Input Impedance for Bow-Tie terminated to a Double Y Balun

Stellenbosch University http://scholar.sun.ac.za

6.8.5 Tapered Line Balun

Figure 6-46 presents a comparison between the predicted tapered line balun /dipole response and the computed tapered line balun /dipole response.

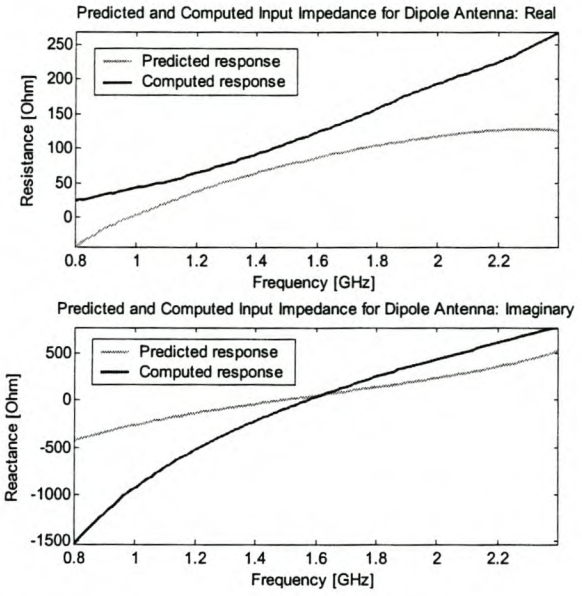

Figure 6-46 Predicted and Computed Input Impedance for Dipole terminated to a Tapered Line Balun

Figure 6-40 presents a comparison between the predicted tapered line balun /bow-tie response and the computed tapered line balun /bow-tie response.

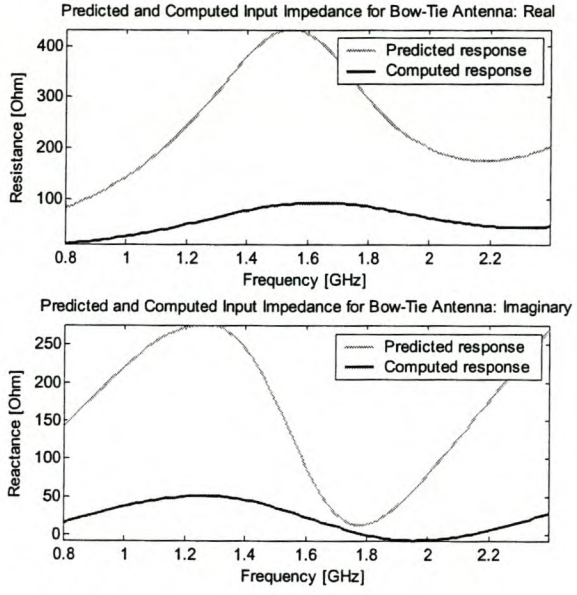

Figure 6-47 Predicted and Computed Input Impedance for Bow-Tie terminated to a Double Y Balun

Stellenbosch University http://scholar.sun.ac.za

Chapter 7. Conclusion

7.1 Comparison of Different Balun Performances

Balun	Balun Ratio Bandwidth % Bandwidth with BR ≥ 20 dB		
	Infinite Dipole	Dipole	Bow-Tie
Bazooka	11.1	23.3	9.2
Quarter wave	∞	∞	∞
Coaxial Marchand	∞	∞	∞
Planar Marchand	NA	26.8	34
Tapered line	0	0	0
Double Y	0	0	0
"Slot line"	0	0	NA
"Log-periodic"	2.8	25	NA

Table 7-1 Comparison of different balun performances

The following bullets summarize the overall performance of the investigated baluns.

- *Quarter wave balun*: Excellent narrow band balun with perfect balance over the whole band. Impedance bandwidth is limited by the loop or quarter wave line. The design and manufacture are very simple and can be done by hand. The factor that limits the balun's performance is the impedance bandwidth. Note that the impedance bandwidth of the dipole is actually increased when the quarter wave balun added to the system. This can be seen in Appendix B.
- *Bazooka balun*: Good narrow band balun. Balance bandwidth is limited to that of a quarter wave transformer. Impedance bandwidth is almost frequency independent. Design and manufacturing is very simple and can be done by hand. The factor that limits the balun's performance is the balance bandwidth.
- *Marchand balun*: Excellent wide band balun for the coaxial case. The balance bandwidth is infinite. The impedance bandwidth is determined in the synthesis procedure and is a trade off for the quality of impedance matching. Bandwidths of 10:1 are easily obtained. The design of the coaxial and the planar Marchand are both

Stellenbosch University http://scholar.sun.ac.za

rather complex. The planar version is manufactured with standard printed circuit board technologies while manufacturing the coaxial version demands workshop skills.

- *Tapered line balun*: The tapered line balun performs excellently as an impedance transformer with good bandwidth. The balance bandwidth is very poor and unpredictable though. **This is not a balun**. The manufacturing is easy and is done with standard printed circuit board technologies.
- *Double Y balun*: This balun does not balance the system at all. The balance results are worse that the results obtained without the balun. The impedance bandwidth on the other hand is perfect, with a theoretical infinite bandwidth arising from the all pass nature of the network. The design is trivial compared to the manufacturing.
- *Slot Line balun*: This balun does not balance the system at all. The balance results is worse that the results obtained without the balun. [21] claims an impedance bandwidth of about 40:1. The design and manufacturing are very simple.
- *Log-Periodic balun*: The balance bandwidth is good. The balun show wide band balance promise and must be investigated further. [19] claims a 8:1 impedance bandwidth. Design and manufacturing is simple.

7.2 Conclusion

Balun performance is governed by two key parameters: The balance and impedance matching. The frequency band that the balun will operate properly in, is thus determined by the key parameter with the smallest bandwidth.

It was proven that many structures that claim to be baluns, are nothing more than impedance matching circuits which do nothing to the balance of the system. In the investigation of these baluns, the following techniques were developed:

- A modelling technique that allows us to divide baluns into two families for explanation purposes: Symmetrical and Choke baluns.
- Characterization of balun performance.
- Computational models that model the physical problem as accurately as possible.

Further investigation is under way to compile an article, presenting these findings to the microwave community.

Stellenbosch University http://scholar.sun.ac.za

References

[1] Author: EM Software & Systems-S.A. (Pty) Ltd: Title: FEKO (www.feko.info): Version: 2.14, FEKO Suite 4.1: Publisher: EM Software & Systems-S.A. (Pty) Ltd: Address: PO Box 1354, Stellenbosch, 7599, South Africa: Date: 2003-07-22

[2] T.T. Wu and R.W.P. King, 'The Cylindrical Antenna with Non-Reflecting Resistive Loading', IEEE Transactions on Antennas and Propagation, vol. AP-13, Nov. 1965

[3] Christian Waldschmidt, 'Antennas for Surface Penetrating Radar', MScEng Thesis, University of Karlsruhe, Germany, December 2000

[4] ATN microwave, 'ATN-4000 series Multiport Network Analyzers', Application

[5] D.E. Bockelman and W.R. Eisenstadt, 'Combined Differential and Common-Mode Scattering Parameters: Theory and Computation', IEEE Transactions on Microwave Theory and Techniques, vol. 43, no. 7, July 1995, pp. 1530

[6] M.W. Van Rooyen,' Simple Broadband Measurement of Balanced Loads Using a Network Analyser', MScEng Thesis, University of Stellenbosch, Stellenbosch, South Africa, November 2000

[7] O. Woodward and S. Perlow, 'Balance Quality Measurement on Baluns', IEEE Transactions on Microwave Theory and Techniques, vol. MTT-31, no. 10, October 1983, pp 821

[8] N. Marchand, ' Transmission-Line Conversion', Electronics, vol. 17, no 12, pp 142-145, December 1944

[9] Jwo-Shion Sun and Tsung-Lin Lee, ' Design of a Plannar Balun', IEEE Proceedings of Antenna an Propagation, 2001, pp. 535

[10] J.H. Cloete, 'Exact design of the Marchand Balun', Microwave Journal, vol 23 no.5, May 1980, pp. 124

[11] J.A.G. Malherbe, 'Microwave Transmission Line Filters', Artech House, 1979

[12] M.C. Horton and R.J. Wenzel, 'General Theory and Design of Optimum Quarter-Wave TEM Filters', IEEE Trans., Vol. MTT, 1965, 316

[13] B. Jokanović and V. Trifunović, 'Dvostruki-Y baluni', Zadužbina Andrejević, 2002

[14] B. Jokanović and V. Trifunović, ' Review of Printed Marchand and Double Y Baluns: Characteristics and Application', IEEE Transactions on Microwave Theory and Techniques, vol. 42, no. 8, August 1994, pp. 1454

[15] B. Jokanović and V. Trifunović, 'Four Decade Bandwidth Uniplanar Balun', Electronics Letters, Vol. 28 No. 6, March 1992, pp. 534

Stellenbosch University http://scholar.sun.ac.za

[16] J.W. Duncan and V.P. Minerva, '100:1 Bandwidth Balun Transformer', Proceedings of the IRE, vol 48, February 1960, pp. 156

[17] R. Mongia, I Bahl and P. Bhartia, 'RF and Microwave Coupled-Line Circuits', Artech House ,1999

[18] D.M. Pozar, 'Microwave Engineering', Second edition, John Wiley & Sons, 1988

[19] M. Basraoui and S.N. Prasad, 'Wideband, Planar, Log-Periodic Balun', IEEE MTT-S, Vol. 2, June 1998

[20] Constanine A. Balanis, 'Antenna Theory', Second edition, John Wiley & Sons, 1997

[21] J. Thaysen, K. B. Jakobsen and J. Appel-Hansen,' A Wideband Balun – How Does it Work', Applied Microwave & Wireless

Stellenbosch University http://scholar.sun.ac.za

Bibliography

[1] W.L. Stutzman and G.A. Thiele, 'Antenna Theory and Design', John Wiley & Sons, 1998

[2] S. Ramo, J.R. Whinnery and T. Van Duzer, 'Fields and Waves in Communication Electronics', Third edition, John Wiley & Sons, 1993

[3] H.A. Haus and J.R. Melcher, ' Electromagnetic Fields and Energy', Prentice Hall 1988

[4] B.K. Woods, 'Development of an Active Pulsed Radar Receiver for a Mono-Static Borehole-Radar tool' , MScEng Thesis, University of Stellenbosch, Stellenbosch, South Africa, February 2003

[5] G. Ghione and C.U. Naldi, 'Coplanar Waveguides for MMIC Applications: Effect of Upper Shielding, Conductor Backing, Finite-Extent Ground Planes, and Line-to-Line Coupling', IEEE Transactions on Microwave Theory and Techniques, vol. MTT-35, no. 3, March 1987

[6] T. Chen, K. Chang, S.B. Bui, H. Wang, G. Dow, L. Lui, T. Lin and W. Titus, 'Broadband Monolithic Baluns and Monolithic Double Balanced Mixer', IEEE Transactions on Microwave Theory and Techniques, vol. 39, no. 12, December 1991

[7] G.J. Laughlin, ' A New Impedance-Matched Wide-Band Balun and Magic T , IEEE Transactions on Microwave Theory and Techniques, vol. MTT 24, no. 3, March 1976

[8] R. Schwindt and C. Nguyen, ' A CAD procedure for the Double-Layer Broadside-Coupled Marchand Balun', IEEE MTT-S, 1994

[9] K. Nishikawa, I. Toyoda, and T. Tokumitsu, 'Compact and Broad-Band Three-Dimensional MMIC Balun', IEEE Transactions on Microwave Theory and Techniques, vol. 47, no. 1, January 1991

[10] T. Rutkowski, W. Zienuitycz, K. Joachimowski,' Wide Band Coaxial Balun for Antenna Application'

[11] K.S. Ang and I.D. Robertson, ' Analysis and Design of Impedance-Transforming Planar Marchand Baluns', IEEE Transactions on Microwave Theory and Techniques, vol. 49, no. 2, February 2001

[12] C. Ng, M. Chongcheawchamnan and I. Robertson, ' Analysis and Design of a High-Performance Planar Marchand Balun', IEEE MTT-S, 2002

[13] K.V. Puglia, 'Electromagnetic Computation of Some Common Balun Structures', IEEE Microwave Magazine, September 2002

[14] J. McLaughlin, D. Dunn and R. Grow, 'A Wide-Band Balun', IRE Transactions on Microwave Theory and Techniques, July

[15] G. Oltman, 'The Compensated Balun', IEEE Transactions on Microwave Theory and Techniques, vol. MTT-14, no. 3, March 1966

Stellenbosch University http://scholar.sun.ac.za

[16] C. Curry, ' How to Calibrate Through Balun Transformers to Accurately Measure Balanced Systems', IEEE Transactions on Microwave Theory and Techniques, vol. 51, no. 3, March 2003

[17] B. Minnis and M. Healy, 'New Broadband Balun Structured for Monolithic Microwave Integrated Circuits', IEEE MMT-S, 1991

[18] M. Tsai, 'A New Compact Wide-Band Balun', IEEE Microwave and Millimetre-Wave Monolithic Circuit Symposium', 1993

[19] D. Raicu, 'Design of Planar, Single Layer Microwave Baluns', IEEE MTT-S, 1998

[20] C. Cho and K. Gupta, 'A New Design Procedure for Single-Layer and Two-Layer Three-Line Baluns', IEEE Transactions on Microwave Theory and Techniques, vol. 46, no. 12, December 1998

[21] J. McLean, 'Balancing Networks for Symmetric Antennas – I: Classification and Fundamental Operation', IEEE Transactions on Electromagnetic Compatibility, vol. 44, no. 4, November 2002

[22] P.R. Foster and Soe Min Tun, 'A Wideband Balun from Coaxial Line to TEM Line', IEE Antennas and Propagation Conference Publication, no. 407, April 1995

[23] Guan-Yu Chen and Jwo-Shiun Sun, 'A Printed Dipole with Microstrip Tapered Line', Microwave and Optical Technology Letters, Vol. 40, No. 4, February 2004

[24] FEKO user manual, EMSS, 2000

[25] C. Nguyen and D. Smith, ' Novel Miniaturised Wide-Band Baluns for MIC and MMIC Applications', Electronics Letters' , vol. 29, no. 2, June 1993

[26] S.J. Paisi, 'Lumped Element Hybrid', IEEE MTT-S Digest, 1989

Stellenbosch University http://scholar.sun.ac.za

Appendix A. Examples of Marchand Baluns

Planar [19]

Specifications

- Topology: Planner
- Order: 4
- Load impedance: 95 Ω
- Source impedance: 50 Ω
- Bandwidth: 3:1
- Return loss: 30 dB

Coupled line parameters

- Z_{0e}^{a} = 191.1Ω
- Z_{0o}^{a} =36.7Ω
- Z_{0e}^{b} = 155.3Ω
- Z_{0o}^{b} = 29.8Ω

Coaxial [20]

Specifications

- Topology: Coaxial
- Order: 2
- Load impedance: 100 Ω
- Source impedance: 50 Ω
- Bandwidth: 10:1
- Reflection coefficient: -9.5 dB

Transmission line parameters

- Z_2 = 21 Ω
- Z_3 = 241

Stellenbosch University http://scholar.sun.ac.za

Coaxial [20]

Specifications

- Topology: Coaxial
- Order: 3
- Load impedance: 100 Ω
- Source impedance: 50 Ω
- Bandwidth: 10:1
- Reflection coefficient: -12.4 dB

Transmission line parameters

- Z_2 = 17.5 Ω
- Z_3 = 215 Ω
- Z_4 = 70.7 Ω

Coaxial [20]

Specifications

- Topology: Coaxial
- Order: 4
- Load impedance: 100 Ω
- Source impedance: 50 Ω
- Bandwidth: 10:1
- Reflection coefficient: -14.9 dB

Transmission line parameters

- Z_1 = 65
- Z_2 = 20 Ω
- Z_3 = 250 Ω

Stellenbosch University http://scholar.sun.ac.za

Appendix B. Balun Performance

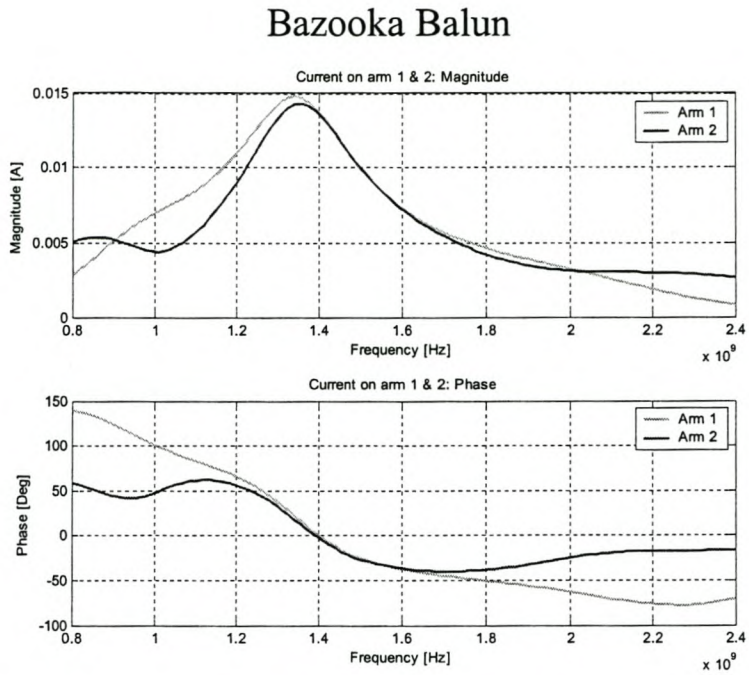

Figure B-1 Current on Dipole Arms

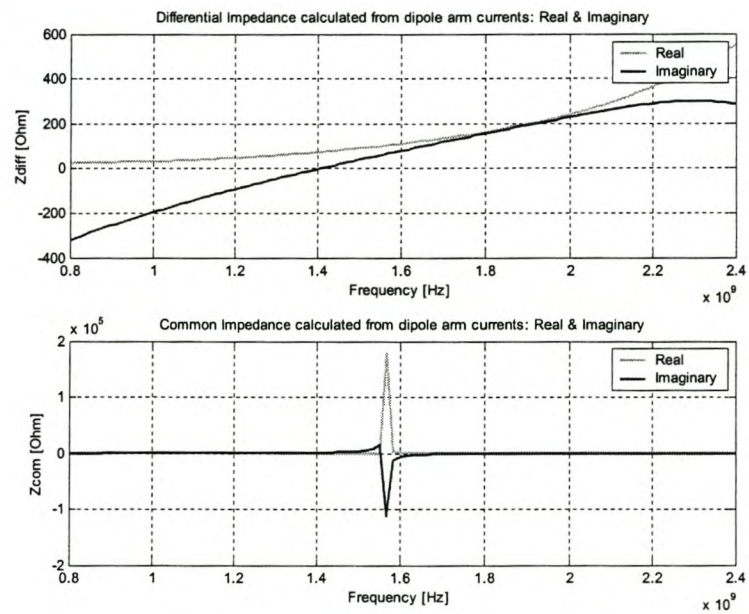

Figure B-2 Common and differential mode impedances measured from Dipole arms at feed point

Stellenbosch University http://scholar.sun.ac.za

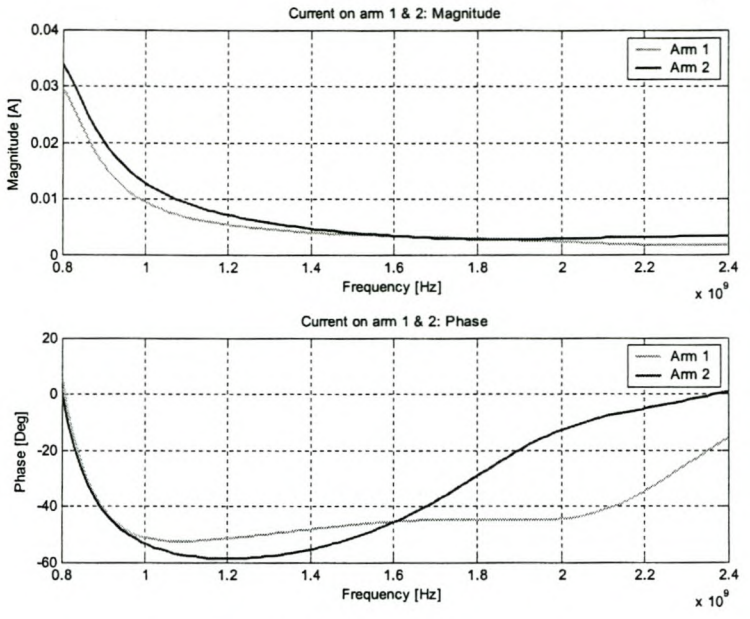

Figure B-3 Currents on Bow-Tie arms

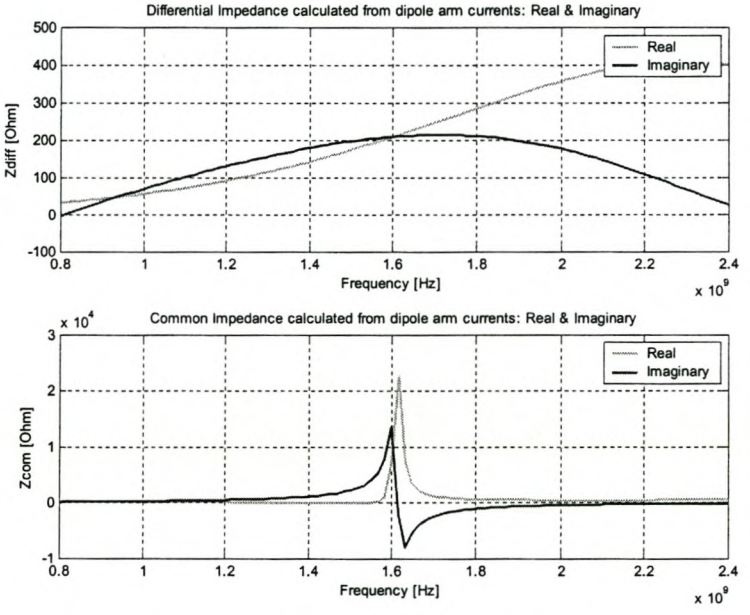

Figure B-4 Common and differential mode impedances measured from Bow-Tie arms at feed point

Stellenbosch University http://scholar.sun.ac.za

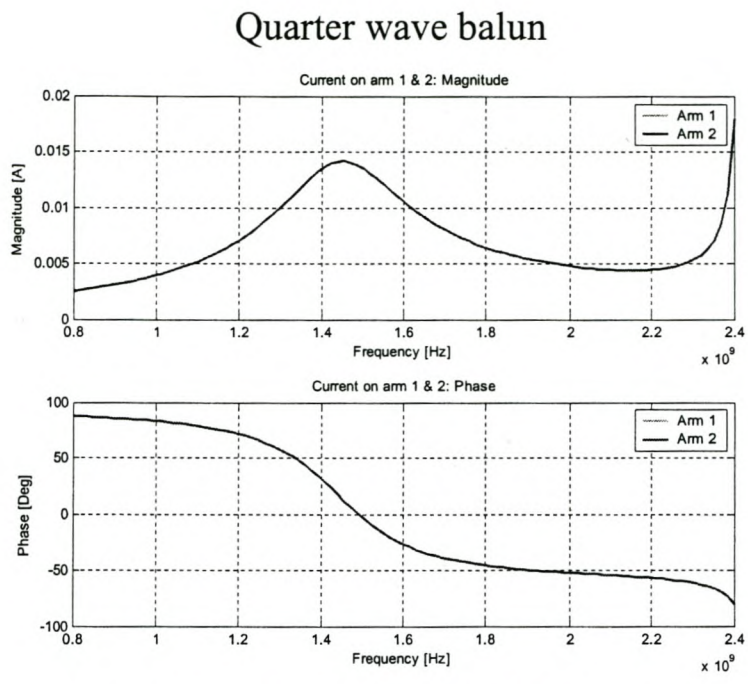

Figure B-5 Currents on dipole arms

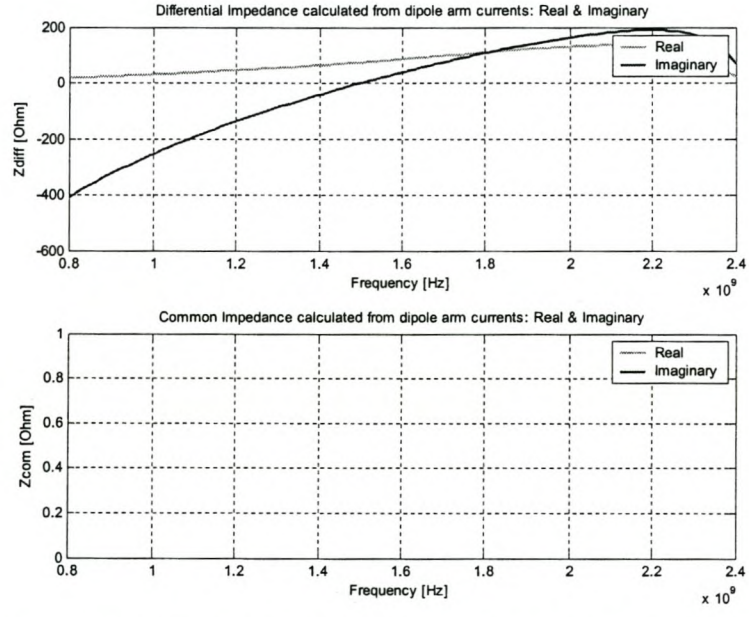

Figure B-6 Common and differential mode impedances measured from dipole arms at feed point.

Stellenbosch University http://scholar.sun.ac.za

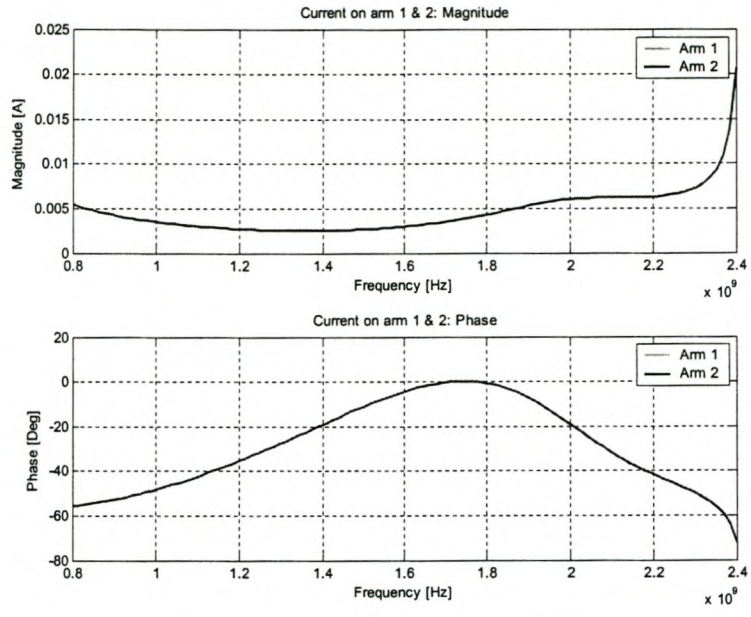

Figure B-7 Currents on Bow-tie arms

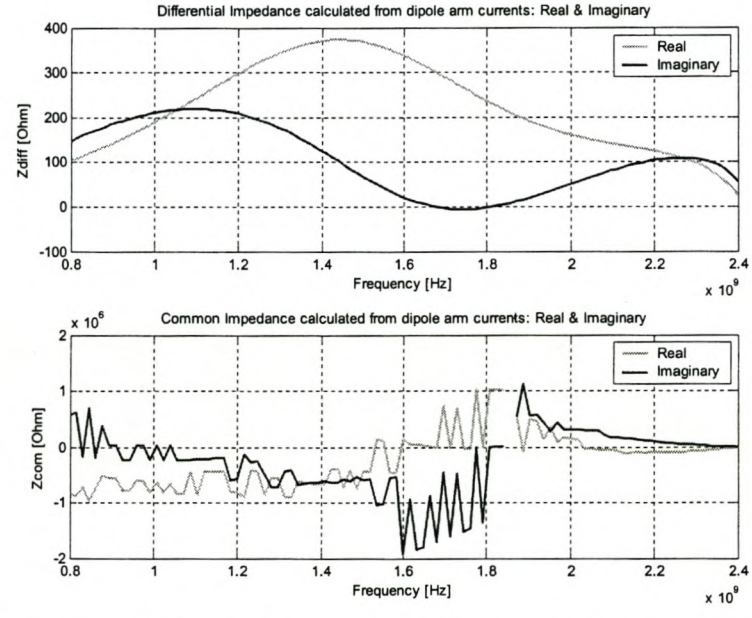

Figure B-8 Common and differential mode impedances measured from Bow-tie arms at feed point.

Stellenbosch University http://scholar.sun.ac.za

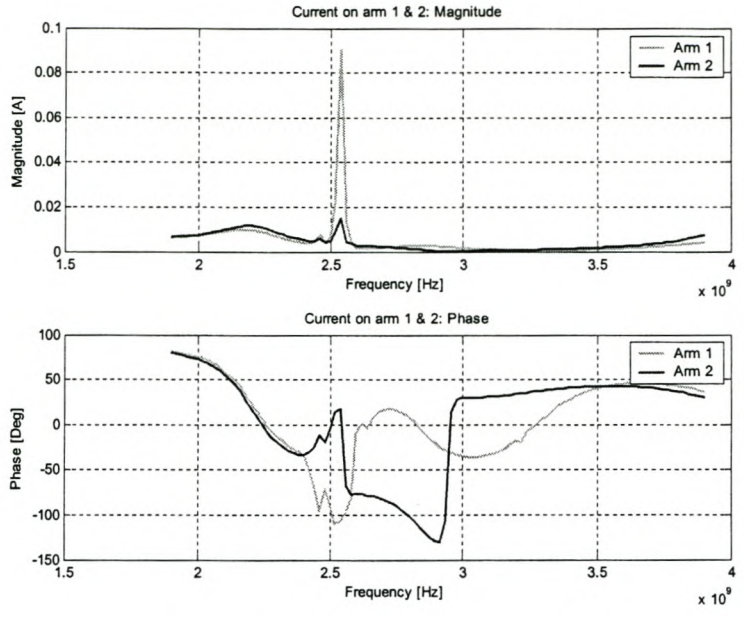

Figure B-9 Currents on Dipole arms.

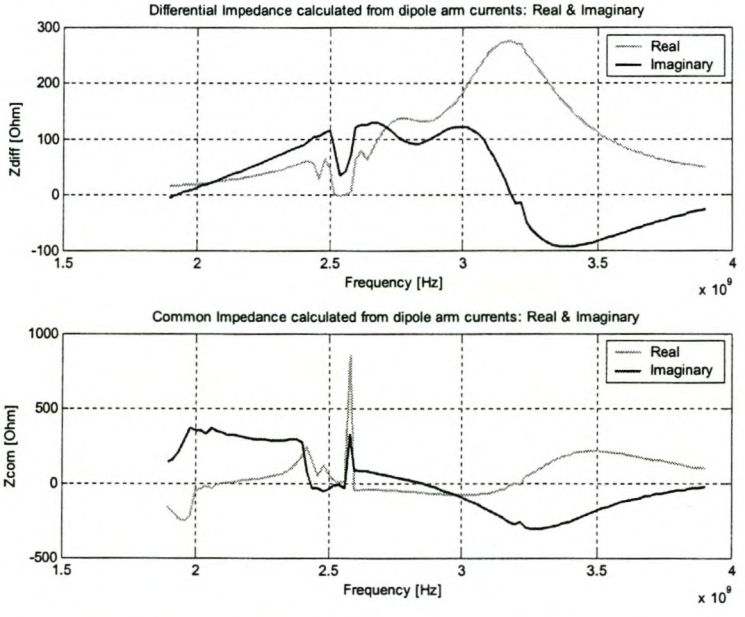

Figure B-10 Common and differential mode impedances measured from Dipole arms at feed point.

Stellenbosch University http://scholar.sun.ac.za

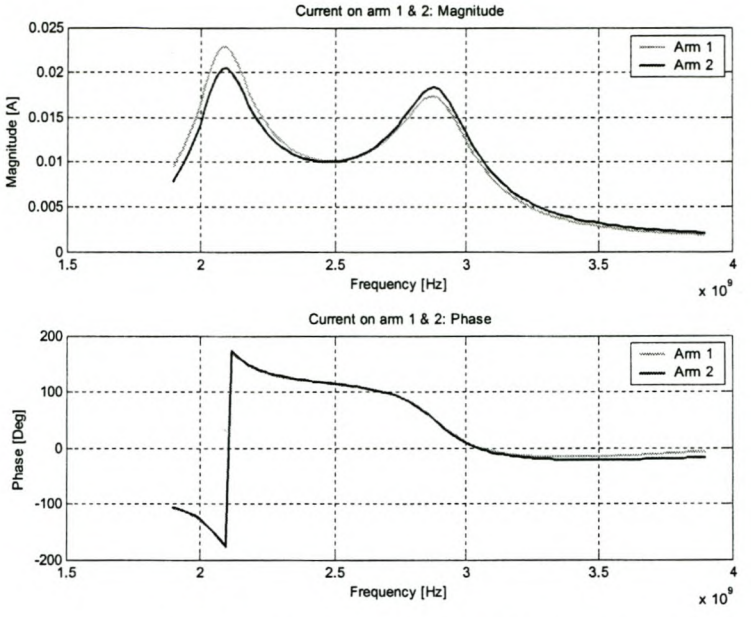

Figure B-11 Currents on Bow-Tie Arms.

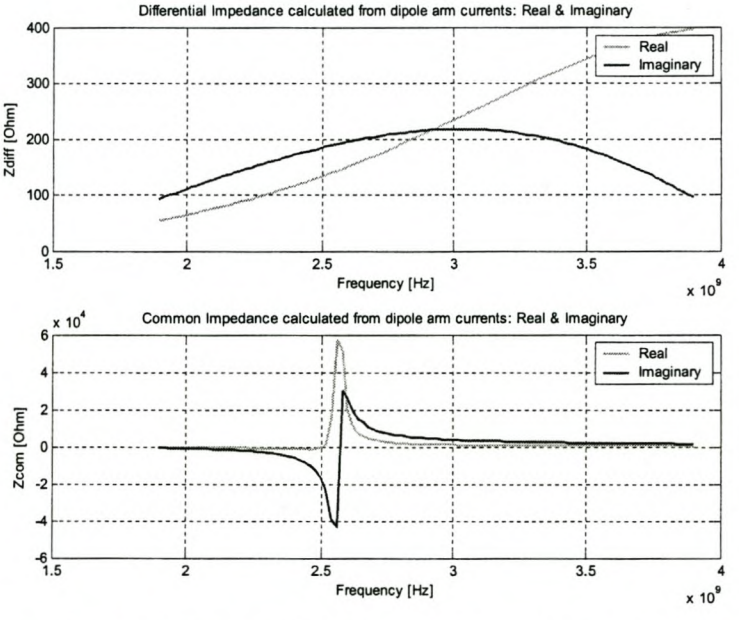

Figure B-12 Common and differential mode impedances measured from Bow-Tie arms at feed point.

Stellenbosch University http://scholar.sun.ac.za

Double Y Balun

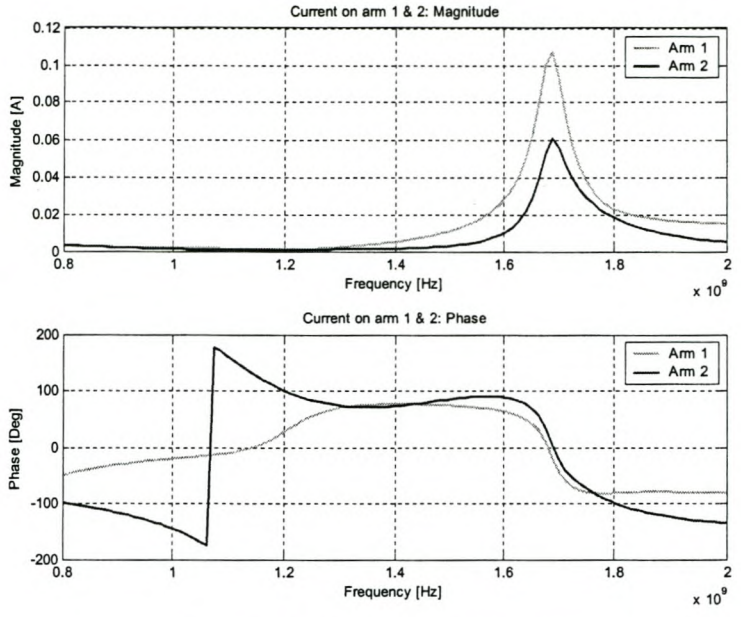

Figure B-13 Current on Dipole Arms

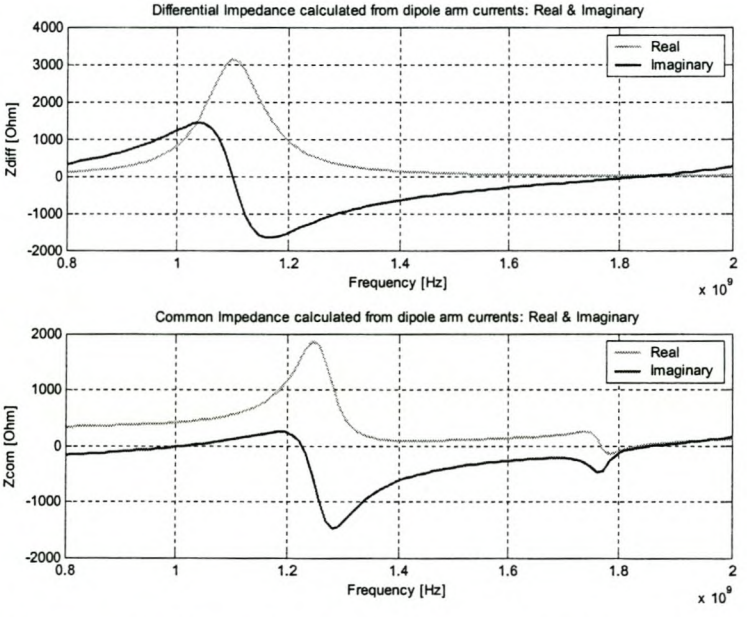

Figure B-14 Common and differential mode impedances measured from Dipole arms at feed point

Stellenbosch University http://scholar.sun.ac.za

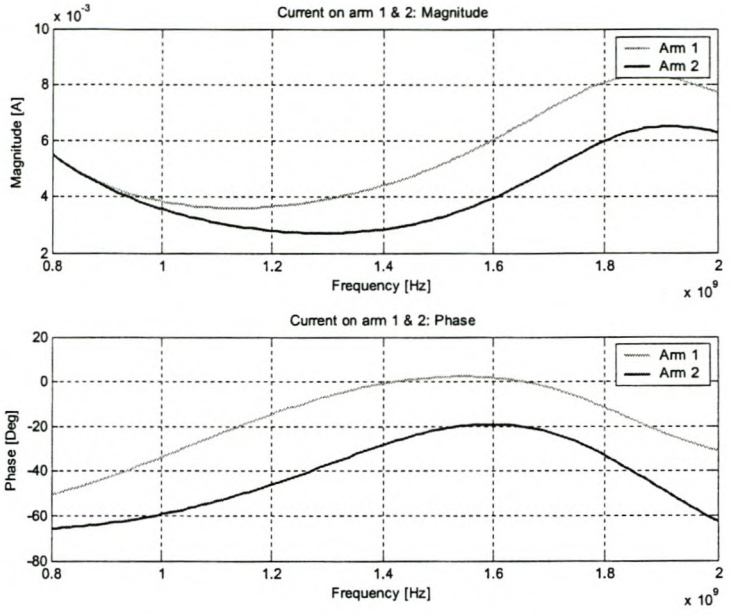

Figure B-15 Currents on Bow-Tie Arms.

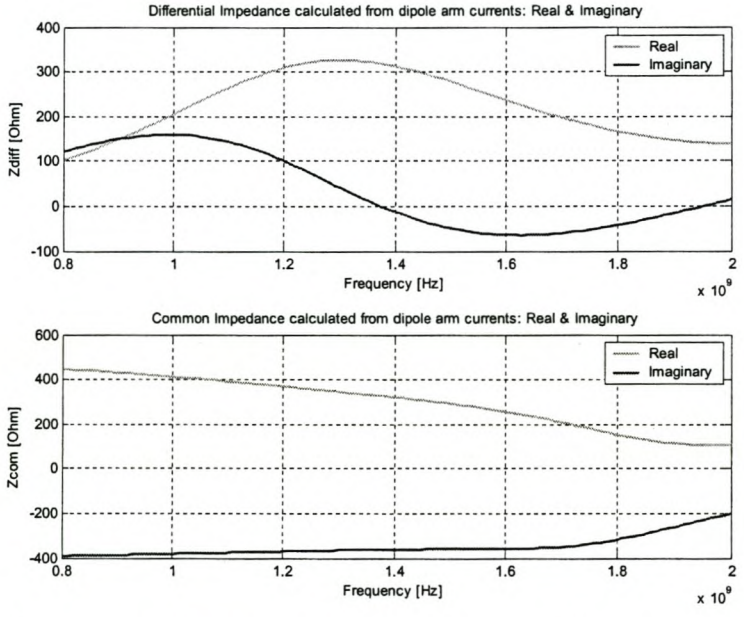

Figure B-16 Common and differential mode impedances measured from Bow-Tie arms at feed point

Stellenbosch University http://scholar.sun.ac.za

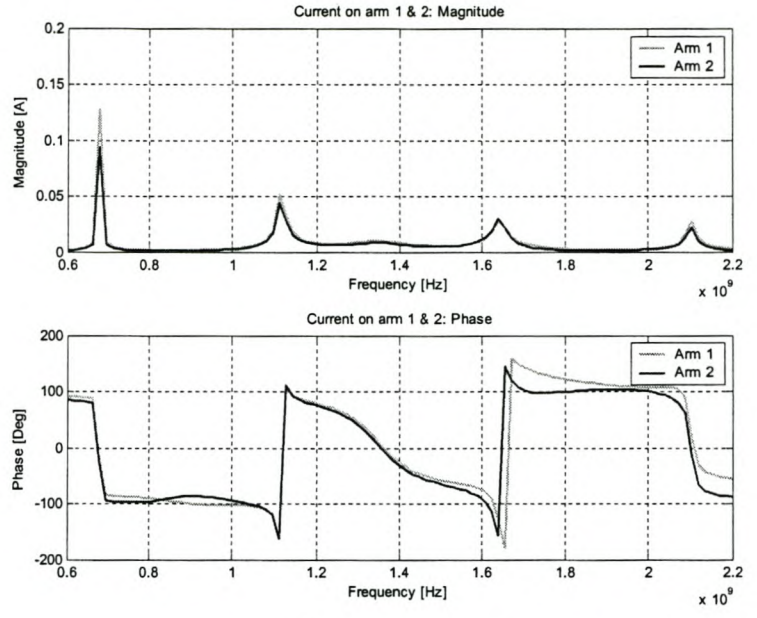

Figure B-17 Current on Dipole Arms

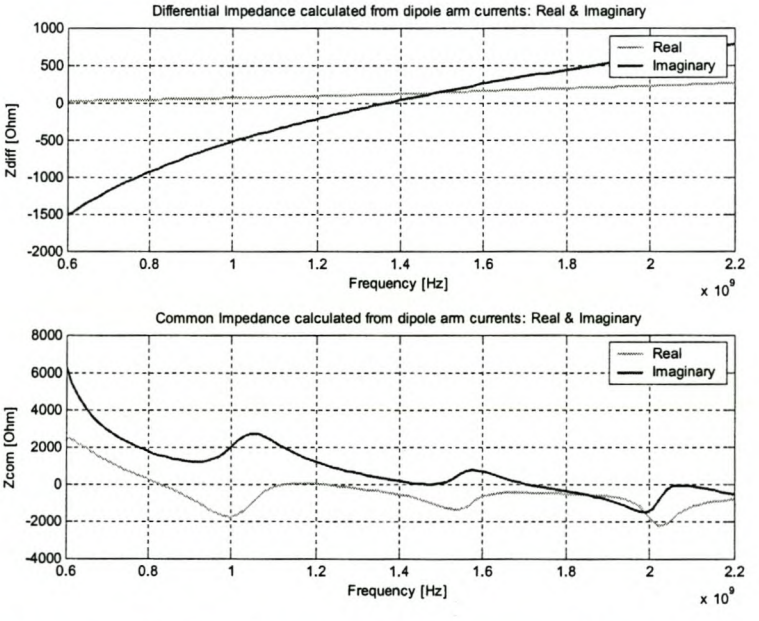

Figure B-18 Common and differential mode impedances measured from Dipole arms at feed point

Stellenbosch University http://scholar.sun.ac.za

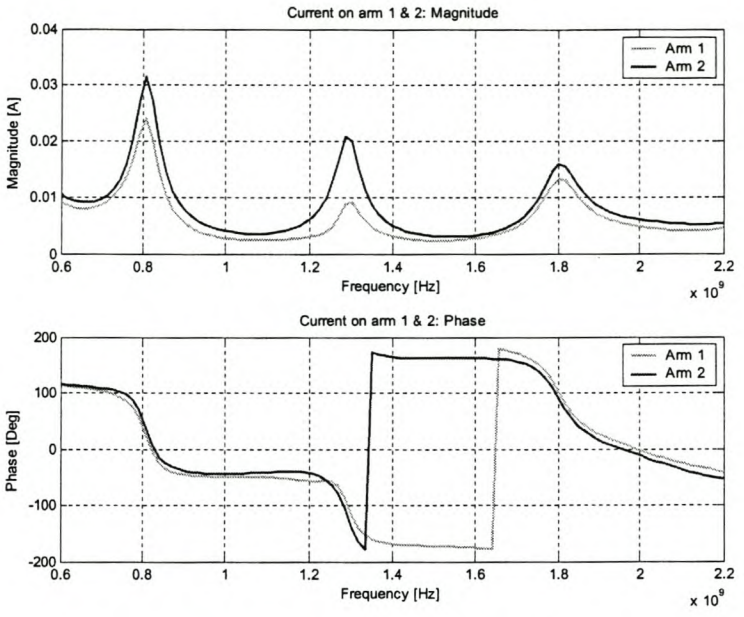

Figure B-19 Current on Bow-Tie Arms

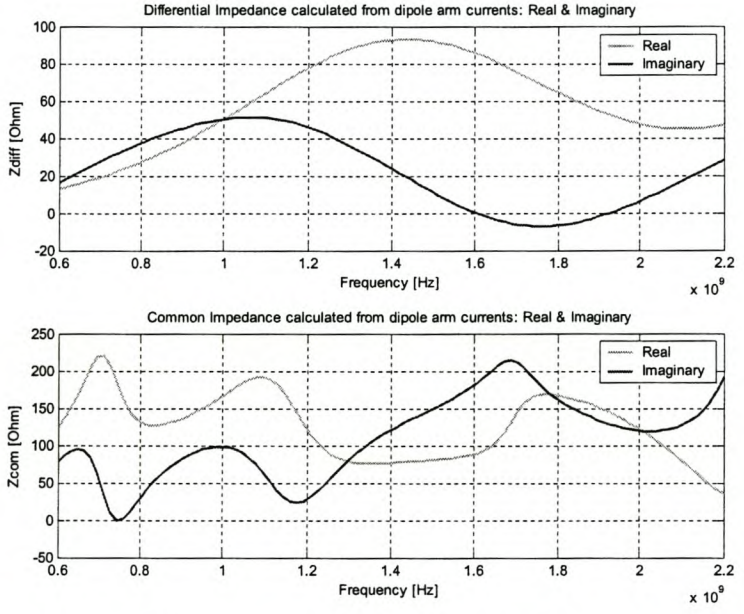

Figure B-20 Common and differential mode impedances measured from Bow-Tie arms at feed point

Stellenbosch University http://scholar.sun.ac.za

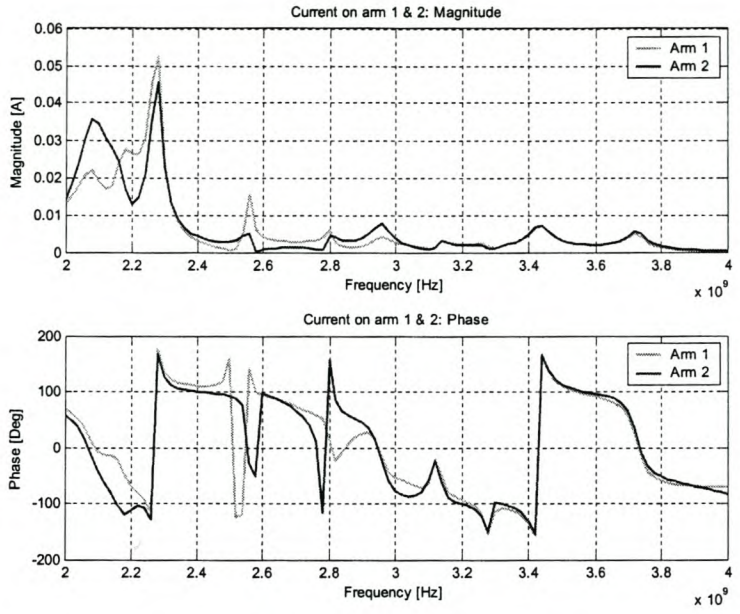

Figure B-21 Currents on Dipole Arms

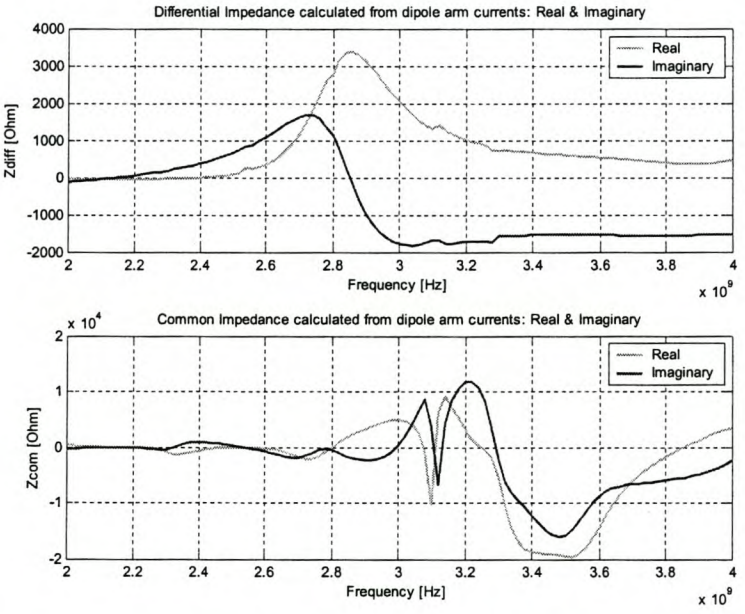

Figure B-22 Common and differential mode impedances measured from Dipole arms at feed points

Stellenbosch University http://scholar.sun.ac.za

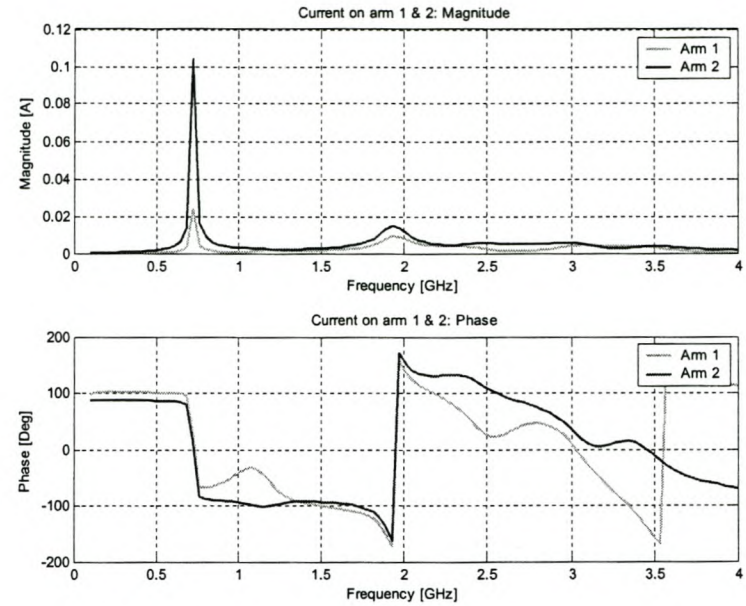

Figure B-1 Currents on Dipole Arms

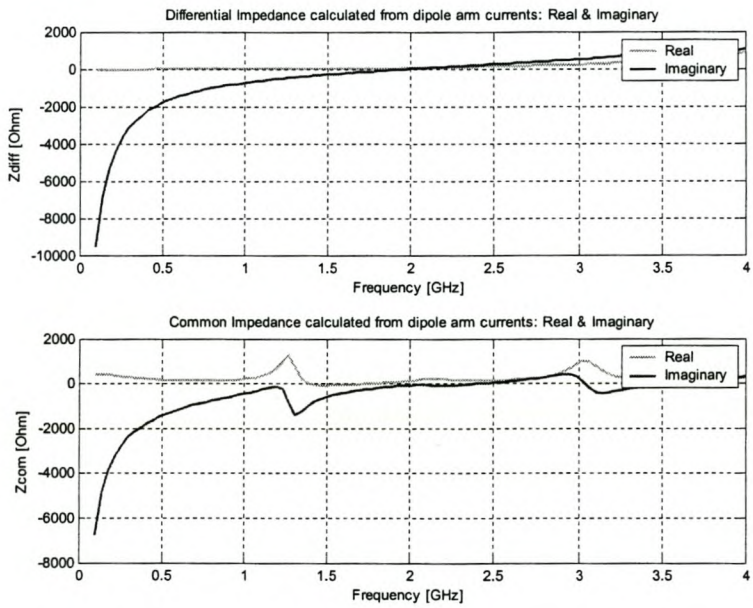

Figure B-23 Common and differential mode impedances measured from Dipole arms at feed points

Stellenbosch University http://scholar.sun.ac.za

Appendix C. Impedance Profile for Wu-King Antenna

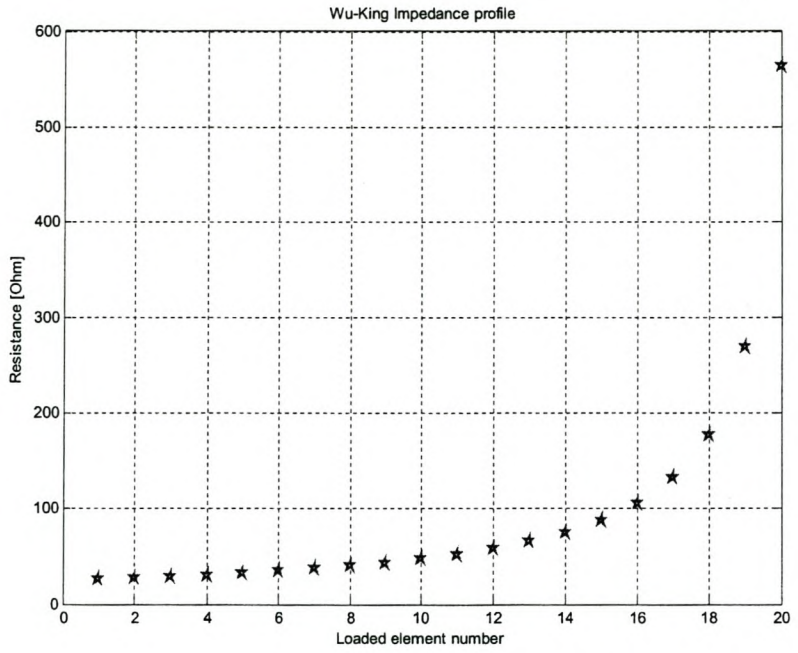

Figure C-1 Impedance profile for Wu-King Antenna

Element Number	Element Value
1	25.9202
2	27.2905
3	28.8136
4	30.5169
5	32.4342
6	34.6086
7	37.0954
8	39.9673
9	43.3212
10	47.2896
11	52.0583
12	57.8966
13	65.2098
14	74.6378
15	87.2526
16	104.9989
17	131.8071
18	176.9981
19	269.3450
20	563.1758

Table C-1 Element values for Resistive